RNAi-mediated Knockdown of Chromatin Modifier Proteins and Their Effect on Long-term Memory in *Drosophila*

A thesis presented to Massey University in partial fulfillment of the requirements for the degree of Master of Science in Genetics

Charles Ellen

2008

Abstract

Memory formation in *Drosophila melanogaster* is composed of two pathways that are genetically distinct, and functionally independent of each other. These are short-term and long-term memory. Short-term memory is a transient phenomenon, located in the cytoplasm of the neuronal cells, which requires no alteration of gene expression. The formation of long-term memory requires a change in gene expression, therefore chromatin-modifying complexes may play an integral part. The mushroom-bodies of *Drosophila* are a distinct bilateral brain structure and are essential for the formation and recollection of long-term memory. Therefore, an alteration in gene expression within the mushroom bodies is essential to the formation of long-term memory. Disruption of a gene within the mushroom-bodies that resulted in an alteration in the formation of long-term memory would indicate that the gene is involved in long-term memory.

In order to investigate the role of the two chromatin-modifying proteins, HDACX and pr-Set7, whose role in memory function is unknown, RNA interference was used to knockdown expression of their respective mRNA. Published GAL4 lines were used to drive down expression in the mushroom bodies. The efficacy of the knockdown on levels of mRNA was measured by quantitative RT-PCR. The effect of these knockdowns on the formation of long-term memory was assayed using conditioned courtship. Additionally, the actual spatial and temporal expression of the GAL4 drivers was investigated using fluorescent proteins, and analysed using fluorescent microscopy.

Both pr-set7 and HDACX appear to play a role in long-term memory function. The RNAi-induced knockdown of the individual mRNAs caused impairment in long-term memory formation, although the exact mode of action is still to be elucidated. The levels of mRNA from these knockdowns were reduced within the head, although not to the extent expected. The fluorescent microscopy analysis indicated that the expression of mushroom-body specific GAL4 drivers was more widespread than previously reported.

Acknowledgment

I would like to thank my supervisor Associate Professor Max Scott for his seemingly endless patience, allowing me to investigate my topic freely, and reining me in if it got to out of hand. I would also like to thank him for having the confidence in me to handle a project that was new to the lab.

I would also like to thank Corey Laverty for putting up with my questions on experimental problems that had absolutely no reference to the topic at hand. Thanks to Anja for her helping me trouble-shoot the qRT-PCR experiments, and to everyone else who is in, or has been in, the Flyspot Lab: Esther, Fang, Abhi, Brandi-lee, Carolina, and Helen. I feel it is also important to mention my sister Fiona, and brother-in-law Andrew, and to thank them for the ready supply of farm meat, and handy clothes drier. The Massey University Alpine Club (MUAC) deserve a mention for simply keeping a flow of interesting people coming into the club, and helping me find places to stay around the world. Finally I would like to thank Emma for providing plenty of distraction and amusing anecdotes while sitting in the either freezing cold, or scorching hot, computer room. It was fun, and Good Luck to all.

Table of Contents

List of Tables

List of Figures

Abbreviations

BDGP	Berkeley *Drosophila* Genome Project
bp	Base Pair
BSA	Bovine serum albumin
PCR	Polymerase chain reaction
dNTP	Deoxynucleoside triphosphates
CIP	Calf Intestinal Phosphatase
LB	Luria-Bertani
Amp	Ampicillin
PNK	Polynucleotide Kinase
X-gal	5-bromo-4-chloro-3-indolyl- beta-D-galactopyranoside
CS2	*chitin Synthase 2* intron
iPCR	Inverse PCR
nt	Nucleotide
RNAi	RNA Interference
HDAC	Histone deacetylase
HMT	Histone methyltransferase
HAT	Histone acetyltransferase
DNase	Deoxyribonuclease
GFP	Green fluorescent protein
mRNA	Messenger RNA
RT-PCR	Reverse transcriptase - polymerase chain reaction
rpm	Revolutions per minute
v/v	Volume per volume
kb	Kilobase-pair
CI	Courtship Index
MB	Mushroom-bodies
ISWI	Imitation Switch
P/CAF	p300/CBP Associated Factor
MYST	MOZ translocation partner, two yeast Sas proteins, and Tip60 protein family

Chapter One

Introduction

1.1 Chromatin

1.1.1 Chromatin Overview

It is well established that DNA in eukaryotes is packaged into a higher order structure known as chromatin. The core component of chromatin is the histone complex. This is composed of two copies of each histone protein H2A, H2B, H3 and H4. These are assembled into an octamer that has 145-147 base pairs (bp) of DNA wrapped around it to form the nucleosome core (Kornberg and Lorch, 1999). These histone proteins have a highly structured, globular C-terminal domain and an unstructured N-terminal 'tail' that makes-up about 25-30 % of the mass of individual histone; these tails are very amenable to post-translational modifications. The nucleosomes, along with approximately 40 bp of linker DNA in between the nucleosomes, are packaged into a solenoid structure forming a 30 nm fibre. The histone protein H1 also binds to the nucleosome core, and is required for the formation of the higher order structure of chromatin. This highly conserved nucleoprotein complex is virtually ubiquitous throughout all eukaryotic genomes (Luger et al., 1997).

The chromatin packaging of DNA has historically been considered a static, non-participating structural element, but now it is becoming increasingly evident that chromatin is very dynamic and has a profound effect on transcription. This appears to be influenced largely through the dynamic interactions of histone tails and histone modifying complexes (Jenuwein and Allis, 2001). These histone-modifying complexes can carry out many different post-translational modifications, such as acetylation of lysine residues (Akhtar and Becker, 2000), phosphorylation of serine residues (Wang et al., 2001), and methylation of both lysine (Muller et al., 2002) and arginine residues (Cakouros et al., 2004). These modifications have varying effects on gene expression, with acetylation being predominantly associated with gene activation whereas methylation can be associated with gene repression or activation. However it is thought that it is the combination of these epigenetic modifications that are responsible for the overall gene expression – the so-called "histone code" (Strahl and Allis, 2000).

1.1.2 Histone Tails

The highly basic, lysine- and arginine-rich N-terminal tails of the nucleosome have a more dynamic and complex role in chromatin structure than the globular C-terminal domain. The tails are defined as the regions of the histone protein that extend out from the globular domains, and in contrast to the highly structured nucleosomal disc, which is bound by the superhelical DNA, appear to be flexible, irregular chains (reviewed in Kornberg (1999)). Histone protein dimers H2A-H2B and H3-H4 must have at least one of their two tails intact in order to maintain viability; this indicates that although histone tails are essential they do show some redundancy in yeast (Ling et al., 1996). In order to restore cell viability, the histone tails need not be attached to their native C-terminal, however the regulation of GAL1 and the silent mating loci by the H3 and H4 tails is highly disrupted by exchange of the histone amino termini.

1.1.3 Histone Acetyltransferase

Histone acetylation is carried out by enzymes collectively known as histone acetyltransferases (HATs). These enzymes, as the name suggests, catalyse the transfer of an acetyl group from acetyl-CoA to the ε-amino groups on the N-terminal tails of histones, and have been implicated in transcriptional activation for many years (Allfrey et al., 1964). Acetylation of these tails results in a decrease in the overall positive charge of histone tails and as a result, diminishes the strength of binding of the tails to the negatively charged DNA. This reduction in electrostatic bond strength may in turn make both tails and nucleosomal DNA more accessible to the factors that bind them, as well as increasing the accessibility of the nucleosomal DNA to transcribing RNA polymerase (Tse et al., 1998). It was observed that actively transcribed regions of chromatin showed enriched histone acetylation, whereas transcriptionally silent regions of chromatin had low levels of acetylated histones. The definitive link between HATs and gene activation came when the *Tetrahymena thermophilus* homologue of yeast transcription co-activator Gcn5 was found to acetylate histones (Brownell et al., 1996). The addition of an acetyl group to a lysine residue alters the charge distribution of the N-terminal tails by neutralising the positive charge. This has implications for gene regulation, as multiple acetylation of histone tails could dramatically change the overall

charge of the nucleosome and in turn affect binding of other proteins, such as the TATA binding protein (Sewack et al., 2001).

Histone acetyltransferases such as Males absent On the First (MOF) in *Drosophila melanogaster*, which belong to a family of HATs that were originally defined by the human MOZ leukemia translocation partner, the two yeast Sas proteins, and the human HIV-Tat interacting protein Tip60, have been shown to be a crucial factor in the up-regulation of the male X chromosome in dosage compensation (Akhtar and Becker, 2000). This up-regulation appears to be achieved via the specific acetylation of the histone H4 tail at the lysine residue 16 (H4K16) (Akhtar and Becker, 2000). This acetylation of H4K16 has been shown to be antagonistic to the action of Imitation Switch (ISWI), a *Drosophila* ATPase subunit of several nucleosome-remodeling complexes, and is required for the maintenance of higher order chromatin structure. It appears that the acetylation of H4K16 interferes with ISWI's function by directly affecting its ability to interact with the nucleosome due to the modification of the histone H4 tail (Corona et al., 2002).

Through these mechanisms it is possible that acetylation of histone tails can produce a two pronged approach to up-regulation of gene regulation. Firstly, the reduction in electrostatic bond strength causes a dissociation of tails from DNA and resulting in a more open chromatin structure. Secondly, and more significantly, the acetylation of the histone tails may alter the recognition sites of heterochromatin-associated proteins and present new sites for proteins associated with gene transcription. This is most evident in the highly conserved domains in chromatin-modifiers, which bind specific chromatin modifications, such as p300/CBP Associated Factor (P/CAF), which contains a bromodomain that is crucial for it to recognise acetylated histone tails (Owen et al., 2000).

1.1.4 Histone Deacetylase

1.1.4.1 Histone Deacetylase

Histone deacetylases (HDACs) are the antagonists of HATs and have been implicated in gene repression (Pikaart et al., 1998). One role of HDACs is to deacetylate lysines on the histone tails. This restores the positive charge to the tails and increases the overall positive charge of the histone. This leads to an increase in the affinity of the DNA to the histone, and to increased stabilisation of the nucleosome via closer histone tail association (Sewack et al., 2001). Regulation of acetylation by HDACs has also been shown to be important for the formation of memory in rats. It is the imbalance of the ratio of HDACs to HATs that results in the enhanced induction of potentiation at synapses, leading to altered long-term memory formation (Levenson et al., 2004). There has also been a link drawn between HDACs and their involvement in cancer, due to their role in gene regulation (reviewed in Wade (2001)).

There are three main classes of HDACs present in mammals through to *D. melanogaster*, based on homology to the three *S. cerevisiae* HDACs. Class I HDACs (HDAC1, 2, 3, 8) are homologous to the yeast Right Parietal Dorsal 3 (RPD3), share a compact structure, and are predominantly nuclear proteins expressed in most tissues and cell lines. Class II HDACs, are homologous to the yeast Histone Deacetylase 1 (HDA1) and are subdivided into two subclasses, IIa (HDAC4, 5, 7 and 9) and IIb (HDAC6 and HDAC10), based on sequence homology and domain organisation. Whereas Class I and II HDACs and their *S. cerevisiae* orthologs, all share some degree of homology in their catalytic domain, Class III HDACs are homologous to the yeast Silent mating type Information Regulation-2 (SIR2), also known as Sirtuins, and are not related to Class I and II proteins (Verdin et al., 2003). *D. melanogaster* have only four Class I and II HDACs: *Drosophila* HDAC (dHDAC)1, dHDAC3, dHDAC4, dHDAC6 (Foglietti et al., 2006), which are named after the relative human homologues. A fourth class has been recently defined, and is present in widely divergent organisms (Gregoretti et al., 2004). At present there is only one HDAC assigned as a Class IV, HDACX (Gregoretti et al., 2004).

1.1.4.2 Histone Deacetylase *HDACX*

Drosophila histone deacetylase X, also known as *HDACX*, *dHDAC11*, or CG31119, is a particularly interesting histone deacetylase. This HDAC has become something of an enigma, with very tissue-specific expression patterns and high conservation between humans and *Drosophila*. In humans its expression is limited to kidneys, heart, brain, skeletal muscles and testes (Gao et al., 2002). In *Drosophila* it shows a 7.4-fold and 7.5-fold increase in expression in the brain and thoracicoabdominal ganglion, respectively (Chintapalli et al., 2007), relative to whole body expression. The evolutionary conservation of the protein, based on protein sequence alignment, is high, with *Drosophila* and humans sharing more than 52 % identity and 67 % similarity (Gao et al., 2002). Despite this high level of conservation, and therefore implication of importance, there has been little if any function ascribed to *HDACX* in *Drosophila* other than sequence homology to the HDAC super family (Foglietti et al., 2006).

An RNA interference screen in *Drosophila* S2 cells could find no growth phenotype or significant deregulation of gene expression when *HDACX* was knocked down, although other dHDACs did show significant alterations in gene regulation (Foglietti et al., 2006). In mice, HDAC11 is localised in the nuclei of the developing brain in a temporal and spatial pattern that correlates with the maturation of neural cells (Liu et al., 2008) There is also abundant expression on the dentate gyrus granule, which is part of the hippocampus and implicated in new memory formation related to spatial learning (Kee et al., 2007), however there is little to no expression in precursor granule neurons in the subgranule layer (Liu et al., 2008).

1.1.5 Histone Methyltransferase

1.1.5.1 Histone Methyltransferase

Histone methyltransferases (HMTs) catalyse methylation of histone N-terminal tails. HMTs use S-adenosylmethionine as a co-factor in order to carry out this methylation. As opposed to acetylation of histones, which only occur at lysine residue, HMTs can methylate histone tails at both lysine and arginine residues (for review see Trievel (2004)). In general, methyl "marks" are read by cells via proteins that have chromo, tudor, or PhD domains that selectively bind methylated lysine. For example, HP1 binds tri-methylated Histone 3 Lysine 9 which is methylated by the HMT Su(var)3-9 (Peters et al., 2002). This regulation is also implicated in long-term expression patterns, like those found on the Barr body in female mammalian cells, which maintain their transcriptionally silent state throughout the life of the organism (Peters et al., 2002).

HMTase often contain an SET (**S**u(var)3-9, **E**nhancer of Zeste, **T**rithorax) domain (Tschiersch et al., 1994). This is a conserved domain that is present in almost all HMTs, however one HMT that does not contain the SET domain, the DOT1 protein (Feng et al., 2002). This protein methylates Histone 3 at Lysine 79, which is within the globular domain of the histone (Feng et al., 2002). Though methylation was historically considered to be a repressive mark, there are several methylation marks that correlated to an increase in gene expression. For instance, all three methylation states of histone 3 lysine 4 correlate to positive expression levels in $CD4^+$ T cells (Barski et al., 2007). Further to this, differing states of methylation of a single lysine residue can markedly change its relation to gene expression. Di- and tri- methylation of histone 3 lysine 9 correlate strongly with inactivated genes, although mono-methylated histone 3 lysine 9 shows a positive correlation with active genes (Bannister et al., 2001; Barski et al., 2007)

1.1.5.2 Histone Methyltransferase *pr-Set7*

The Drosophila gene *pr-Set7*, also known as *SET8*, or CG3307 in *Drosophila*, encodes a histone methyltransferase of the Suppressor of variegation 3-9, Enhancer of zeste, Trithorax (SET) family of methyltransferases (Nishioka et al., 2002). *pr-Set7* is essential for survival in *Drosophila*, although deletion mutants survive to late second instar larvae. Further, homozygous mutants show no methylation of histone 4 lysine 20, indicating it is the primary methylase for this lysine (Nishioka et al., 2002). PR-SET7 specifically methylates histone 4 lysine 20, and more specifically mono-methylates the lysine residue (Xiao et al., 2005). The mono-methylation, as well as di- and tri-methylation, of histone 4 lysine 20 is developmentally regulated (Karachentsev et al., 2007). Mono- and tri-methylated histone 4 lysine 20 residues are present in early embryos, throughout larval and pupal stages, ovaries, and in adults. The di-methylated form of histone 4 lysine 20 is not detected in ovaries or early embryos, and only appears 4 to 8 hours through embryogenesis; it then however remains present throughout development (Karachentsev et al., 2007).

PR-SET7 is also important in cell cycle progression. In *Drosophila* larvae, tissues with higher rates of cell divisions, such as imaginal discs, are severely affected by the depletion of PR-SET7. Homozygous *pr-Set7* mutant discs are smaller than wild type because they contain only 25 % as many cells as wild type, although actual DNA content per cell is increased significantly. (Karachentsev et al., 2005). In the null *pr-Set7*^{20} allele the PR-SET7 protein is missing from the first instar larvae onwards, and the *Drosophila* survive until the transition to pupae, where a reduction of mono-methylated histone 4 lysine 20 was detected (Sakaguchi and Steward, 2007). In the mutant third instar larval brains mono-methylated histone 4 lysine 20 was strongly reduced, and progression through early mitosis was delayed. Abnormalities in the mitotic progression was rescued when the DNA damage checkpoint was abolished, this indicates that DNA damage checkpoint is activated in these *pr-Set7* mutants (Sakaguchi and Steward, 2007).

1.1.5.3 Histone Demethylase

Whereas HATs and HDACs dynamically regulate histone acetylation, histone methylation has been considered a rather permanent modification. Shi *et. al.* (2004) described the first histone demethylase (HDM), Lysine Specific Demethylase (LSD1). It has been shown that LSD1 has a *Drosophila* homologue, su(var)3-3, which is capable of demethylating mono- and di-methylated histone 3 lysine 4 (Rudolph et al., 2007). Further to this, Rudolph *et. al.* (2007) also showed that this function was important in the regulation of euchromatin and heterochromatin boundaries in early development (Rudolph et al., 2007). Subsequently, other HDMs have been discovered in *Drosophila*, such as *Drosophila* G9a, which demethylates histone 3 lysine 9 (Kato et al., 2008), and *Drosophila* KDM2 with targets di-methylated histone 3 lysine 36 (Lagarou et al., 2008). With the increase in our understanding of the control of gene expression at the epigenetic level, the complex nature of higher functions in organisms can started to be elucidated.

1.2 Memory

1.2.1 Memory Overview

Memory is the retention and recollection of knowledge and experience. Recently acquired knowledge is stored in short-term memory. If that knowledge is reinforced through repetition, it is consolidated into long-term memory (LTM). The latter is modified over time with either the acquisition of new information and further reinforcement of the synaptic circuits or through disuse, and pruning of such circuits (Hubel et al., 1977; Lichtman and Colman, 2000). The process of consolidation of learning and memory is very crucial to the survival of organisms and there is great interest in understanding the underlying mechanism of this process. To achieve this, a popular strategy is to use the simpler and more easily manipulated nervous systems of invertebrates to generate information that can be applied to the more complex nervous systems of vertebrates (Ito et al., 1998; Kandel, 2001; Isabel et al., 2004).

From the study of memory formation in *Drosophila melanogaster* it has become apparent that memory is composed of two pathways that are genetically distinct, and function independently of each other (Tully et al., 1994; Shirahata et al., 2006). These two components are short-term memory (STM) and long-term memory (LTM). STM is short-lived, with no detectable memory after one or two days, where as LTM, as the name suggests, lasts for longer periods of time, often with no appreciable reduction in function over seven days (Tully et al., 1994). Short-term memory is a transient phenomenon, isolated in the cytoplasm of the neuronal cells, which requires no alteration of gene expression. The formation of long-term memory, by contrast, requires a change in gene expression. It has been shown that long-term memory consolidation is susceptible to protein synthesis inhibitors, such as cyclohexamide (CXM) (Gong et al., 1998). Therefore chromatin-modifying complexes may play an integral part in the formation of LTM.

1.2.2 Long-Term Memory Consolidation

Studies of implicit memory in the Californian sea slug, *Aplysia californica*, and explicit memory in mice, show that STM and LTM storage is a result of distinct phases of synaptic plasticity within the neurons (Guan et al., 2002). Implicit memory is the recollection of previous experiences that adds to a current task without conscious recollection, whereas explicit memory is the conscious, intentional, recollection of a previous experience.

The signaling pathway that is crucial for the conversion of STM to LTM is also critical for the conversion of short-term and long-term phases of synaptic plasticity. The pathway is highly conserved from *Aplysia californica* to humans (Guan et al., 2002). The pathway involves activation of the cAMP-dependent protein kinase and p42 MAP kinase, their translocation to the nucleus and induction of gene expression. The expression cascade initiates with the activation of c-AMP response element-binding protein 1 (CREB1) and the removal of repression by CREB2. CREB1 also induces the CAAT box enhancer binding protein (C/EBP), leading to *de novo* synapse formation and an increase in synaptic strength (extensively reviewed in Kandel 2001).

At the cellular level, long-lasting synaptic plasticity depends on CREB-mediated gene transcription and subsequent structural and functional modification of relevant synapse. How this synaptic plasticity is actually achieved downstream of the CREB-mediated transcription is not clear, but appears to involve the staufen/pumilio mRNA transport pathway (Dubnau et al., 2003).

1.2.3 Mushroom-Bodies

In *Drosophila melanogaster* there are distinct bilateral brain structures termed the mushroom-bodies (MBs) (Figure 1.1). These MBs are formed and rearranged sequentially during embryonic and post-embryonic development (Armstrong et al., 1998; Nassif et al., 1998; Lee et al., 1999). The adult *Drosophila* MBs are a pair of easily recognisable neuropils comprised of approximately 5000 neurons, called Kenyon cells, running on either side of the central complex from back to front and downward through the protocerebrum (Heisenberg, 1998). Three sets of neuronal bundles make up five lobes on each half of the MBs (Figure 1.1). Two sets branch to give rise to a vertical and a medial lobe, the α/β and the α'/β', respectively (Figure 1.1). The third neuronal bundle makes up the medial γ lobe (Crittenden et al., 1998; Lee et al., 1999). Axons extending from the Kenyon cells that form these lobes also extend into the regions of the forebrain. Conversely regions of the forebrain also extend axons into the vertical and medial lobes of the MBs (Ito et al., 1998). This unique structuring of the *Drosophila* brain indicates that these lobes have distinct functions (Pascual and Preat, 2001).

1.2.3.1 Mushroom-Body Development

Neurons projecting into the γ lobe of the adult MB develop first, prior to the mid-third instar larval stage. Neurons projecting into the α'/β' lobes develop between the mid-third instar larval stage and pupa formation. Finally, neurons projecting into the α/β lobes develop after pupae formation (Lee et al., 1999). During the larval stage, axons of all MB neurons bifurcate into both the dorsal and medial lobes. Shortly after pupa formation larval MB neurons are selectively pruned according to the order of their development. Degeneration of axon branches means γ lobe neurons retain only their main processes in the peduncle, which then project into the adult γ lobe without bifurcation (Lee et al., 1999). In contrast, the basic axon projections of the α'/β' lobes are preserved during metamorphosis. (Lee et al., 1999).

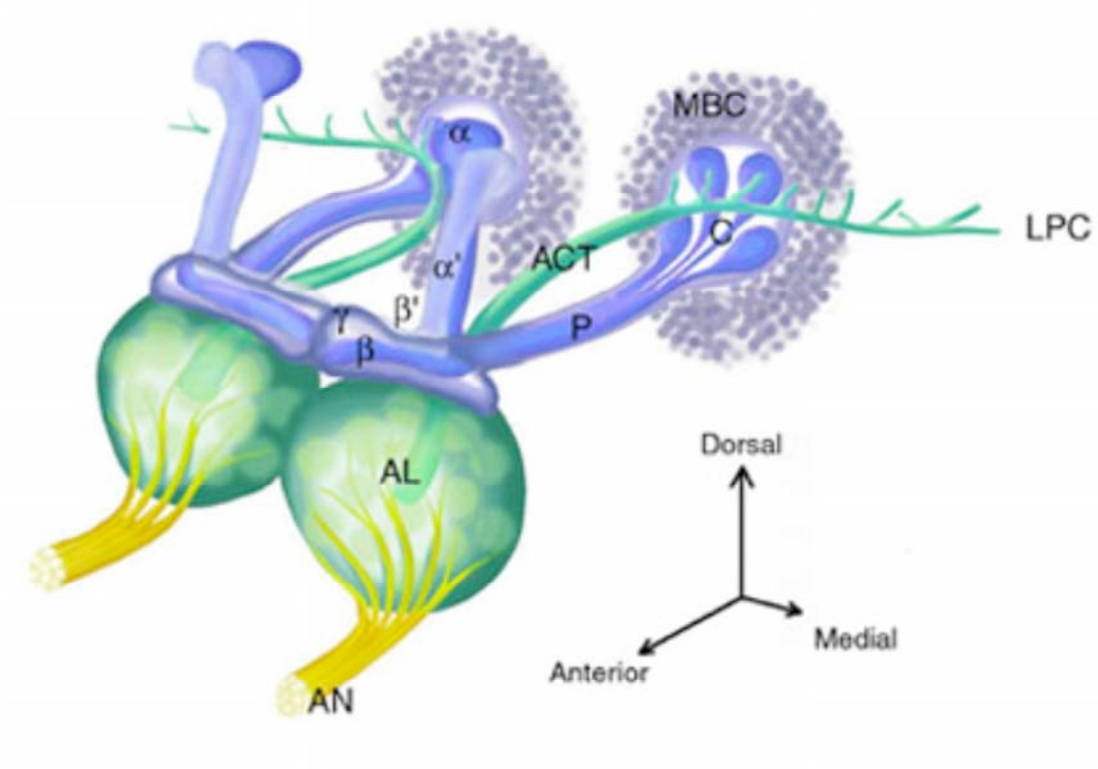

Figure 1.1 Diagram of the *Drosophila* Mushroom-Bodies

Diagram of the *Drosophila* mushroom-bodies. The α/β are α'/β' and γ are indicated. The antennal nerve (AN) and antennal lobe (AL) are seen in yellow and green respectively. The mushroom-body cell bodies (MBC) called Kenyon Cells, are in grey, feed into the calyx (C) and extend axons into the peduncles (P). The antennal cerebral tract (ACT) transmits olfactory information from the antennal lobe to the calyces. The ACT proceeds laterally to synapse with other neurons in the lateral protocerebrum (LPC). Diagram to the right of mushroom-bodies indicates the mushroom-bodies orientation within the *Drosophila* head. ACT and LPC are not discussed in this introduction. Figure from McGuire et al., 2001.

1.2.3.2 Mushroom-Bodies and Long-Term Memory Function

The MBs of *Drosophila* are important for olfactory learning and memory (Han et al., 1992). Genetic and chemical disruption of the MBs produces flies that are normal for general behaviors but are defective in olfactory learning (de belle and Heisenberg, 1994; Pascual and Preat, 2001). Many genes involved in olfactory learning and memory show enriched expression in the MBs, particularly those encoding components of the cyclic adenosine mono-phosphate signaling pathway. Interestingly restoring the *rutabaga* gene product, which is an adenylyl cyclase, specifically to the MBs of *rutabaga* mutants is sufficient to restore short-term memory in these flies (Zars et al., 2000).

Pascual and Preat (2001), alerted by the distinct architectures of the MBs and the axonal positioning of lobes within distinct regions of the forebrain, used the *alpha-lobes-absent* (*ala*) mutant to elucidate the distinct region necessary for LTM. The phenotype has absentee α/α' lobes, however this mutant does not always have complete loss of α/α', approximately 10 % of cases have all five lobes present, and more than 35 % lack the β/β' lobes also. With these different phenotypes it was possible to show that the vertical lobes of the mushroom-bodies were required for LTM. It was also shown that it was necessary to have the medial lobes present for LTM (Pascual and Preat, 2001). Further to this, STM memory was normal without either vertical or the medial lobes (Pascual and Preat, 2001).

Subsequent experiments on the different MB lobes at a higher resolution have allowed more detailed analysis of their individual function (McGuire et al., 2001; Krashes et al., 2007). McGuire *et al.* (2001) showed through the inhibition of neurotransmitters in the MBs that synaptic transmission in the α/β lobes was necessary for the memory retrieval, but not during acquisition or consolidation. Work by Krashes *et al.* (2007) has further elucidated the roles of separate lobes in memory formation. Using a similar system to block neurotransmitters as that use by McGuire *et al.*, they showed that synaptic transmission in the α'/β' lobes was required during and after training to acquire and stabilise memory (Krashes et al., 2007).

1.2.4 Assays for Long-Term Memory

It is well established that *Drosophila* have long-term memory (McGuire et al., 2006), and also have distinct behaviours that can be quantified (Sakai et al., 2004). These two attributes and the well establish protocols for genetic manipulation make *Drosophila* invaluable for the study of LTM. By disrupting genes in the mushroom-bodies of *Drosophila*, effects on LTM can be quantified, and thus elucidate the mechanisms of LTM.

1.2.4.1 Olfactory Conditioning Assay

Drosophila can form associative memories, where one stimulus is associated to another stimulus. The olfactory conditioning assay exploits this by placing flies in a copper lined tube, where they are exposed to an odour (Odour A), and are given a series of electric shocks. Flies are then exposed to a second odour (Odour B), which is not coupled with a series of electric shocks. The flies are then rested, and subsequently exposed to both odour A and odour B in a T-maze; flies with intact memory will avoid Odour A (McGuire et al., 2006). Flies with disrupted long-term memory function will show no preference for either odour.

1.2.4.2 Courtship Conditioning Assay

Drosophila males have characteristic courtship behaviours, including orienting themselves towards the female, following female movement, tapping the female abdomen with their forelegs, and vibrating their wings to generate a courtship song. A virgin male paired with a non-virgin female will reduce his courtship behaviour after repeated rejection by the female (conditioning). Subsequent exposure to females by the males, even to virgin females who would be receptive to courtship, show a reduction in their courtship (Sakai et al., 2004). This behaviour can be used to assay for effects in long-term memory. By disrupting genes that may be involved in memory function, flies show an inability to learn from repeated rejection from non-virgin females, and continue to court at the same rate even after three to seven days of their conditioning when presented with a virgin female.

1.2.5 Histone Acetylation during Memory Formation

With the implication of multiple gene regulatory events involved in memory formation, chromatin-modifying complexes such as HATs are also suspected of being involved in memory formation (Levenson et al., 2004). Increased acetylation of histone H3 in the CA1 region of the rat hippocampus was regulated in context with fear conditioning. Addition of the HDAC inhibitor sodium butyrate enhanced long-term potentiation at synapses in the CA1 area. Furthermore, animals injected with sodium butyrate prior to fear conditioning enhanced formation of long-term memory (Levenson et al., 2004). Further to this, Guan *et. al.* (2002) have shown in *Aplysia* that neurons receiving facilitatory signals recruit CREB1 and HATs, whereas inhibitory signals induce CREB2 and HDAC5, which displace CREB1 and inhibit memory formation (Guan et al., 2002). This indicates that heterochromatin undergoes structural alteration during the formation of long-term memory, and that histone acetylation plays an integral part.

1.3 RNA Interference

1.3.1 RNA interference

RNA interference (RNAi) results in the targeted down-regulation of gene expression (knockdown), and is triggered by double-stranded RNA (dsRNA)(for review see Hannon (2002)). RNAi was first discovered in *Caenorhabditis elegans* as a response to dsRNA, which resulted in sequence specific gene silencing (Fire et al., 1998). The dsRNA is at least ten-fold more potent in silencing a specific gene than either sense or anti-sense RNA alone. In addition to this, even a few dsRNA molecules per cell in a parental organism triggered gene silencing in F_1 progeny.

1.3.2 Molecular Mechanism of RNAi

The molecular mechanism by which RNAi acts (Figure 1.2) was elucidated by the discovery that injection of dsRNA into *Drosophila* embryos induced silencing at the post-translational level, and that embryonic extracts were also RNAi competent (Turner, 1998). The nuclease responsible was isolated from *Drosophila* S2 cells, and termed RNA-induced silencing complex (RISC) (Hammond et al., 2000). Long dsRNA transcripts are processed into ~22 nt fragments, the fragments also contained 5′-phosphylated termini, a 2 nt 3′-overhang, and the processing is ATP-dependent (Zamore et al., 2000). The enzyme involved in the processing of the dsRNA into siRNA is an RNase III enzyme containing dual catalytic domains, a helicase domain, and PAZ domain, known as Dicer (Bernstein et al., 2001). The PAZ domain is a ~110 residue conserved region present in Piwi, Argo and Zwille/Pinhead proteins. Once Dicer has processed the siRNA, it induces RNAi via the RISC complex. The siRNA is loaded into the RISC complex; this then guides the complex to mRNA via Watson-Crick base-pairing. The RISC precursor is ~250 kDa, which upon activation forms ~100 kDa complex that cleaves substrate mRNA via endonuclease activity. Cleavage occurs only in the region homologous to the siRNA (Bernstein et al., 2001).

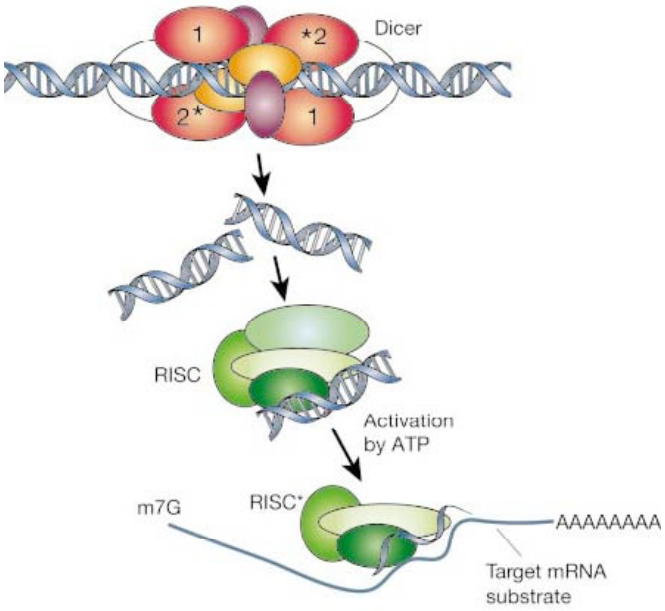

Figure 1.2 Mechanism of Dicer/RISC mediated RNAi

RNAi is initiated by the Dicer enzyme (two Dicer molecules with five domains each are shown), which processes dsRNA into ~22 nt siRNAs. Cleavage into precisely sized fragments is determined by the fact that one of the active sites in Dicer is defective (*), shifting the periodicity of cleavage from ~9-11 nt to ~22 nt. The siRNAs are loaded into RISC (green). RISC needs to be activated by unwinding of the siRNAs. RISC then uses the siRNA to target sequence specific mRNA for degradation. Figure from (Hannon, 2002).

1.4 GAL4 Responsive Promoter

To date, the most widely used system in *Drosophila* for achieving spatially restricted gene expression is the yeast GAL4 upstream activation sequence (UAS) system (Brand and Perrimon, 1993). A *P* element carrying the yeast transcription activator GAL4 is randomly inserted within the genome, trapping the expression of GAL4 under the control of endogenous tissue-specific enhancers. A target transgene containing a minimal promoter and an UAS multimer is then transformed into separate fly lines. To carry out the induction, these two lines are crossed and within the offspring the transgene is expressed in the same fashion as the GAL4 activator. There are a number of advantages to this system. Firstly, the GAL4 activator and transgene are carried in separate fly lines, permitting viable fly lines even when the transgene is toxic. Secondly, generated GAL4 lines can be used to drive any $GAL4_{UAS}$ transgene, conversely, once a $GAL4_{UAS}$ transgene is generated the transgene can be expressed in a variety of tissues.

1.4.1 Mushroom-Body Specific Drivers

Mushroom-body specific drivers are GAL4 expressing drivers that have been reported to express GAL4 in the mushroom-bodies. Three of these lines were used in this thesis; MB247, MBc739, and MBc772.

Pavlopoulos *et al.* (2008) have reported, using a UAS-*LacZ* reporter and immunostaining, that the MB247 and MBc772 drivers direct expression of GAL4 in peripheral neurons of the α/β lobes, with much lower expression in the γ lobes, in contrast, c739 was expressed in internal neurons of the α/β lobes, complementary to that of c772 and MB247 (Pavlopoulos et al., 2008). The expression pattern of MB247 is corroborated by Tanaka *et al.* (2008) who used a UAS-GFP to visualise the expression pattern, and also found that MB247was expressed in the α/β neurons and not the α′/β′ (Tanaka et al., 2008).

1.5 Site-Specific Integration Using Phage ϕC31 Intergrase

Transformation by *P*-element integration has been a powerful tool to study gene function (Rubin and Spradling, 1982). However, due to the random integration of the *P*-element, position effects can strongly influence the gene expression, which in turn can complicate analysis (Levis et al., 1985). The site-specific intergrase from phage ϕC31 requires no cofactors and mediates recombination between the *attB* and *attP* sites, to create a stable transformant (Thorpe and Smith, 1998).

To this end, a *P*-element vector can be transformed into *Drosophila* carrying an *attP* site and supplemented with the ϕC31 recombinase. It is possible to subsequently transform a vector into that site if that vector is carrying the *attB* site. This mechanism allows for many different vectors or gene constructs to be inserted into the same position, therefore removing any position effects and allowing for consistent analysis (Groth et al., 2004).

1.6 Experimental Overview

1.6.1 Aim

The aim of this study is to investigate the role of two specific chromatin-modifying proteins in *Drosophila* in long-term memory.

1.6.2 Genes of Interest

1.6.2.1 *Drosophila* Histone Deacetylase HDACX

Drosophila HDACX (CG31119), is an almost completely unstudied protein in *D. melanogaster*. It contains a conserved HDAC domain and it has a novel human homologue HDAC11 (Gao et al., 2002). It is the only Class IV HDAC, therefore it may have distinct physiological roles to that of other known HDACs. *HDACX* shows a 7.4-fold and 7.5-fold increased expression in the brain and thoracicoabdominal ganglion respectively (Chintapalli et al., 2007) relative to whole flies.

1.6.2.2 *Drosophila* Methyltransferase *pr-Set7*

Drosophila PR-SET7 (CG3307), is a histone lysine methyltransferase that is associated with heterochromatin and gene silencing, and is known to methylate lysine 20 on histone 4 (H4K20). Mutations of prSet7 are lethal; second instar larval death shows a direct correlation to the loss of H4K20, indicating *pr-Set7* has a fundamental role in development (Nishioka et al., 2002).

1.6.3 Hypothesis

That reduction of CG31119 or CG3307 transcript levels in adult mushroom-bodies of *Drosophila* will cause a disruption in long-term memory function.

1.6.4 Project Objectives

1. To confirm that the published GAL4 drivers express GAL4 in the mushroom-bodies, using fluorescent protein reporter under the control of UAS_{GAL4} promoter.

2. To make RNAi constructs targeted specifically to CG31119 and CG3307 gene transcripts under GAL4 spatial control. Transform *Drosophila melanogaster* with these gene constructs and cross to appropriate GAL4 driver line.

3. To quantify the levels of RNAi-mediated knockdown of CG31119 and CG3307 transcript using qRT-PCR.

4. To use courtship conditioning to assay the effects these knockdowns have on long-term memory

Chapter Two

Materials and Methods

2.1 Chemicals and Enzymes

The following were purchased from New England BioLabs: ATP, BSA, CIP, *Eco* RI, *Xba* I, *Nsi* I, *Bam* HI , *Bgl* II, *Nhe* I, *Mfe* I, *Nru* I, *Sac* I, *Xho* I, *Fsp* I, *Afl* I, *Bst* BI, T4 DNase Ligase, T4 polymerase, and T4 PNK.

2.2 Buffers and Solutions

All buffers and solutions were prepared according to Sambrook *et. al.* (1989) or Ashburner (Ashburner, 1989).

2.3 Culture Media

The following media was prepared according to methods described in Sambrook *et al.* (Sambrook et al., 1989): SOB, SOC, LB, and Terrific Broth. Where required, ampicillin (100 mg/mL) was added to a final concentration of 50μg/mL. For blue/white selection in sub-cloning with applicable vectors, X-Gal was used as a substrate.

2.4 Bacterial Strains

The *Escherichia coli* strains DH5α, with the genotype FΦ80*lac*ZΔM15Δ(*lac*ZYA-*arg*F) U196 *deo*R *rec*A *end*A1 *hsd*A1 *hsd*R1 (r_k^-, m_k^+) *pho*A *sup*E44 λ^- *thi*-1 *gyr*A96 *rel*A1, were used for all preliminary transformations. The final sub-cloning step of the completed inverted repeat constructs were transformed into Stbl2™ cells, with the genotype F^- *mcr*A Δ(*mcr*BC-hsdRMS-*mrr*) *rec*A1 *end*A1*lon gyr*A96 *thi sup*E44 *rel*A1 λ^- Δ(*lac-pro*AB).

2.5 Chemically Competent Cells

DH5α *E. coli* chemically competent cells were made as described in (Inoue et al., 1990). Stbl2™ chemically competent cells were made using a modified method (Section 2.5.1).

2.5.1 Modified Method for Creating Chemically Competent Stbl2™ Cells

Stbl2™ chemically competent cells were made using a modified method of (Inoue et al., 1990). Terrific Broth was used in place of LB. Transformation Buffer was made according to (Inoue et al., 1990). Frozen stocks of Stbl2™ in glycerol were streaked on a Terrific Broth agar plate, and cultured for ~36 hrs at 30 °C. Several large colonies were inoculated into 250 mL of SOB medium in a baffled 2 L flask, and grown to an A_{600} of 0.6 at 22 °C. The rest of the protocol was carried out according to (Inoue et al., 1990).

2.6 Culture Storage

Transformed bacterial cultures were incubated at 37 °C for 12-15 hrs in 5 mL of LB media containing 50 μg/mL of ampicillin at 200 rpm. 850 μL of this culture was added to a cryotube (Cryovial, Simport Plastics, inc.) with 250 μL of glycerol. Cultures were quickly frozen in liquid nitrogen. Storage was at -80 °C.

2.7 Isolation of Nucleic Acids

2.7.1 RNA

All solutions and equipment for use with RNA were prepared in an RNase-free manner. All solutions except those containing Tris, SDS, or solvents, were treated with DEPC according to Sambrook *et. al.* (1989).

2.7.2 Small-Scale Preparations of Plasmid DNA

The procedure outlined in Sambrook *et. al.* (1989) for isolation of plasmid DNA from bacterial cultures was used. Plasmid DNA was also isolated using QIAPrep® Spin Miniprep Kit (Qiagen) according to manufacturer's instructions.

2.7.3 Large-Scale Preparations of Plasmid DNA

Larger scale plasmid DNA preparations from bacterial cultures were preformed using the QIAGEN® Plasmid Midi Kit (Qiagen) according to the manufacturer's instructions.

2.7.4 Isolation of Genomic DNA

Genomic DNA was isolated as described in Ashburner (1989).

2.7.5 Isolation and Purification of Total RNA

50 mg of eggs, larvae, whole adult flies, or fly heads were homogenised in 500 μL of TRIzol® reagent (Invitrogen) in a 2 mL Kontes Glass homogeniser, and transferred to a 1.5 mL microfuge tube and incubated at room temperature for 10 min. 200 μL of chloroform was added, mixed vigorously for 15 sec, and incubated for 5 min at room temperature, followed by centrifugation at 12,000 g for 10 min. The upper aqueous layer was transferred to a fresh tube, to which was added 500 μL of isopropanol. After 10 min incubation at room temperature, the RNA was pelleted by centrifugation at 12,000 g for 15 min. The pellet was washed in 75 % (v/v) ethanol, re-centrifuged at 7,500 g for 10 min, and air dried for 10 min at room temperature. RNA was re-suspended in 150 μL of DEPC treated dH_2O (Section 2.7.1). 150 μL of phenol:chloroform:isoamyl alcohol (25:24:1) was added, the mixture was then shaken vigorously for 15 sec, and centrifuged at 12,000 g for 15 min. 125 μL of upper aqueous layer was transferred to a fresh 1.5 mL microfuge tube was combined with 125 μL of chloroform and centrifuged again at 12,000 g for 15 min. 100 μL of the aqueous upper layer was transferred to a fresh 1.5 mL microfuge tube with 400 μL of 100 % ethanol and 10 μL of 3 M sodium acetate. RNA was precipitated for at least 6 hrs at -20 °C.

RNA was then pelleted at 12,000 g for 15 min, washed with 75 % ethanol (v/v), centrifuged for a further 15 min at 12,000 g, and air dried for 10 min at room temperature. The pellet was re-suspended in 50 μL of DEPC treated dH_2O and stored at -80 °C.

2.7.6 DNase Treatment of Total RNA

30 μg of total RNA was added to 5 μL of 10 x TURBO™ RNase-free DNase Buffer (Roche), 3 μL of TURBO™ RNase-free DNase (Roche), and DEPC treated dH_2O to a volume of 50 μL. The reaction mixture was incubated for 1 hr at 37 °C. 100 μL of DEPC treated dH_2O was added to the mix and then heated for 20 min at 65 °C to inactivate the DNase. The DNA-free RNA was extracted with organic solvents and ethanol precipitated as described in Section 2.7.5. The final volume of re-suspended RNA was adjusted to 10 μL.

2.7.7 Gel Extraction

The QIAquick® Gel Extraction Kit (Qiagen) was used according to the manufacturer's instructions.

2.7.8 PCR Purification

The QIAquick® PCR Purification Kit (Qiagen) was used according to the manufacturer's instructions.

2.8 Nucleic Acid Quantification

Plasmid and genomic DNA as well as total and DNase treated RNA samples were quantified using a NanoDrop® ND-1000 Spectrophotometer (BioLabs) with NanoDrop Version 3.1.0 software (BioLabs).

2.9 DNA Sequencing

2.9.1 Sequencing

DNA samples where prepared according to Section 2.7. Samples were diluted to appropriate concentrations, according to operator's instructions. If required sequencing primers were added to appropriate concentrations. DNA was sequenced by the Allan Wilson Centre Genome Service, Massey University, Palmerston North. Sequencing was preformed with an ABI 3730 Automated Sequencer (Applied Biosystems), using BigDye™ Terminator Version 3.1 Ready Reaction Cycle Kit (Applied Biosystems) according to manufacturers instructions.

2.9.2 Sequence Analysis

Sequences were compiled and edited using Sequencer 4.5 (Gene Codes Corporation)**.** Completed sequences were compared with the public genomic database NCBI (http://blast.ncbi.nlm.nih.gov/Blast.cgi) using the BLAST algorithm (Altschul et al., 1990). Primers used for sequencing are listed in Table 2.1.

Sequence analyses and plasmid map creation was done using MacVector™ 7.2.3 or 10.0 software (Accelrys Incorporated).

Name	Sequence	Size (nt)	Comment
RNAiCS2Plus	5′-AAGCGACTCCCACTTACCTG-3′	20	Sequencing pUASp-NBa-CS2-BgX out from CS2 intron into MCS
RNAiCS2Minus	5′-CTCCGCAAATACCGCATTGG-3′	20	Sequencing pUASp-NBa-CS2-BgX out from CS2 intron into MCS
PlusCS2Plus	5′-CAATCACTGGTAATCGCAAG-3′	20	Sequencing pUASp-NBa-CS2-BgX out from MCS into promoter region
2ndCS2Minus	5′-CTCCCCGAAAAGGACGAAAC-3′	20	Sequencing pUASp-NBa-CS2-BgX out from MCS into K10 terminus region
attBNsiIRNAiF	5′-AATGCGTCGTTTAGAGCAGCA-3′	21	Sequencing and screening colonies for attB insert into pUASp-NBa-CS2-BgX
attBNsiIRNAiR	5′-TGTGACCTGTTCGGACTGATT-3′	21	Sequencing and screening colonies for attB insert into pUASp-NBa-CS2-BgX
Pwht1	5′-GTAACGCTAATCACTCCGAACAGGTCACA-3′	29	Forward primer for inverse PCR
Plac1	5′-CACCCAAGGCTCTGCTCCCACAAT-3′	24	Reverse primer for inverse PCR

Table 2.1 Oligonucleotide primers for Sequencing and iPCR

2.10 Polymerase Chain Reaction

2.10.1 PCR

PCR was used for DNA amplification and gene isolation, with the following typical PCR reaction mix was used: 1 μL DNA, 1 μL of each primer (Sigma-Aldrich) at 10 mM, 1 μL of deoxyribonucleoside triphosphates at 10 mM (Roche), 2.5 μL PCR Buffer containing magnesium (Roche), 0.25 μL *Taq* DNA polymerase (Roche), and 18.25 μL dH_20. Standard cycling conditions consisted of an initial denaturation step at 94 °C for 2 min, followed by 35 cycles consisting of 1 min at 94 °C, annealing temperature for 1 min, and extension at 72 °C for 2 min. The final extension was at 72 °C for 10 min, and then cooled to 4 °C. Primer used in PCR are listed in Table 2.2.

2.10.2 PCR on Colony

When applicable, a single colony was isolated using a sterile toothpick and suspended in 20 μL of H_20. The suspended colony was heated at 94 °C for 10 min to lyse bacterial cells; 1 μL of the solution was then used as the DNA source for PCR (Section 2.10.1).

2.10.3 cDNA Synthesis

DNase treated total RNA (section 2.7.5) was reverse transcribed using Expand reverse transcriptase (Roche), with added dNTPs, according to the manufacturer's instructions. Random N_6 oligo (Roche) were used to prime cDNA synthesis.

2.10.4 Inverse PCR

Inverse PCR using primers for *P*-element vectors was conducted according to BDGP iPCR protocol (www.fruitfly.org). The primer sequence used for inverse PCR and sequencing of the resulting PCR product are described in Table 2.1.

Name	Gene Sequence	5′- restriction tag	Total Size (nt)	Gene Position
HDACXbaIF	5′-TTCAGCGTTCCTATTTGCGACCC-3′	XbaI – 5′-TCTAGA-3′	29	367-389
HDACBamHIR	5′-ACCCCTGCGGATGCCTTCAAGTAG-3′	BamHI – 5′-GGATCC-3′	30	985-962
prSet7XbaIF	5′-CCCACCAAAGCCTCCAGCATAAAG-3′	XbaI – 5′-TCTAGA-3′	30	1104-1127
prSet7BamHIR	5′-GAAGAAGTCCGTCATCTCACGATTGC-3′	BamHI – 5′-GGATCC-3′	32	1868-1843
MSL2XbaIF	5′-CCCAAAACCACACACAGGAGTTCATTCG-3′	XbaI – 5′-TCTAGA-3′	32	751-776
MSL2BamHIR	5′-GCGTCTTCAACGGTCTCTTCAACCAG-3′	BamHI – 5′-GGATCC-3′	32	1460-1435
LacZXbaIF	5′-AACCGTCACGAGCATCATCCTCT-3′	XbaI – 5′-TCTAGA-3′	29	1063-1086
LacZBamHI	5′-CGCCAAAATCACCGCCGTAAG-3′	BamHI – 5′-GGATCC-3′	27	1780-1760

Table 2.2 Oligonucleotide primers used for PCR

2.10.5 Quantitative Real-Time PCR

Quantitative real-time PCR was conducted using the LightCycler 480 SYBR Green I (Roche) reaction master mix in a LightCycler 480 Instrument (Roche) according to manufacturer's instructions. 1 μL of template, 5μL of LightCycler 480 SYBR Green I (Roche), 0.5 μL of each primer (10 μM) and 3 μL of PCR grade dH_2O was added to each well. A typical assay consisted of 10-fold dilution of cDNA in triplicate and a sample without reverse transcriptase. To establish primer efficiency a series of 5-fold, 10-fold, 50-fold, and 100-fold dilutions, or 10-fold, 50-fold, 100-fold, and 500-fold dilutions, depending on the native concentration of the transcripts, was prepared and analysed. Each cDNA sample was assayed in triplicate. The LightCycler protocol used is described in Table 2.3. Crossing points were automatically determined by the LightCycler 480 software (Roche). Results were analysed using the LightCycler 480 software (Roche). Primers used for qRT-PCR are listed in Table 2.4.

2.11 Agarose Gel Electrophoresis

1 x loading dye was added to each sample, then loaded into 0.8-2.0 % agarose gel, and run at 50-120 volts. With each gel 10 μL of 1 kb Plus ladder (invitrogen) was loaded to either side of the set of samples being run. Gels were stained with 0.5 μg/mL ethidium bromide for 15 minutes on a shaker at ~30 rpm. Gels were visualised under a short wave ultra violet light using the GelDoc 2k (Bio-Rad) and Quantity One software (Bio-Rad).

2.12 Enzymatic Manipulations

2.12.1 Analytical Restriction Digestions

Plasmid DNA (Section 2.7.2) was digested using 1 μg of DNA, 5-10 Units of each restriction enzyme, 1 X reaction buffer, 100 μg/mL BSA (where applicable), dH_2O to a total volume of 10 μL. The reaction was incubated in a water bath at the appropriate temperature for 1-3 hours. The reaction was stopped by heat inactivation at 65 °C for 20 minutes.

Program:	**Denaturation**		**Cycles: 1**
Segment nuimber	*Temperature (°C)*	*Hold Time (s)*	*Acquisition Mode*
1	95	600	None
Program:	**Amplification**		**Cycles: 45**
1	95	10	None
2	57	10	None
3	72	20	Single
Program:	**Melting Curve**		**Cycles: 1**
1	97	60	None
2	65	15	None
3	95	0	Continuous
Program:	**Cooling**		**Cycles: 1**
1	40	30	None

Table 2.3 LightCycler 480 protocol used for Quantitative Real-Time PCR

Name	Sequence	Size (nt)	Gene Position	Primer Pair Efficiency
HDAC11qRTPCR2F	5′-GAGGAGGTTGTCTGGGT-3′	17	48-64	1.838 ± 0.024
HDAC11qRTPCR2R	5′-GCACAGGAGCTTGTGAAT-3′	18	200-183	
prSet7qRTPCR2F	5′-ATTGAGAACTTCTTCAAAGCC-3′	21	466-486	1.909 ± 0.0638
prSet7qRTPCR2R	5′-TCTGCCAGCTTTAGCAC-3′	17	623-607	
MSL2qRTPCR2F	5′-GGTCATGTGCAAACAGAAT-3′	19	1603-1621	1.912 ± 0.044
MSL2qRTPCR2R	5′-CGGGTTCTCTTTCGCTT-3′	17	1772-1756	
rp49-596F	5'-CGGTTACGGATCGAACA-3	17	579-596	1.963 ± 0.0137
rp49-720R	5'-CGATCTCGCCGCAGTAAA-3	18	720-738	

Table 2.4 Oligonucleotide primers used for Quantitative Real-Time PCR

2.12.2 Preparative Restriction Digestions for Cloning

Restriction digests used in cloning steps consisted of 5-10 μg of DNA 30-50 Units of each restriction enzyme, 1 X reaction Buffer, 100 μg/mL BSA (where applicable) and dH_20 to 25 μL. The reaction was incubated for at least 3 hrs. The reaction was stopped by heat inactivation at 65 °C for 20 minutes.

2.12.3 Dephosphorylation of 5′ Ends

Calf Intestine Alkaline Phosphatase (CIP) was used to remove 5′ phosphate groups from linearised plasmid preparations. A typical reaction consisted of 5-10 μg DNA, 1X supplied buffer, 5-30 Units of CIP, and dH_2O up to 15 μL. The reaction was incubated at 37 °C for 60 minutes.

2.12.4 Phosphorylation of 5′ Ends

T4 Polynucleotide Kinase (T4 PNK) was used to add 5′ phosphate groups to PCR products for ligation (Section 2.10.). The reaction consisted of up to 2 μg of DNA, 1 μL ATP, 1 x T4 PNK Buffer, and 10 Units of T4 PNK. The reaction was incubated at 37 °C for 30 minutes.

2.12.5 Blunt End Formation

Digested DNA (Section 2.12.2) with cohesive ends was treated with T4 DNA polymerase to form blunt ends. The reaction consisted of 1-4 μg of DNA, 1X T4 DNA polymerase Buffer, 5 pmol dNTPs, and dH_20 to 40 μL. The reaction was incubated at 12 °C for 20 minutes.

2.12.6 Ligation

A typical ligation reaction consisted of 200 ng of vector and a 3-fold molar excess of insert. 1 μL of T4 ligase (400 units), 1X T4 DNA Ligase Buffer, and dH_20 to a total volume of 10 μL. The reaction was incubated at 16 °C overnight.

2.12.7 Transformation of DH5α Chemically Competent Cells

Transformation of DH5α chemically competent cells was carried out as in Sambrook *et. al.* (1989) with some modification. 5 μL of the ligation reaction (Section 2.12.6) was added to 100 μL of chemically competent cells (Section 2.5) and incubated for 30 minutes on ice. The cells were heat shocked at 42 °C for 45 seconds, 800 μL of LB was added, and the cells shaken at 200 rpm for 45 minutes at 37 °C. After the incubation, cells were centrifuged at 6,000 rpm for 5 minutes in a Biofuge pico centrifuge. The supernatant was discarded and the pellet was re-suspended in 200 μL of fresh LB. 180 μL and 20 μL were plated onto two LB Amp plates. Plates were incubated overnight at 37 °C. Plates were then stored at 4 °C.

2.12.7.1 Transformation of Stbl2™ Chemically Competent Cells

Transformation of Stbl2™ chemically competent cells was carried out as in Sambrook *et. al.* (1989) with some modification. 5 μL of the ligation reaction (Section 2.16.6) was added to 100 μL of chemically competent Stbl2 cells (Section 2.5.1) and incubated for 30 minutes on ice. The cells were heat shocked at 42 °C for 45 seconds, 800 μL of Terrific Broth was added, and the cells shaken at 200 rpm for 45 minutes at 30 °C. After the incubation, cells were centrifuged at 6,000 rpm for 5 minutes in a Biofuge pico centrifuge. The supernatant was discarded and the pellet was re-suspended in 200 μL of fresh Terrific Broth. 180 μL and 20 μL were plated onto two Terrific Broth Amp plates. Plates were incubated for ~36 hr at 30 °C. Plates were then stored at 4 °C.

2.13 *Drosophila* Care and Manipulation

Normal *Drosophila* stocks were raised on standard cornmeal agar (Section 2.13.2) sprinkled with yeast granules and incubated at 18 °C, 21 °C, or 25 °C. Stocks and crosses used for behavioural assays were raised at 25 °C, with a 12 hr light dark cycle.

2.13.1 Drosophila Strains

Fly strains used are listed in Table 2.5 and fly strains made in this study are listed in Table 2.6.

2.13.2 *Drosophila* Culture Media

2.13.2.1 Cornmeal Agar

Cornmeal agar *Drosophila* culture media consisted of: 10 g agar, 32 g active dry yeast (New Zealand Food Industries), and 110 g organic cornmeal (Polenta) added to 1 L of dH_20. This mixture was then brought to the boil and simmered for two minutes. The mixture was then cooled slightly and 3.3 g of p-Hydroxybenzoic Acid Methyl Ester (SIGMA) dissolved in 37 mL of 95 % ethanol, 128 g sucrose (Pam's), and 100 mL of molasses (Red Seal Natural Health) were added. The mixture was then poured into 30 mL sterile plastic vials (Labserv) or 100 ml glass bottles (SCHOTT). Bottles and vials were stopped with cotton wool.

2.13.2.2 Egg Laying Media

Egg laying *Drosophila* culture media consisted of: 20 g agar and 60 g organic cornmeal (Polenta) added to 1 L of dH_20. This mixture was then brought to the boil and simmered for two minutes. The mixture was then cooled slightly and 3.3 g of p-Hydroxybenzoic Acid Methyl Ester (SIGMA) dissolved in 37 mL of 95 % ethanol, and 40 mL of molasses (Red Seal Natural Health) were added. Media for laying chambers was used for both collection of eggs for injection (Section 2.13.3.2), and for the collection of developmental stages (Section 2.13.7).

Name	Genotype	Phenotype	Linkage	Comment	Source
#4	*y w*	Yellow body, white eyes	X	Used for injections in early rounds	JCL[1]
#6	*WT*	Canton S		Used in behavioural assays	BSC[2]
#8	*y w;L²/CyO, pr cn² y⁺*	Yellow body, white eyes, curly wing	X;2	Balancer, used for linkage analysis	JCL
#9	*y¹ w¹; TM3, y⁺ Ser¹/Sb¹*	White eye, serrate wing, stubble bristles	X;3	Balancer, used for linkage analysis	BSC 1614
M8	*w*; P{w⁺ mW.hs= GAL4-arm.S}11*	Wild type, some curly wing	2	Constitutively expresses GAL4	BSC 1560
M29	*w¹¹¹⁸; P{w^mc=Sgs3-GAL4.PD}TP1*	Wild type	3	Expresses GAL4 in salivary glands	BSC 6870
M30	*w*; P{w^mc=GMR-ninaE-GAL4}*	Wild type	2	Expresses GAL4 in eye	BSC 1104
CS10	*w*	White eyes	X	*w* in CantonS genetic back ground	RD[3]
MB247	*P{GawB}*	Wild type	3	Expresses GAL4 in the mushroom bodies	RD
MBc739	*y¹ w67c23; P{w⁺ mW.hs= GawB}c739*	Wild type	2	Expresses GAL4 in the mushroom bodies	BSC 7362
MBc772		Wild type		Expresses GAL4 in the mushroom bodies	RD
	w; TM2, Ubx/TM6B-P, Tb	Tubby larvae, enlarged halteres	3	Balancer in Canton S background	RD
	w; Sco/CyO	Loss of scutellar bristles, curly wings	2	Balancer in Canton S background	RD
Adult	*w¹¹¹⁸; P{w⁺ mW.hs= GawB}EDTP^OJ628*	Wild type	3	Expresses GAL4 in adult flies	BSC 8176

Table 2.5 Fly lines used in this study

[1] John C. Lucchesi
[2] Bloomington Stock Centre
[3] Ron Davis

Name	Genotype	Phenotype	Linkage
M2R2	*w*; P{w^{+mW}=UAS-MSL2$_{IR}$.CS2$_{intron}$}*	WT body, WT eyes	2
M2R3	*w*; P{w^{+mW}=UAS-MSL2$_{IR}$.CS2$_{intron}$}*	WT body, WT eyes	3
HDR1	*w*; P{w^{+mW}=UAS-HDACX$_{IR}$.CS2$_{intron}$}*	WT body, Orange eyes	2
HDR2	*w*; P{w^{+mW}=UAS-HDACX$_{IR}$.CS2$_{intron}$}*	WT body, WT eyes	3
spSR3-3	*w*; P{w^{+mW}=UAS-prSet7$_{IR}$.CS2$_{intron}$}*	WT body, Red eyes	2
spSR4-1	*w*; P{w^{+mW}=UAS-prSet7$_{IR}$.CS2$_{intron}$}*	WT body, Red eyes	3
pUAS-attB	*w*; P{w^{+mW}=UAS-RNAi-attB53}*	*y* body, Orange eyes	X

Table 2.6 Fly lines produced in this study

2.13.3 Creation of Transgenic Fly Lines

2.13.3.1 Co-Precipitation with Helper Plasmid pΔ2-3

20 μg of the required construct was mixed with 5 μg pΔ2-3 helper plasmid (Table 2.7) and TE buffer was used to make a 200 μL solution. To this solution 20 μL of sodium acetate (3 M) and 1 mL 95% ethanol was added, and precipitated overnight at 4 °C. The solution was centrifuged at 13,000 rpm for 20 minutes, and the supernatant was discarded. The pellet was washed with 70 % ethanol and centrifuged for 13,000 rpm for 10 minutes. The supernatant discarded and the pellet air-dried. The pellet was re-suspended in 50 mL of injection buffer (0.1 mM naH_2PO_4 (pH 6.8), 50 mM KCl).

2.13.3.2 Microinjection

Drosophila eggs were microinjected essentially as described by Spradling and Rubin, (1982). The chorion was removed using forceps and double-sided tape; the eggs were dehydrated with silica beads to an appropriate level, where they were able to accommodate the DNA to be injected. After dehydration the eggs were covered in halocarbon oil (Series 700, Halocarbon Products Corporation) to prevent further dehydration and reduce cytoplasm leakage after injection. The posterior end of the eggs was injected with a small amount of DNA using an Eppendorf Transjector 5246 and a micromanipulator (Leica). The needles used were made from thin walled glass capillary (A-M Systems, Inc.) on a Sutter Instrument Co. model P-2000 needle puller (Sutter Instrument Co.)

Injected eggs were placed in a humidity chamber that was enriched in oxygen and pressurised to approximately 2 atmospheres. The chamber was incubated at 18 °C overnight and 21 °C for 48 hours. Emerging larvae (G_0) were collected and transferred into a plastic vial containing cornmeal agar medium (Section 2.13.2).

Name	Description	Source
pUASp-NBa-CS2-BgX	pCaSpeR derived plasmid, containing two MCS separated by a *CS2* intron, used to construct inverted repeats	(Zhu and Stein, 2004)
pUASp-RNAi-attB53	Derived from pUASp-NBa-CS2-BgX, contains an attB site between *miniWhite* and 5′-repeat in the 5′ to 3′ direction	This Study
pUASp-RNAi-attB35	Derived from pUASp-NBa-CS2-BgX, contains an attB site between *miniWhite* and 5′-repeat in the 3′ to 5′ direction	This Study
pGEM®-T Easy	Linearised plasmid with single nucleotide 5′ and 3′ Thymine overhangs	Promega
pTAattB	pCR2.1 plasmid vector containing attB site	(Groth et al., 2000)
pGEMt-HDAC11	pGEM®-T Easy containing HDAC11 PCR fragment with restriction endonuclease tags	This Study
pGEMt-prSet7	pGEM®-T Easy containing pr-Set7 PCR fragment with restriction endonuclease tags	This Study
pGEMt-MSL2	pGEM®-T Easy containing MSL2 PCR fragment with restriction endonuclease tags	This Study
pΔ2-3	Plasmid encoding functional *P* element transposase	(Robertson et al., 1988)
pBS II KS	BlueScript plasmid for routine sub-cloning and blue white selection	Stratagene
pBSKII-CS2intron	BlueSript plasmid containing *CS2* intron from pUASp-NBa-CS2-BgX, sub-cloned for sequencing	This Study
pUAS-$MSL2_{IR.CS2_{intron}}$	pUASp-NBa-CS2-BgX derived plasmid with a MSL2 gene fragment in either MCS. Produces inverted repeat for RNAi	This Study
pUAS-$HDACX_{IR.CS2_{intron}}$	pUASp-NBa-CS2-BgX derived plasmid with a HDACX gene fragment in either MCS. Produces inverted repeat for RNAi	This Study
pUAS-$prSet7_{IR.CS2_{intron}}$	pUASp-NBa-CS2-BgX derived plasmid with a pr-Set7 gene fragment in either MCS. Produces inverted repeat for RNAi	This Study
pUAS-$LacZ_{IR.CS2_{intron}}$	pUASp-NBa-CS2-BgX derived plasmid with a LacZ gene fragment in either MCS. Produces inverted repeat for RNAi	This Study

Table 2.7 Plasmids Used or Made in this Study

2.13.4 Microinjection Crosses

A single G_0 fly was crossed to 3 *w* CantonS virgins at 25 °C, and the progeny selected for w^+. The G_1 offspring were collected and crossed again to 3 *w* CantonS virgins. The w^+ G_2 heterozygous flies were crossed with a balancer for the chromosome that carries the transgene (Section 2.13.6), and the offspring backcrossed. The offspring of this cross had the balancer marker selected against, to establish homozygous transformant stocks to be used for further experiments and examination.

2.13.5 Virgin Collection

Bottles containing newly emerging flies were cleared of adult flies. Bottles were incubated at 25 °C and cleared every 8 hours. Flies emerging within this time are considered to be virgin. Collected flies were separated and used in later crosses and assays.

2.13.6 Collection of *Drosophila* Heads

Drosophila heads used for RNA extraction were collected by anaesthetising male flies with CO_2 and transferring them to a 1.5 mL microfuge tube and then frozen in liquid nitrogen. The microfuge tube was then vortex vigorously for 30 s, and placed back in liquid nitrogen. This was repeated 3 times. The vortexing shears legs, wings, and heads, away from the body. Fly body parts were then sorted under a dissecting microscope and the heads re-frozen in liquid nitrogen and either used immediately for total RNA extraction (Section 2.7.5) or kept at -80 °C for later use.

2.13.7 Linkage Analysis

To determine the chromosome carrying the insert, three separate crosses were conducted. Firstly, w^+ male flies carrying the transgene were crossed to *y w* virgin females (section 2.13.6) at 25 °C. If the transgene is on the X chromosome, then all the male offspring would have white eyes, and all females would be w^+. Secondly, w^+ male flies carrying the transgene on an autosome were crossed with *w;*L^2*/CyO* virgin females at 25 °C, and *CyO* w^+ male off spring were selected and test crossed to *y w* virgin females. If the transgene is on the second chromosome then the *CyO* chromosome will segregate from the transgene with the w^+ marker and thus all *CyO* flies are *w*. Thirdly, w^+ male flies carrying the transgene on an autosome were crossed with *w*;*Sb/*TM3, *Ser* virgin females at 25 °C, and *Ser* w^+ male off spring were selected and test crossed to *y w* virgin females. If the transgene is on the third chromosome then the *Ser* segregate from the transgene with the w^+ marker and all *Ser* flies are *w*.

2.13.8 Collection of Developmental Stages

Different developmental stages were collected by aging newly laid eggs collected from laying chambers (Section 2.13.2.2). A paste of dried yeast pellets and water was made and a thin strip placed in the middle of the plate. Laying flies were placed in the chamber and allowed to lay for an hour. Flies where removed and the plates were incubated for the appropriate time at 25 °C; a method modified from Ashburner (1989).

2.13.9 Drosophila Brain Dissection for Confocal Microscopy

Adult male flies aged between 36-48 hrs old were anaesthetised with CO_2 and the heads were removed with a scalpel blade. The fly heads where then fixed in 95 % Ethanol for 10 min. After fixation heads where blotted dry on tissue paper and placed face-dawn on a slide in quick-drying cement, leaving the back of the head exposed above the cement. The cement was allowed to dry, and care was taken not to let too much alcohol evaporate, which would dehydrate the brain. Once the cement was dry, a small drop of Ringers solution (Section 2.2) was placed over the brain to prevent any further drying and to aid dissection. The back of the head was peeled away using sharp pointed forceps, in a radial fashion to expose the brain. The forceps were then used to separate the optical lobes of the brain from the ommatidia. The brain was then gently agitated with the forceps to free it from the front of the head. The brain was then floated free into the Ringers solution. The brain was then removed from the Ringers solution and imaged with confocal microscopy (Section 2.13.11).

2.13.10 Fluorescent Microscopy

Fluorescent microscopy on *Drosophila* was carried out using an Olympus SZX12 microscope and an Olympus U-RFL-T mercury burner lamp. Images were captured using an Olympus U-TVO.SXC-2 digital camera, and images were processed using Olympus DPController and DPManager software.

2.13.11 Confocal Microscopy

Brains collected from Section 2.13.9 were mounted on a slide, in a PBS/glycerol (50:50 v/v) solution. Confocal images were obtained and processed using the Leica TCS SP5 DM6000B Confocal Microscope and associated software (Lieca)

2.13.12 Viability Assay

The inverted repeat fly lines were crossed to *w*; *Sco/Cyo* and w^{+}*/CyO* males were crossed to a GAL4-expressing line *arm-GAL4* (Table 2.3). 10 pairs of flies were allowed to lay in a bottle (Section 2.13.2.1) for 4 days, then removed. Flies were sorted into male, female, curly, and non-curly, and counted 18 days after the bottle was set. Bottles were set in triplicate. This allowed for an internal control of the viability of the flies. As a further control against possible effects on viability by the balancer chromosome, a line not carrying an IR over a balancer was also crossed to the *arm-GAL4* driver.

2.14 Behavioural Conditioning of Drosophila

Assays were performed essentially following the procedures of *(Sakai et al., 2004)* with minor modifications. All flies were raised at 25 °C with a light source on a periodic timer producing a 12 hr light/dark cycle.

2.14.1 Preparation of Female Flies for Conditioning Assay

CantonS virgin males and females aged between 3 and 5 days were mated 12-18 hrs prior to use in the conditioning assay (Section 2.14.3). The virgin female flies were set in vials with 10 females and 15 males and allowed to mate. Flies were not anaesthetised.

2.14.2 Preparation of Male Flies for Conditioning Assay

Virgin male flies from either CantonS, or crosses with IR lines were aged for 3 days. Flies were anaesthetised soon after eclosion in order to collect them (Section 2.13.5). All subsequent manipulation of these flies were done by aspiration and not anaesthetic.

2.14.3 Conditioning of Male Flies

Mated females (Section 2.14.1) were aspirated into a conditioning chamber that measured 15 mm in diameter by 15 mm in depth containing 10-12 mm of cornmeal agar fly food (Section 2.13.2) (Figure 2.1). Male flies (Section 2.14.2) were aspirated into the chamber with the female and left in the conditioning chambers for 9 hrs.

After conditioning, the male flies were removed by aspiration and placed in a fresh chamber of the same diameter and kept for use in the conditioned assay (Section 2.14.4). As a control, a virgin male of equivalent age was introduced into another conditioning chamber without a mated female.

2.14.4 Behavioural Assay Method and Materials

In this assay, a decapitated virgin female was used as a target. Females were anaesthetised and the heads removed with a scalpel blade. After decapitation, fly bodies were allowed to recover from anaesthesia for 10 min. Flies regained rudimentary faculties such as self-stabilisation, and cleaning reflexes. The assays were recorded using a Panasonic DMR-ES15 DVD recorder, via a WAT 213 analogue camera through an Olympus SZ61 dissecting microscope.

Conditioning and test chambers were made of transparent acrylic plastic and covered with a rectangular acrylic plastic at the top with dimensions of 13 mm in diameter by 3 mm in depth (Figure 2.1). After each assay the chamber was washed with 95 % ethanol to remove any possible contaminants or accumulation of odours that could interfere with the assay. Chambers were allowed to air dry for 30 min to remove any excess ethanol.

Conditioned and non-conditioned male (Section 2.14.3) flies were assayed 2 days after the females were removed (Section 2.14.3). A male fly was aspirated into an assay chamber with a target female (Section 2.14.4). Active courtship preformed by the male was recorded for 10 min.

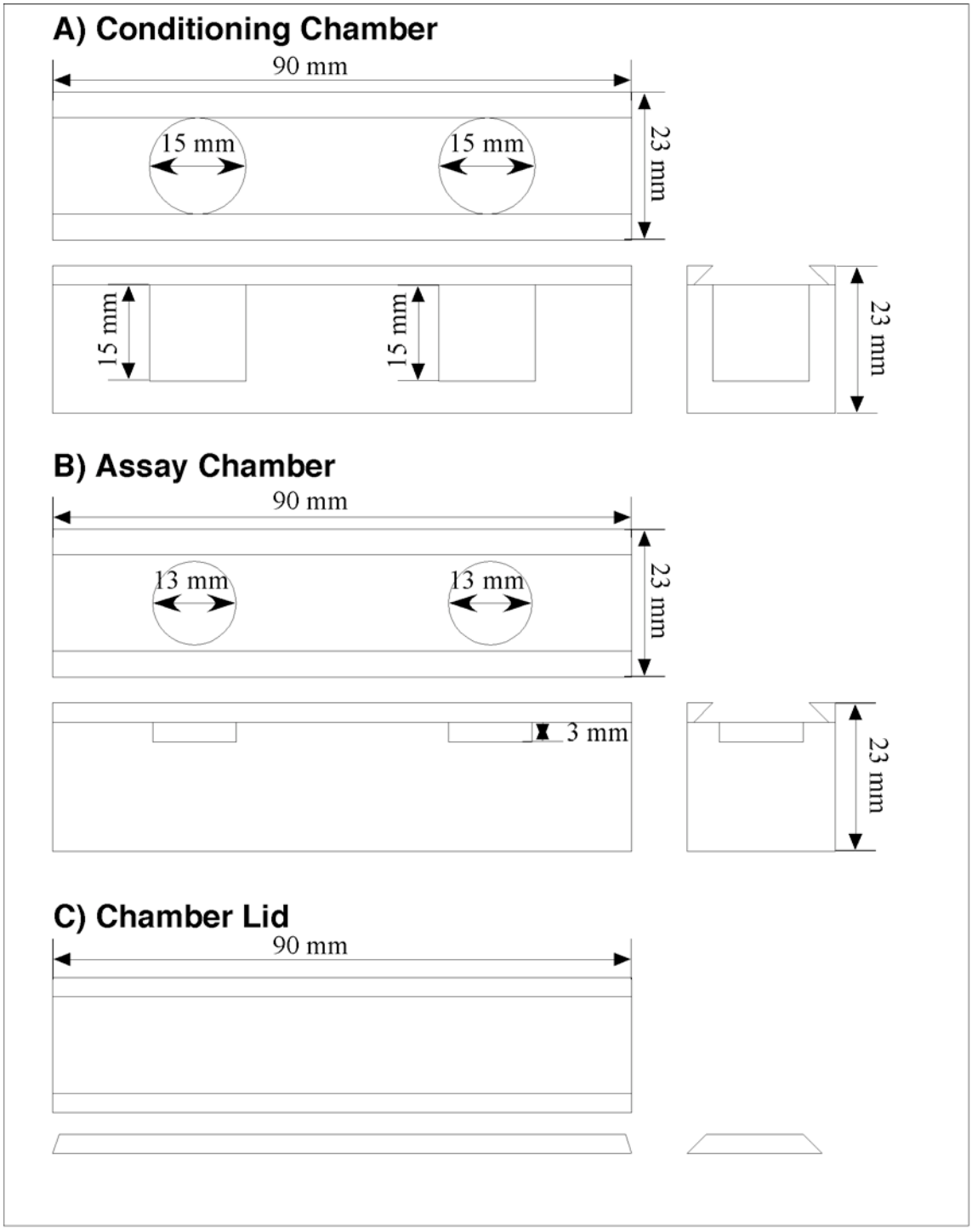

Figure 2.1 Behavioural Conditioning and Assay Chamber

(A) Conditioning chamber for behavioural assay (B) Assay chamber used to observe conditioned *Drosophila* (C) Lid of both conditioning and assay chamber

Recordings were viewed and analysed for the time spent in active courtship by the male. As an indicator of male courtship activities, a courtship index (Section 1.15) was calculated. Courtship activity of a conditioned male was compared with those of a naïve male. Within genotypes the courtship index was normalised to the naïve males, giving a representation of relative changes in courting behaviour.

Male flies were removed from the 25 °C incubator and immediately assayed at 21 °C. This is not ideal, however technical constraints meant assays could not be carried out at 25 °C. Assays were carried out under double blind control, to avoid bias.

2.14.5 Statistical Analysis

To analyse the statistical significance of the behavioural data collected, these data were assumed to be normally distributed. Raw courtship times were averaged and the standard deviation was calculated. From these data the 95 % confidence level was calculated. A courtship index was calculated by dividing time spent courting with total allowable courtship time. Conditioned assay data were normalised to unconditioned data by dividing the mean scores from the conditioned data by the unconditioned score in each fly line. This allowed for a comparison to be drawn between fly lines, even if their unconditioned courtship times differed significantly.

Chapter Three

Results

3.1 Molecular Cloning

3.1.1 Overall Strategy for Molecular Cloning

The overall strategy of this section was to create a *P*-element vector with an inverted repeat of a gene of interest that would produce enough dsRNA *in vivo* to induce the knockdown of the target gene at the mRNA level. The base *P*-element vector used, pUASp-NBa-CS2-BgX, was from Zhu and Stein, (2004)(Table 2.7). Sequence analysis (Section 3.1.3) was carried out on the areas of interest of pUASp-NBa-CS2-BgX to produce a more detailed and accurate map (Appendix 6.1).

The final goal of this section was to create a vector to allow the targeted integration into the fly genome and to produce dsRNA. The targeted insertion should prevent variation in expression due to position effects caused by the random integration of independently transformed lines with the *P*-element system.

3.1.2 Creation of pGEM-T Easy Clones

A pGEM®-T Easy clone of each gene of interest was created for use in further cloning steps. Primers for the PCR of the gene fragment were designed using MacVector™ (Section 2.9.2). Predicted products of 500-800 bp were screened for *Xba* I, *Bgl* II, *Nhe* I, or *Bam* HI restriction sites. Predicted products that did not contain these restriction sites had *Xba* I and *Bam* HI restriction sites placed on the 5′ ends, and were subjected to a second round of screening. To avoid possible off target effects, the available primer pairs with the largest predicted products were then visually screened for CAN repeats (Ma et al., 2006). The primer pairs that passed through these screens and had the highest annealing temperature were used to amplify the gene of interest. The PCR products were purified through a QIAquick® PCR Purification Kit (Qiagen) (Section 2.7.9) and ligated (Section 2.12.6) with pGEM®-T Easy. Ligation products were transformed into DH5α cells and grown on LB Amp/X-gal plates (Section 2.12.7). Part of each selected white colony was used to inoculate a 5 mL LB Amp broth and part was used as a source for a PCR-based screen (Section 2.10.2). Plasmid DNA was purified

from the LB Amp broth colonies, which were positive in the PCR screen. The purified DNA was sequenced and analysed with the BLAST alignment tool (Section 2.9)

3.1.2.1 Creation of *HDACX* pGEM-T Easy Clone

To amplify the *HDACX* gene fragment, primers HDACXbaIF and HDACBamHIR were used (Table 2.2). The primers bind at 367-389 bp and 985-962 bp respectively, of the predicted gene transcript. There was a single PCR product of approximately 631 bp. Sequence analysis showed that the sub-cloned PCR product was the expected *HDACX* sequence (Appendix 6.1). The clone was designated pGEMt-HDAC11 (Table 2.7), and a glycerol stock was created (Section 2.6).

3.1.2.2 Creation of *pr-Set7* pGEM-T Easy Clone

To amplify the *pr-Set7* gene fragment, primers prSet7XbaIF and prSet7BamHIR were used (Table 2.2). The primers bind at 1104-1127 bp and 1868-1843 bp respectively, of the predicted gene transcript. There was a single PCR product of approximately 777 bp. Sequence analysis showed that the sub-cloned PCR product was the expected *pr-Set7* sequence (Appendix 6.2). Also discovered in the sequence analysis was a *Bam* HI restriction site. This resulted in a 363 bp fragment when digested for subsequent cloning (Section 3.1.4.2). The clone was designated pGEMt-prSet7 (Table 2.7) and a glycerol stock was created (Section 2.6).

3.1.2.3 Creation of *msl-2* pGEM-T Easy Clone

To amplify the *msl-2* gene fragment, primers MSL2XbaIF and MSL2BamHIR were used (Table 2.2). The primers bind from 751-776 bp and 1460-1435 bp respectively, of the predicted gene transcript. There was a single PCR product of approximately 722 bp. Sequence analysis showed that the sub-cloned PCR product was the expected *msl-2* sequence (Appendix 6.3). The clone was designated pGEMt-MSL2 (Table 2.7) and a glycerol stock was created (Section 2.6).

3.1.3 Analysis of pUASp-NBa-CS2-BgX

To gain a greater understanding of the features and sequence of the pUASp-NBa-CS2-BgX vector, areas of importance were sub-cloned and sequenced. However, in order to sequence important areas of pUASp-NBa-CS2-BgX, initial sequences needed to be already known. The solution to this problem was to digest the vector and sub-clone a region into another vector that already had well-established sites for sequencing primers. Then primers could be designed to specific regions within the original vector and further sequencing could be carried out without the use of sub-cloning.

3.1.3.1 Sub-Cloning of Important Regions of pUASp-NBa-CS2-BgX

The *chitin synthase 2* (CS2) intron area of pUASp-NBa-CS2-BgX was sequenced first (Appendix 6.9). The pUASp-NBa-CS2-BgX DNA was transformed into DH5α cells (Section 2.12.7) and a large-scale plasmid preparation was performed (Section 2.7.3). To remove the CS2 region for sub-cloning, the pUASp-NBa-CS2-BgX was digested with *Bam* HI and *Xba* I (Section 2.12.2). This produced a fragment approximately 800 bp when separated on a gel. A pBS II KS^+ plasmid was digested with *Bam* HI and *Xba* I (Section 2.12.2) and purified through a QIAquick® PCR Purification Kit (Qiagen) (Section 2.7.9). The PCR purification column was used because the fragment between the two restriction sites was too small to be retained in the column. The CS2 intron region was then ligated into the digested pBS II KS^+ plasmid (Section 2.2.6). Ligation product was transformed into DH5α cells and grown on LB Amp plates (Section 2.12.7). Ampicillin-resistant colonies were picked and grown in LB Amp Broth (Section 2.12.7). Small-scale plasmid preparation was carried out (Section 2.7.2) and the plasmids were digested with *Bam* HI and *Xba* I (Section 2.12.2). Several clones with the expected insert size were sent for sequencing (Section 2.9) using T7 primers provided by the sequencing service. The resulting sequence data was analysed and annotated using MacVector and BLAST (Section 2.9). The BLAST analysis showed that the fragment was the intron of the *chitin synthase 2* gene (Appendix 6.9).

3.1.3.2 Sequencing of Flanking Regions of the pUASp-NBa-CS2-BgX

To further analyse the important regions of pUASp-NBa-CS2-BgX, primers were designed to sequence in both the 5′ and 3′ direction from the central CS2 intron across the two predicted multiple cloning sites, and into the promoter region and the K10 terminus. The two primers that were designed to bind within the CS2 intron were 2ndRNAiCS2Minus, to sequence toward the K10 terminus, and RNAiCS2Plus, to sequence towards the promoter region. The sequences returned from these primers were high quality, and were assembled into a larger contig with the sequences produced in Section 3.1.3.1 using MacVector (Section 2.9) (Appendix 6.16).

Using the sequences produced from the RNAiCS2Plus and 2ndRNAiCS2Minus primers as a template, another set of primers were designed to further sequence into the pUASp-NBa-CS2-BgX region. The two primers that were designed were PlusCS2Plus to sequence further into and past the K10 terminus, and 2ndCS2Minus, to sequence further into the 5′ region of the promoter. The sequences returned from these primers were high quality, and the sequences were compiled into the contig produced from the previous set of sequencing primers.

The contig produced from these series of sequencing steps was then compared with the pCaSpeR backbone plasmid (Appendix 6.13) sequence used to create the pUASp-NBa-CS2-BgX. Analysis of these data allowed for an estimated vector sequence to be created (Appendix 6.4). By noting at which point along the contig the sequences aligned, and which point they ceased to align, it was possible to identify which portions of the original sequence had been removed and where the important features of the pUASp-NBa-CS2-BgX had been inserted. This proved to be an efficient way to analyse the pUASp-NBa-CS2-BgX. As all the important regions had been sequenced, the combination with the pCaSpeR backbone sequence provided an accurate compilation sequence and a robust restriction enzyme map (Appendix 6.4).

3.1.4 Creation of pUASp-NBa-CS2-BgX Inverted Repeats

The strategy of this section was to create a series of vectors that would produce an inverted repeat *in vivo* to induce a dsRNA-mediated knockdown of the target mRNA transcript. It is important to note in this section is that the second sub-cloning steps, which produced the final constructs to be injected into the *Drosophila* lines, were amplified in Stbl2™ cells (Section 2.4). This cell is a recombination deficient strain that reduces the risk of the inverted repeats being disrupted.

A two-step cloning strategy was used to produce the inverted repeats (Figure 3.1). The same restriction digest from the pGEM®-T Easy clones was used in both cloning steps. Firstly, an insert was removed from the respective pGEM®-T Easy clone by a digestion with *Xba* I and *Bam* HI and cloning this fragment into pUASp-NBa-CS2-BgX that had been digested with *Nhe* I and *Bam* HI. Sites produced by *Nhe* I and *Xba* I have compatible ends. Thus the ligation of the gene fragment is directionally cloned into the pUASp-NBa-CS2-BgX in the 5′ to 3′ direction. Ligation product was then transformed into DH5α cells and grown on LB Amp plates (Section 2.12.7). Several Ampicillin-resistant colonies where grown in a 5 mL Amp LB broth overnight and small-scale plasmid preparations were made (section 2.7.2). These samples were sent for sequencing (Section 2.9) using the CS2Plus sequencing primer (Table 2.1). A clone that was positive for the insert was grown in a 25 mL LB Amp broth and a large-scale plasmid preparation was performed (Section 2.7.3).

The sub-cloned vector was subsequently digested with *Xba* I and *Bgl* II. The same fragment from the first insert digestion was ligated into the digested vector. Sites produced by *Bgl* II and *Bam* HI have compatible ends. Therefore the ligation of the gene fragment is directionally cloned into the pUASp-NBa-CS2-BgX in the 3′ to 5′ direction. Ligation product was transformed into Stbl2™ cells and plated on Terrific Broth Amp agar plates. Ampicillin-resistant colonies were picked and grown in 5 mL Terrific Broth Amp at 30 °C. Due to the inverted repeats in the vector creating unusable sequence reads, it was not possible to sequence the second insert to confirm its correct orientation. To confirm the second insert was correct, a series of restriction digests were carried out. The correct fragments are described in the following sections.

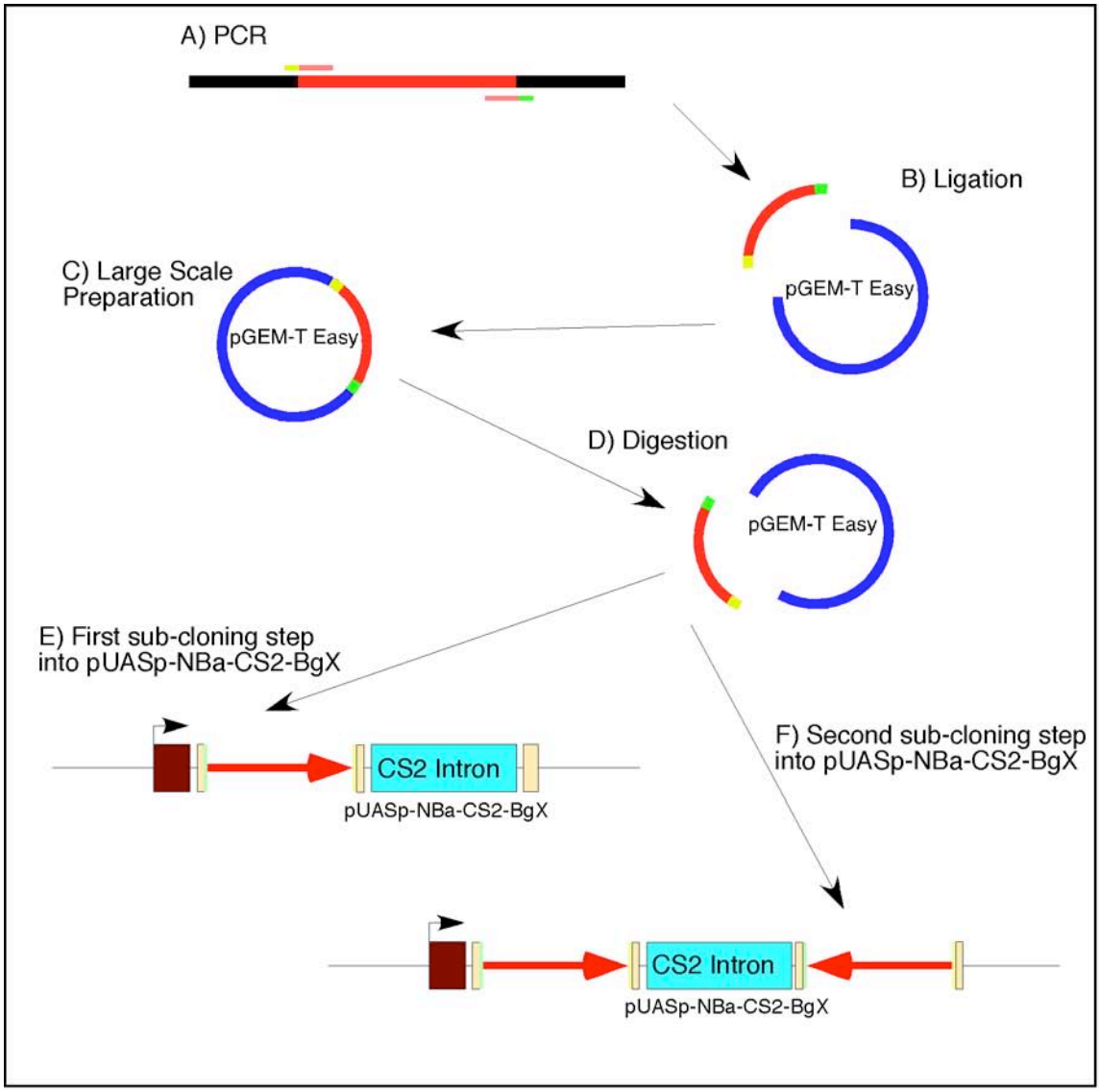

Figure 3.1 Cloning Strategy for RNAi Vector

(A) Primers with restriction tags were used to amplify the gene of interest. (B) PCR product was ligated into the pGEM-T Easy vector. C) Large-scale plasmid preparation from transformed cells. (D) Plasmid preparation was digested with *Xba* I and *Bam* HI. (E) Excised fragment was sub-cloned into a *Nhe* I and *Bam* HI digested pUASp-NBa-CS2-BgX . (F) The fragment excised from (D) was sub-cloned into a *Xba* I and *Bgl* II digested product produced in (E) to produce the final vector.

3.1.4.1 Confirmation of *HDACX* Inverted Repeats

The vector with the *HDACX* inverted repeats was designated pUAS-$HDACX_{IR}.CS2_{intron}$. To confirm the correct orientation, the vector was digested with three restriction enzymes individually (Figure 3.2); *Xho* I, *Eco* RI, and *Fsp* I (Appendix 6.1). The *Xho* I digestion produced five restriction products: 9206 bp, 1098 bp, 862 bp, 520 bp, and 254 bp. *Eco* RI produced two restriction products; 11006 bp, and 934 bp. *Fsp* I produced three restriction products; 7085 bp, 3513 bp, and 1342 bp.

3.1.4.2 Confirmation of *pr-Set7* Inverted Repeats

The vector with the *pr-Set7* inverted repeats was designated pUAS-$prSet7_{IR}.CS2_{intron}$. Due to a mistake made in the initial primer design and screening of *pr-Set7* (Section 3.1.2.2) there was a *Bam* HI site included within the 777 bp clone in pGEM®-T Easy. This resulted in a 363 bp fragment being used instead of the initial full clone. The vector pUAS-$prSet7_{IR}.CS2_{intron}$ was digested with three restriction enzymes individually (Figure 3.2); *Bst* BI, *Afl* II, and *Xho* I (Appendix 6.2). The *Bst* BI digest produced five restriction products; 4259 bp, 3747 bp, 1719 bp, 1440 bp, and 225 bp. The *Xho* I digest produced three restriction products; 9206 bp, 1685 bp, and 499 bp. The *Afl* II digest produced two restriction products; 7929 bp and 3461 bp.

3.1.4.3 Confirmation of *msl-2* Inverted Repeats

The vector with the *pr-Set7* inverted repeats was designated pUAS-$MSL2_{IR}.CS2_{intron}$. The vector pUAS-$MSL2_{IR}.CS2_{intron}$ was digested with three restriction enzymes individually (data not shown); *Mfe* I, *Nru* I, and *Sac* I (Appendix 6.3). The *Mfe* I digest produced four restriction products; 8150 bp, 2030 bp, 988 bp, and 952 bp. The *Nru* I digest produced three restriction products; 6685 bp 3539 bp, 2196 bp. The *Sac* I digest produced five restriction products; 6047 bp, 2897 bp, 1632 bp, 1138 bp and 406 bp.

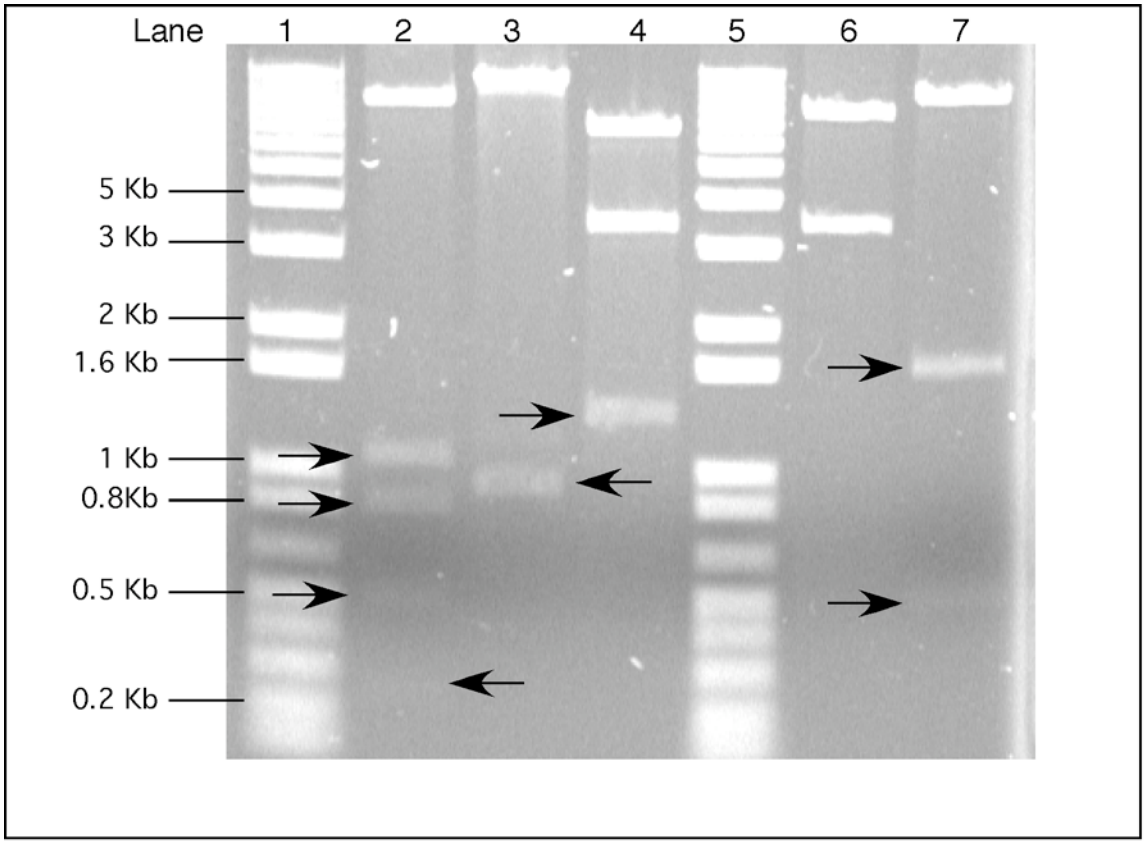

Figure 3.2 Example of Restriction Digest for Inverted Repeat Confirmation

Lane 1) 1 Kb Plus ladder (Invitrogen). Lane 2-4)Restriction digest of HDACX inverted repeat. 2) Xho I, 3) Eco RI, 4) Fsp I. Lane 5) 1 Kb Plus Ladder (Invitrogen). Lane 6 and 7) Restriction digest of pr-Set7 inverted repeat. 6) Afl II, 7) Xho I. Scale indicates fragment size of 1 Kb Plus Ladder. Arrows indicate bands present but difficult to observe.

3.1.5 Creation of pUASp-RNAi-attB

The strategy of this section was to insert an attB site into the pUASp-NBa-CS2-BgX vector to allow the targeted insertion into a pre-determined site within the *Drosophila* genome, the attP site (Section 1.5).

To produce this vector the restriction map produced in Section 2.1.3 was analysed with MacVector (Accelrys Incorporated) to find sites to insert the attB site. Of the sites analysed, the *Nsi* I site was the only one that was not situated within critical regions of the vector. This restriction site occurs once between the *miniWhite* gene and 5′ repeat (Appendix). The attB fragment was obtained from the pTAattB plasmid (Table 2.7) by digesting with *Eco* RI and gel extraction (Section 2.7.8). The 5′ cohesive ends produced by the *Eco* RI digestion were filled in to produce non-cohesive ends (Section 2.12.5) and the 5′ ends were phosphorylated (Section 2.12.4). The pUASp-NBa-CS2-BgX vector was digested with *Nsi* I and 5′ ends were dephosphorylated (Section 2.12.3) to avoid re-ligation. The attB fragment was ligated into the *Nsi* I digested pUASp-NBa-CS2-BgX (Section 2.12.6) and transformed into DH5α cells and grown on LB Amp plates (Section 2.12.7). Ampicillin-resistant colonies were screened with PCR on colony (Section 2.10.2) using the primers attBNsiIRNAiF and attBNsiIRNAiR (Table 2.1), which bind either side of the *Nsi* I restriction site (Appendix 6.5). As it was possible for the fragment to ligate in either orientation, several PCR-positive clones were picked and grown in 5 mL LB Amp broth. A small-scale plasmid preparation (Section 2.7.2), of several PCR positive clones, were sequenced using the same primers as used in the PCR on colony.

From this cloning strategy, two pUASp-NBa-CS2-BgX vectors containing the attB fragment in the *Nsi* I restriction site were created. These two clones differed in the orientation of the attB site. The pUASp-RNAi-attB53 had the attB insert in the 5′ to 3′ orientation and pUASp-RNAi-attB35 had the insert in the 3′ to 5′ orientation (Table 2.7). Both these inserts were confirmed by sequence analysis (Appendix 6.17).

3.2 *Drosophila* Transformations

3.2.1 Transformation of *Drosophila* with the pUAS-IR-CS2 Vector

Creation of transgenic fly lines was performed as described in Section 2.13.3. The first transformant lines were created in a *y,w* genetic background (Table 2.5). A second series of lines were created in the *w* Canton-S genetic background (Table 2.5).

Lines created in *y,w* were backcrossed to produce a homogenous genetic background congruent with current literature that considers the CantonS genetic background the standard for memory and learning assays (Sakai et al., 2004)(Table 2.6). The lines were backcrossed for five generations through w^+ virgin female crossing to male *w* CantonS.

A number of independent lines were produced from these injection experiments with varying degrees of efficiency of transformation (Appendix 6.14). Two independent lines were selected from each construct and backcrossed, where necessary, to CantonS *w* males (Table 2.6).

3.2.2 Transformation of pUAS-CS2-attB into *Drosophila*

The pUASp-RNAi-attB53 vector was used in these transformations. The vector was prepared as described in Section 2.13.3, with the exception of the co-precipitation of the helper plasmid as described in Section 2.13.3.1. The vector was injected into the appropriate genetic background containing both the *phi* c-31 intergrase transgene and the attP integration site on the X chromosome (Table 2.5) (Thorpe and Smith, 1998).

The transformation was very efficient and produced eight independent lines from twenty-six fertile crosses, giving a transformation efficiency of 31 %. This was a significant improvement over the *P*-element system (Appendix 6.14). All of the lines were X linked, indicating that they were targeted to the attP site located on the X chromosome.

3.2.3 Transgene Integration Sites of Selected Transformant Fly Lines

Inverse PCR (iPCR) was performed as described in Section 2.10.4 to find the position of insertion of the *P*-element vectors. The sequences are presented in Appendix 6.15. The flanking regions of the insert are reported in the following sections.

3.2.3.1 pUAS-HDACX$_{IR}$.CS2$_{intron}$ Insertion Position

The iPCR results for the strain HDR1 (Table2.7), containing the transgene UAS-HDACX$_{IR}$.CS2$_{intron}$, showed that it inserted between CG6424, which is 5′ of the insert, and CG10934, which is 3′ of the insert, on the 2R chromosome. Both these genes have no phenotypic data and no proposed function for the predicted proteins. The vector did not insert within a gene, and did not directly disrupt any predicted coding region.

3.2.3.2 pUAS-prSet7$_{IR}$.CS2$_{intron}$ Insertion Position

The iPCR results for the strain spSR3-3 (Table 2.7), containing the transgene UAS-prSet7$_{IR}$.CS2$_{intron}$, showed that it inserted between CG12464, which is 5′of the insert, and CG17716, which is 3′of the insert, on the 2R chromosome. The vector inserted into a region that was relatively distant from other predicted genes. The closest genes were 13.8 kb in the 5′, and 31.4 kb in the 3′ direction. The CG12464 gene had no phenotypic data and no proposed function for the predicted protein. The CG17716 gene is also known as *faint sausage* (*fas*) and refers to the phenotype of the embryo. The *fas* gene is involved in embryogenesis and development of the central nervous system (Lekven et al., 1998).

3.2.3.3 pUAS-MSL2$_{IR}$.CS2$_{intron}$ Insertion Position

The iPCR results for the strain M2R3 (Table 2.7), which carries the transgene UAS-MSL2$_{IR}$.CS2$_{intron}$, showed that it inserted between the LpR1 (CG31094) and LpR2 (CG31092) genes on the 3R chromosome. The LpR1 gene is 3′, and LpR2 is 5′, of the inserted vector. The LpR1 and LpR2 genes are a Lipophorin receptor that has been linked to lipid use in *Drosophila* larvae starvation (Gutierrez et al., 2007). The vector did not insert within a gene, and did not directly disrupt any predicted coding region.

3.3 Analysis of GAL4 Driver Lines by Fluorescence

The objective of this section was to analyse the expression pattern of different promoters driving expression of GAL4, within various fly tissues and through development. Two fluorescent markers were used: DsRed-nls, and GFP. The expression of both fluorescent markers is regulated by GAL4-UAS, only permitting expression where GAL4 is being expressed. It is also important to note that the DsRed-nls fluorescent marker has a nuclear localisation signal, resulting in only the nucleus being fluorescent. The GFP marker does not have any localisation signal, and therefore produces fluorescence throughout the cytoplasm and nucleus. The offspring of a cross between a GAL4 expressing line and fluorescent marker line were used for analysis.

3.3.1 Analysis of GAL4 Expression by DsRed-nls Fluorescence

There were three objectives to this section. Firstly, to observe the expression of the DsRed-nls fluorescent marker under the control of an artificial promoter, such as the synthetic promoter element *GMR*. Secondly, to observe the specificity of expression of enhancer trapped lines, such as GAL4 driver BSC 8176 (Table 2.7). This particular fly line is reported as having expression in adult flies, increasing with age. Thirdly, to observe the expression of the GAL4 enhancer trapped lines that were reported as being mushroom-body specific.

3.3.1.1 Analysis of Artificial Promoters

The expression pattern of the artificial promoters is very demarcated (Figure 3.3). There is no significant observable fluorescence in any unexpected tissues. The control used in this experiment is the UAS-DsRed-nls fly line without any GAL4 driver. This control would detect any possible ectopic expression that could have occurred from the UAS-DsRed-nls due to any positional effects, as well as possible auto-fluorescence.

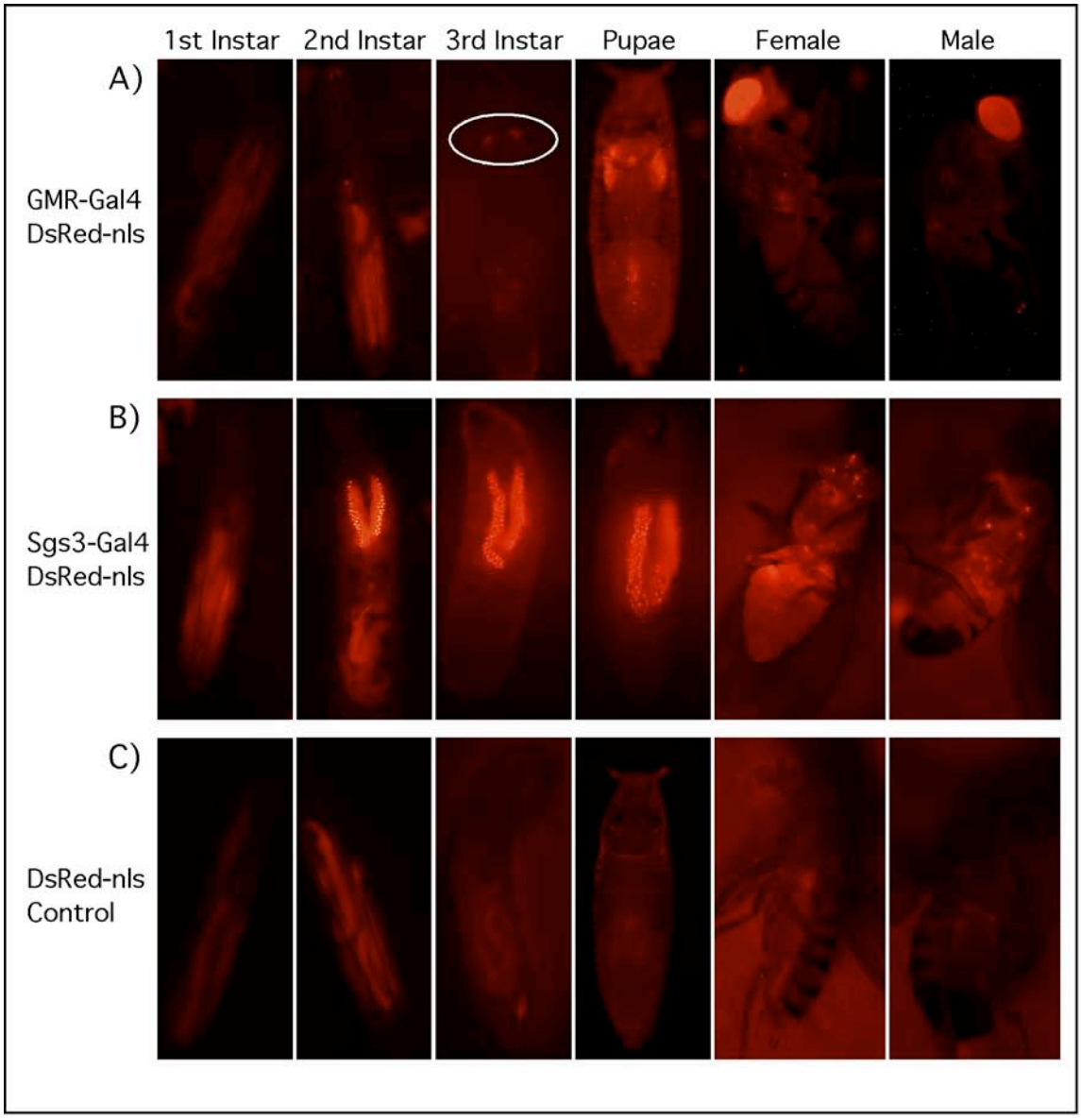

Figure 3.3 GAL4 Regulated expression of DsRed-nls Throughout Development

Adult Flies, pupae and larvae that contain the UAS-DsRed-nls transgene either, (A) GAL4 driven by the *GMR* promoter, (B) GAL4 driven by the *Sgs3* promoter, or (C) no GAL4 driver. White circle in (A) indicate eye imaginal disks.

The *GMR*-GAL4 promoter shows no significant observable fluorescence until the late third instar larvae, at which point fluorescence is observed in the imaginal discs, in keeping with the expected expression behind the morphogenic furrow (Figure 3.3 A). In the pupae the fluorescence was clearly visible through the pupal casing. Adult flies had very intense fluorescence of the eyes, but not in any other tissue. These data show that *GMR*-GAL4 is a very specific promoter, with no significant observable ectopic fluorescence.

The Sgs3-GAL4 line showed a very clear expression in the salivary glands (Figure 3.3 B). The expression of the DsRed-nls can be clearly seen within the enlarged nuclei of the salivary gland. The third instar larvae show the greatest intensity of fluorescence. In the pupal stage there was a loss of specific fluorescence in the nuclei of the salivary gland, as they senesce as the adult fly develops. The adult flies seem to retain some residual fluorescence.

The *arm*-GAL4 shows expression throughout all tissues and developmental stages (Figure 3.4 A). This result is expected, as the expression of *armadillo* is ubiquitous throughout *Drosophila* development (Vincent et al., 1994). There is a distinct punctate appearance to the whole body of the larvae and pupae. An interesting observation was the lack of any observable expression in the salivary glands, as the level of expression of *armadillo* is 2.45 fold increased in the salivary glands relative to the expression average of the whole fly (Chintapalli et al., 2007). The *arm*-GAL4 driver would be expected to express strongly in the salivary glands. The body of the adult flies still retained a punctate appearance (Figure 3.4).

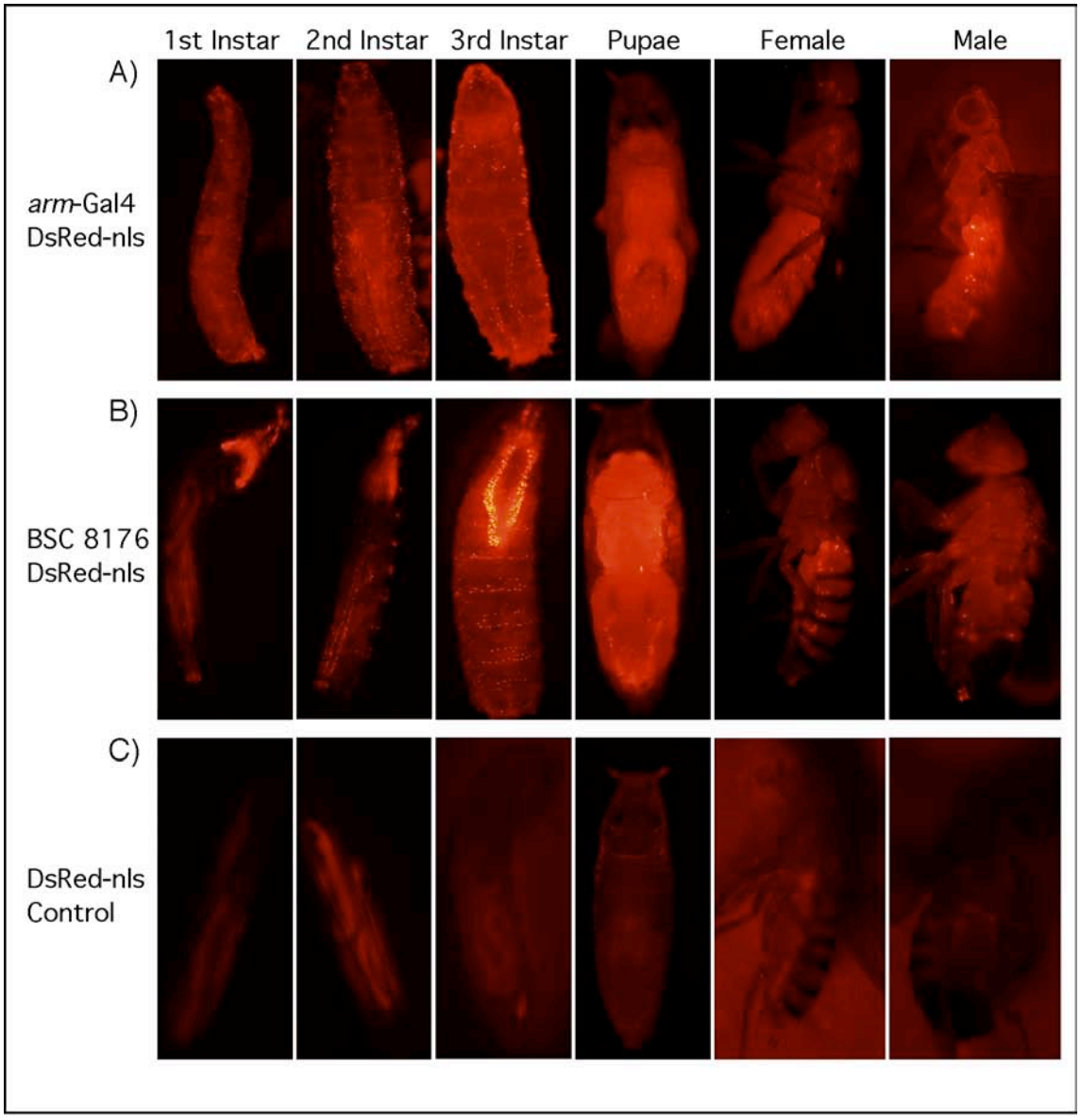

Figure 3.4 GAL4 Regulated Expression of DsRed-nls Throughout Development

Adult Flies, pupae and larvae that contain the UAS-DsRed-nls transgene either, (A) GAL4 driven by the *armadillo* promoter, (B) GAL4 driven by BSC 8176 enhancer trap, or (C) no GAL4 driver.

3.3.1.2 Analysis of Enhancer-Trap Line BSC8176

The enhancer-trap line BSC8176 has been reported to express in the adult fly muscles and to increase with age (Bloomington Stock Center). The BSC8176 line showed very high expression in the salivary glands throughout the development of the larvae. There is also an increase in expression in other tissues over development. There is an increase in fluorescence in cells surrounding the tracheal system of the larvae (Figure 3.4 B). There is also an increase of fluorescence of cells surrounding the ventral denticle belts. The pupae have intense fluorescence though out the body. There is fluorescence throughout the whole adult fly, although there appears to be increased fluorescence in the thorax, relative to the rest of the body. The thorax contains large flight muscles (Figure 3.4 B).

3.3.2 Analysis of GAL4 Expression by Fluorescence of Mushroom-Body Specific Enhancers

Three different mushroom-body drivers were assayed for their expression through development; MB247, MB739, and MB772 (Table 2.5). The expected expression patterns of the three mushroom-body drivers are described in Section 1.4. These were assayed to assess which gave the most specific expression of GAL4 within the mushroom-body. However, it became apparent that the expression of the GAL4 drivers crossed to UAS-DsRed-nls were not limited to the mushroom-bodies. The third instar larvae of the offspring MB739 and MB772 crossed to UAS-DsRed-nls were rotated onto their backs to expose the salivary glands. This was done to show the intense expression of the salivary glands, which tended to obscure the fluorescence of other tissues. There was no observed change in expression patterns of the MB739 and MB772 crosses between the second and third instar larvae.

3.3.2.1 Analysis of MB247 by Fluorescence

The expression pattern of the MB247 mushroom-body driver was much more expansive than expected (Figure 3.5). In the first and second instar larvae there was extensive fluorescence along the main tracheal tubes running dorsally (Figure 3.5). The third instar shows an increase in expression along the main dorsal trunk and extending into the transverse connective trachea. Also observable in the third instar larvae is the expression in the head region that appears to be the antenomaxillary complex (Figure 3.5). Expression in the antenomaxillary complex region was lost in the pupal stage (Figure 3.5). However, there was clear expression in the abdominal region, with a decrease in the fluorescence from the main tracheal tubes. This was probably due to the senescence of the larval trachea, and the development of the adult trachea. The pupae show expression in the larval tracheal dorsal trunk as well as in the transverse connective trachea. Both the adults appear to have ubiquitous expression, with no obvious specificity to the brain.

Figure 3.5 GAL4 Regulated Expression of DsRed-nls and GFP Throughout Development by MB247

Adult Flies, pupae and larvae that contain the either the UAS-GFP or UAS-DsRed-nls transgene. (A) MB247-GAL4 driving UAS-DsRed-nls, or (B) MB247-GAL4 driving UAS-GFP.

The fluorescence pattern of MB247 in GFP appears similar to that of DsRed-nls. The fluorescence pattern is much more dispersed than that of DsRed-nls, as the GFP does not have a nuclear localisation signal. In the first and second instar larvae there was fluorescence along the main tracheal tubes running dorsally (Figure 3.5). The third instar showed an increase in expression along the main tracheal tubes running dorsally and extending into the transverse connective tracheal tubes. Also observable in the third instar larvae is the expression in the head region that appears to be the antenomaxillary complex (Figure 3.5). The pupae seem to have lost the expression in the antenomaxillary complex region (Figure 3.5). However, there is clear expression in the abdominal region, with a loss of fluorescence from the main tracheal tubes, probably due to the senescence of the larval trachea, and the development of the adult trachea. Both the adults appeared to have a ubiquitous expression, with no obvious specificity to the brain. Important to note in the larvae is the high levels of auto-fluorescence, which were not present in the DsRed-nls lines.

The expression of MB247 by confocal microscopy in the *Drosophila* brain was analysed with DsRed-nls and GFP independently. The brains were prepared as described in Section 2.13.9, and imaged using confocal microscopy as described in Section 2.13.10. The expression pattern of MB247 driving the expression of DsRed-nls showed an extensive fluorescent pattern throughout the brain (Figure 2.6 A). There appears to be no especially intense fluorescence localised to the Kenyon cells, where it would normally be expected. However, there is strong DsRed-nls expression in the region of the brain known to contain the Kenyon cells, as indicated by the white circles in Figure 3.6 A. This confirmed that the MB247 driver is expressing GAL4 within the mushroom-bodies as well. A three dimensional representation of the fluorescence confocal image is shown in Figure 3.6 B.

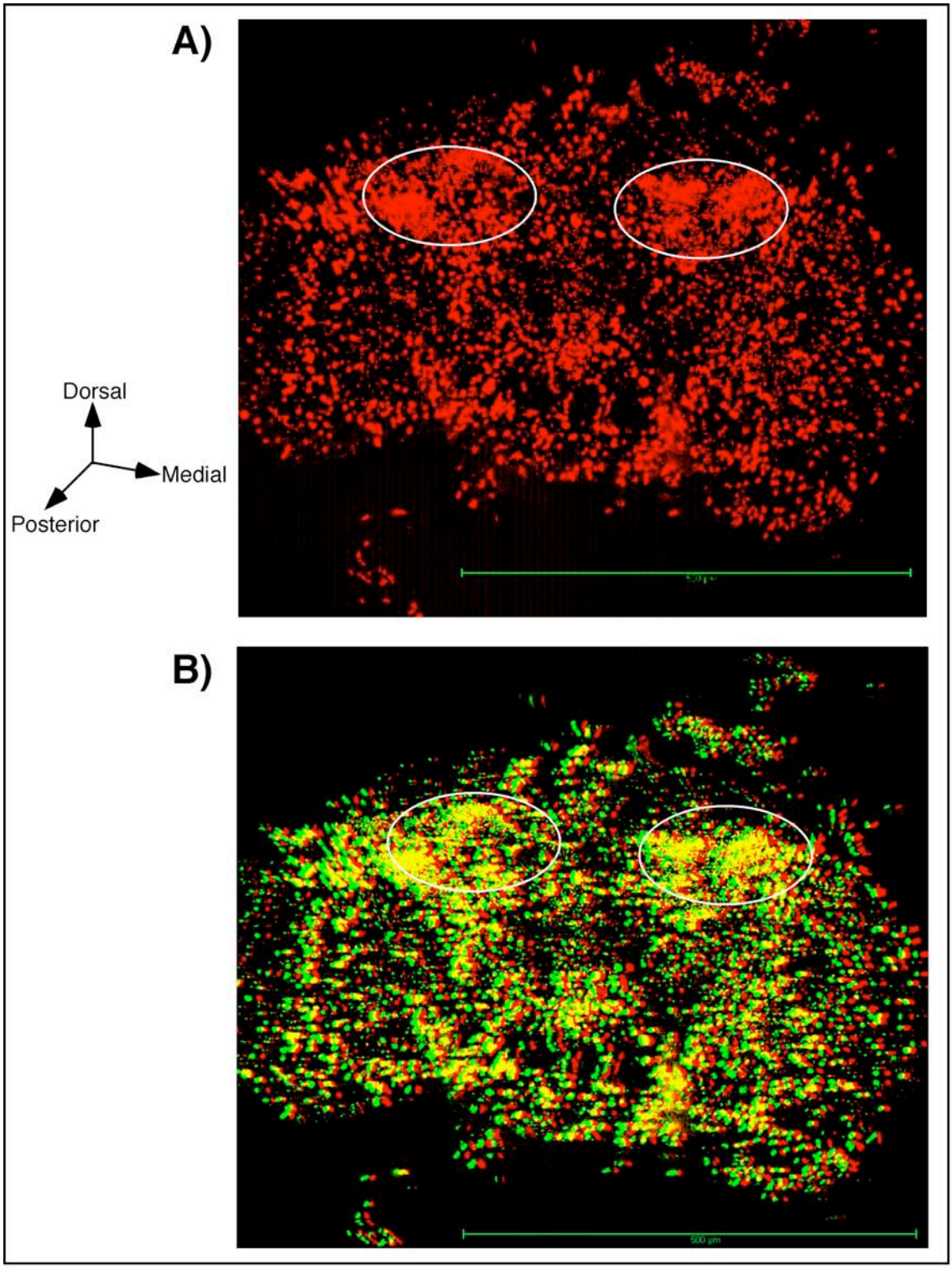

Figure 3.6 Confocal Microscopy Image of MB247-GAL4 driving DsRed-nls

Adult male brain of MB427-GAL4 crossed to UAS-DsRed-nls. (A) Original confocal image, and (B) 3-Dimensional representation. White circles indicates Kenyon cells. The green and red Images in (B) were both rotated ± 10° before merging.

The expression pattern of MB247 driving the expression of GFP showed a much more localised expression pattern (Figure 3.7 A). The mushroom-body structure is clearly visible within the α/α′ lobe region, although no distinction can be made between the lobes. There is also intense fluorescence along the β/β′lobe region, although, similar to the α/α′, no distinction could be made between the lobes (Figure 3.7 A). Although more localised, there was still strong auto-fluorescence in the brain, particularly in and around the antennal lobes, obscuring portions of the mushroom-body. A three dimensional representation of the fluorescence confocal image is shown in (Figure 3.7 B).

3.3.2.2 Analysis of MB739 by Fluorescence

The expression pattern of MB739 driving expression of DsRed-nls appeared to be even more extensive than MB247 in the larval stages (Figure 3.8). The expression increases with the development of the larval stages. There is strong expression in the salivary glands, increasing with age. There is also fluorescence along the main tracheal tubes running dorsally. The fluorescence along the gut of the larvae is very distinct, being the most intense around the proventriculus. In contrast to MB247, the MB739 pupae show little expression in the abdomen in comparison to the thorax and head regions (Figure 3.8). Similar to the adults of MB247, there was a ubiquitous expression throughout the adult, with no observable specificity for the *Drosophila* head.

The expression of MB739 driving expression of GFP is most intense in the salivary gland, with an increase from the first to third instar (Figure 3.8). There was a clear expression pattern along the gut of the larvae, increasing with age. The pupae exhibited a low-level ubiquitous expression throughout, although this was often obscured by auto-fluorescence. The adults both showed ubiquitous expression with no apparent bias for the head, similar to that of MB739 DsRed-nls.

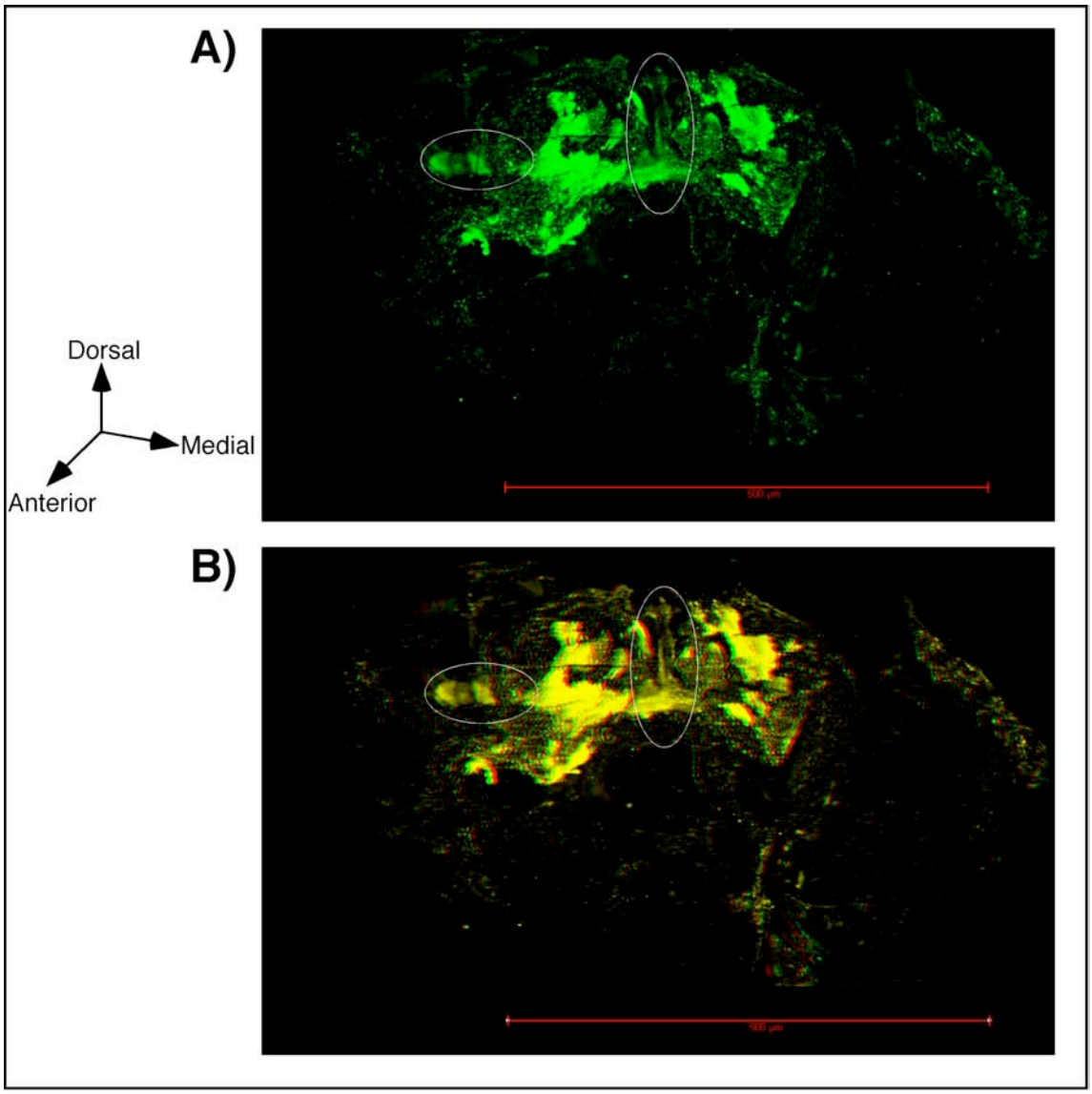

Figure 3.7 Confocal Microscopy Image of MB247-GAL4 Driving GFP

Adult male brain of MB427-GAL4 crossed to UAS-GFP. (A) Original confocal image, and (B) 3-Dimensional representation. White circles indicates mush-room-bodies. The green and red Images in (B) were both rotated ± 5° before merging.

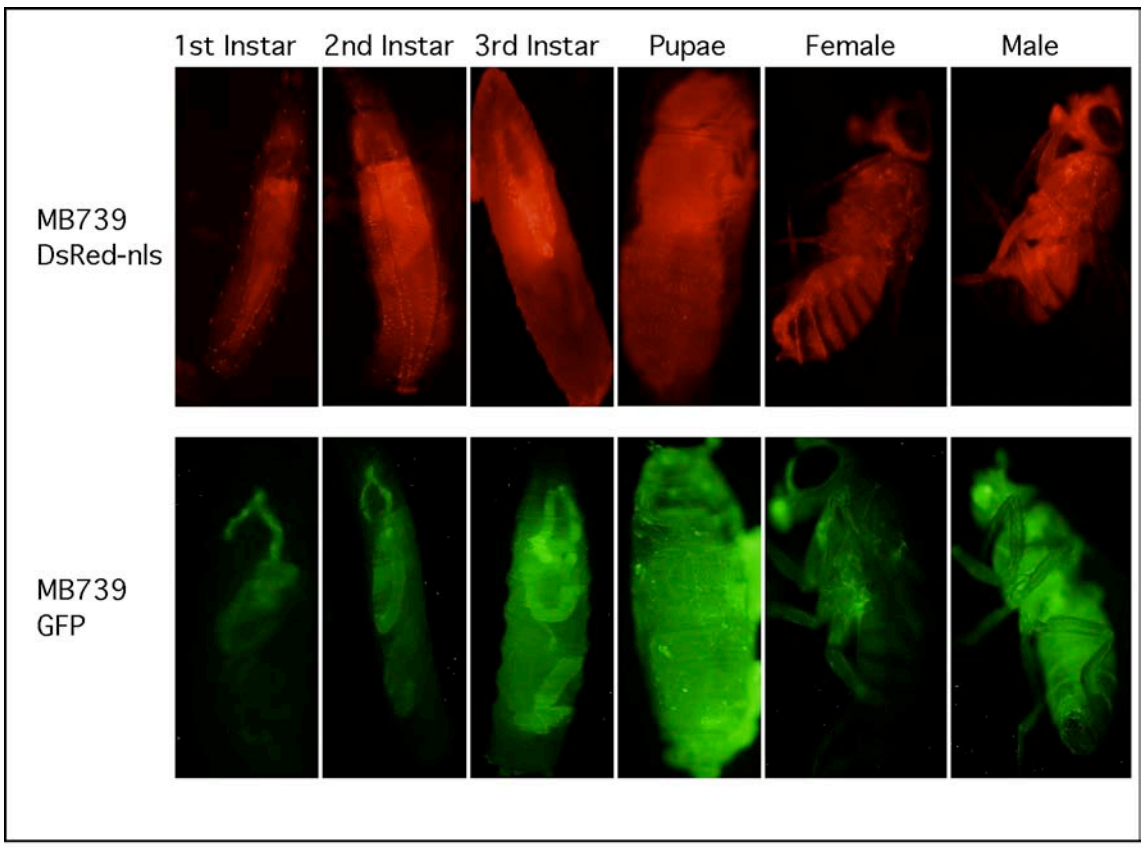

Figure 3.8 GAL4 Regulated Expression of DsRed-nls and GFP Throughout Development by MB739

Adult Flies, pupae and larvae that contain the either the UAS-GFP or UAS-DsRed-nls transgene. (A) MB739-GAL4 driving UAS-DsRed-nls, or (B) MB739-GAL4 driving UAS-GFP.

3.3.2.3 Analysis of MB772 by Fluorescence

Similar to MB739, the fluorescence of MB772 was, more extensive in the larval stages than MB247. There was extensive punctation in the first instar throughout the larvae (Figure 3.9). The second instar had fluorescence along the main dorsal trunk as well as the gut. The second instar also showed fluorescence in the salivary glands, although the glands are slightly obscured by the fluorescence from the gut. The third instar larvae show the same fluorescence as the second instar, although there is an increased fluorescence in the salivary gland (Figure 3.9). The pupae show a similar expression to that of MB739, with limited expression in the abdominal region, however there was clear fluorescence in the thorax and head (Figure 3.9). In contrast to MB739 and MB247, the fluorescence in the adults was more punctate and discrete. This indicated that expression was generally lower, as high levels of fluorescence tend to mask expression of DsRed-nls in the individual nuclei.

The expression of MB772 GFP is most intense in the salivary glands, with an increase from first to third instar (Figure 3.9). There was a clear expression pattern along the gut of the larvae, increasing with age. The pupae exhibited a low-level ubiquitous expression throughout, although this was often obscured by auto-fluorescence (Figure 3.9). The pupae were earlier in development than the pupae pictured in the previous sections, and the salivary gland is still visible. The adults showed very similar expression to the other driver lines, with no observable fluorescent bias to the head.

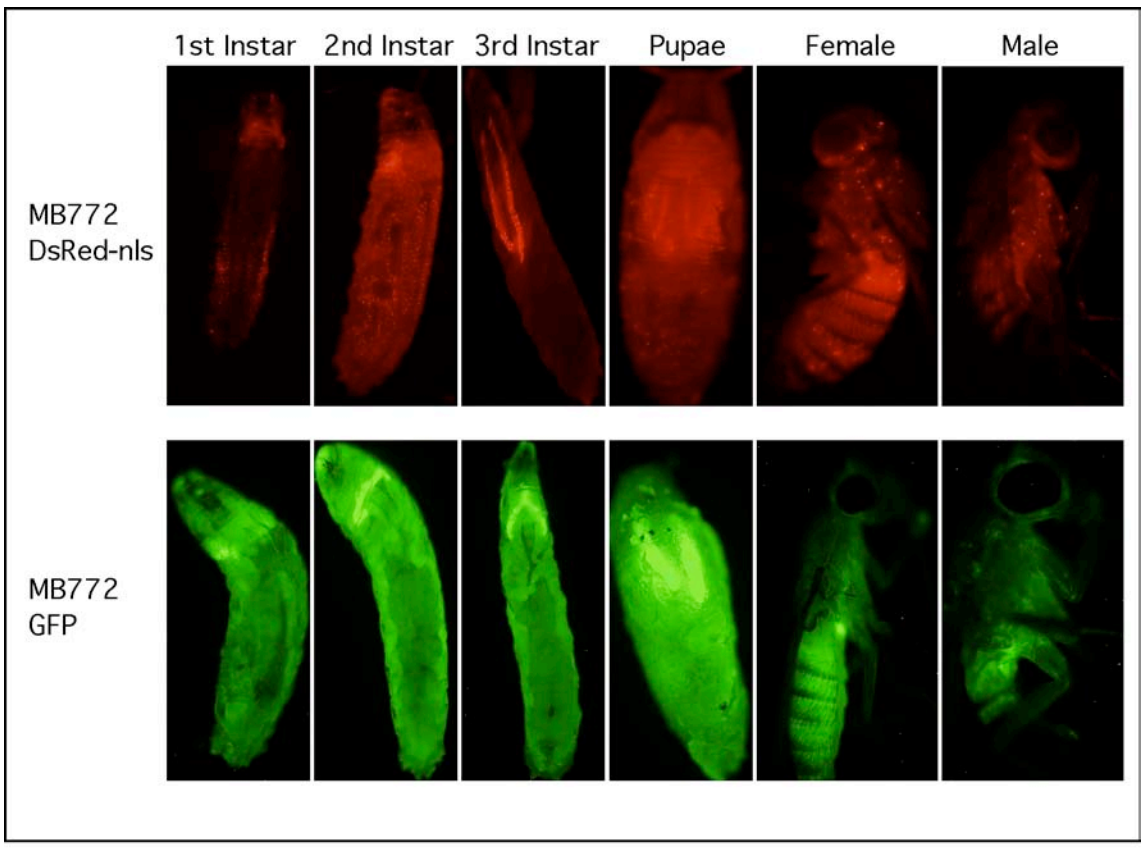

Figure 3.9 GAL4 Regulated expression of DsRed-nls and GFP Throughout Development by MB772

Adult Flies, pupae and larvae that contain the either the UAS-GFP or UAS-DsRed-nls transgene. (A) MB772-GAL4 driving UAS-DsRed-nls, or (B) MB772-GAL4 driving UAS-GFP.

3.4 RNAi-mediated Reduction of Expression of Targeted Genes

The objective of this section was to quantify the effectiveness of the expression of dsRNA on the relative levels of target mRNA. Two different GAL4 drivers were used in these experiments. Firstly, the whole-body knockdown induced by the *arm*-GAL4 driver, and secondly, the knockdown induced by the MB247 mushroom-body driver in *Drosophila* heads (Table 2.5).

All experiments were carried out in triplicate on a minimum of two independent biological samples. Primers used in this section are presented in Table 2.4, along with their relative efficiencies, and the run-protocol used for qRT-PCR is presented in Table 2.3. All primers designed in this section bind outside of the inverted repeat target region of the mRNA transcript to avoid reporting false levels of mRNA from the vector transcript. Adult males that were aged for three days were used for both sections, as they were the target of the behavioural assay. Crossing points of samples from the qRT-PCR are presented in Appendix 6.7. It was anticipated that expression of a hairpin dsRNA would cause a 75 % decrease in the total expression of the target gene (Dietzl et al., 2007).

3.4.1 Whole Fly qRT-PCR of *arm*-GAL4 Induced Transformant Lines

Three-day old males were collected, and samples were prepared as described in Section 2.7.1. Samples were analysed as described in Section 2.10.5.

3.4.1.1 Relative Levels of *HDACX* mRNA in Whole Flies

The assay was carried out on the offspring of the homozygous HDR1 line crossed to the *arm*-GAL4 driver. The relative level of *HDACX* mRNA in adult males was 0.70 ± 0.04 that of wild type male CantonS. This was a lower reduction in gene expression than expected (Figure 3.10).

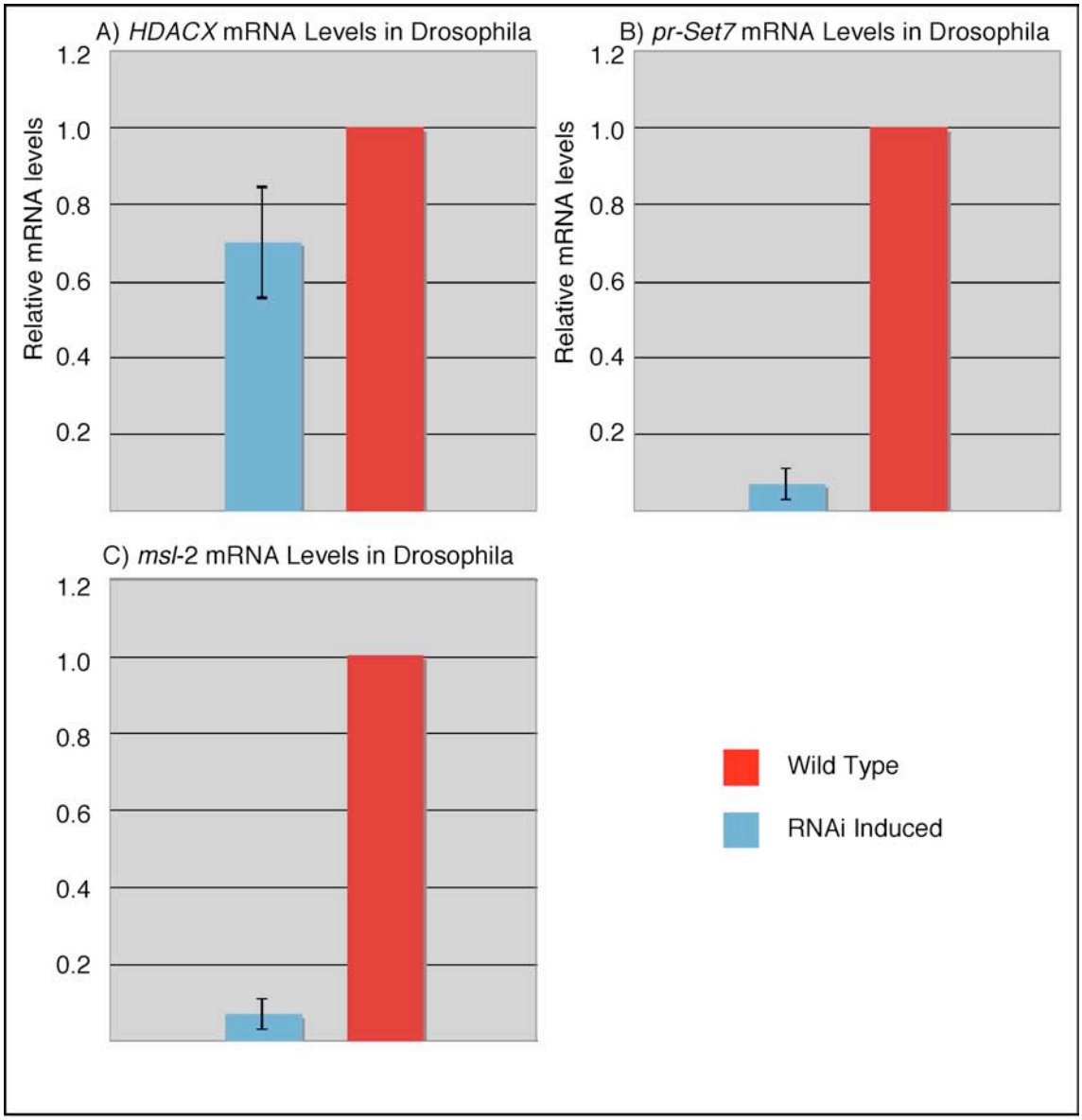

Figure 3.10 Relative mRNA Levels of RNAi Induced Transgenic Lines in Whole Flies

Relative mRNA levels in the whole body of adult flies that contain the *arm*-GAL4 transgene and either, (A) UAS-*HDACX* inverted repeat, (B) UAS-*pr-Set7* inverted repeat, or (C) UAS-*msl*-2 inverted repeat. Error bars represent 95 % confidence interval. Score normalised to wild-type levels.

3.4.1.2 Relative Levels of p*r-Set7* mRNA in Whole Flies

The assay was carried out on the offspring of the homozygous spSR3-3 line crossed to the *arm*-GAL4 driver. The mRNA levels of *pr-Set*7 were significantly reduced; the relative level in adult males was 0.12 ± 0.05 that of wild type male CantonS. This was greater than a 8-fold decease in the amount of *p-rSet*7 mRNA (Figure 3.10).

3.4.1.3 Relative Levels of *msl*-2 mRNA in Whole Flies

The assay was carried out on the offspring of the homozygous spSR3-3 line crossed to the *arm*-GAL4 driver. The mRNA levels of *msl*-2 were significantly reduced; the relative level in male adults was 0.07 ± 0.04 that of wild type male CantonS males. This was equivalent to almost a 15-fold decease in the amount of *msl*-2 mRNA (Figure 3.10).

3.4.2 Analysis of mRNA Levels by qRT-PCR of MB247 Induced Transformant Lines

The heads of three-day old males were collected as described in Section 2.13.6, and samples were prepared as described in Section 2.7.1. Samples were analysed as described in Section 2.10.5.

The assay was carried out on the offspring of the homozygous HDR1 line crossed to the MB247 GAL4 driver. The relative level of *HDACX* mRNA in this line was 0.63 ± 0.13 that of wild type levels found in male CantonS brains (Figure 3.11 A). This was a similar low level of reduction of expression as seen with the *arm*-GAL4 (Section 3.4.1.1). This was unexpected as the *HDACX* gene is expressed at a 7.4-fold increase in the brain (Chintapalli et al., 2007).

The assay was carried out on the offspring of the homozygous spSR3-3 line crossed to the MB247 GAL4 driver. The relative level of *pr-Set7* mRNA in this line was 0.75 ± 0.16 that of wild type levels found in male CantonS brains (Figure 3.11 B). The level of *pr-Set7* mRNA reduction was very different to that seen with the *arm*-GAL4 driver (Section 3.4.1.2).

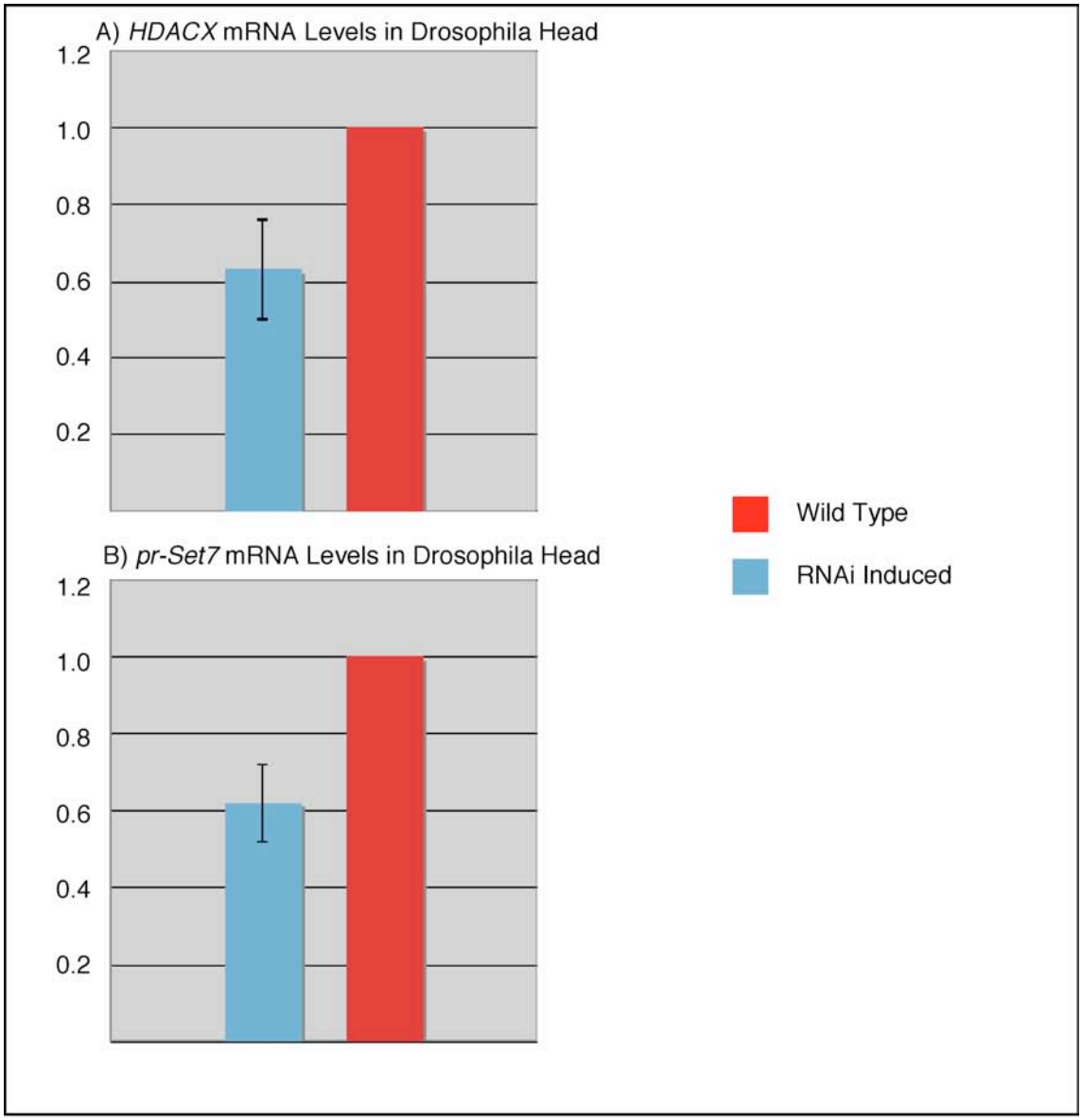

Figure 3.11 Relative mRNA Levels of RNAi Induced Transgenic Lines in Fly Heads

Relative mRNA levels in the heads of adult flies that contain the MB247 transgene and either, (A) UAS-*HDACX* inverted repeat, or (B) UAS-*pr-Set7* inverted repeat. Error bars represent 95 % confidence interval. Score normalised to wild-type levels.

3.5 *HDACX* Developmental Expression

The objective of this section was to analyse the expression of *HDACX* mRNA throughout the development of the *Drosophila*. This was due to the limited data on the expression of *HDACX* throughout development, although there was some expression data on larval tubules and fat bodies. Samples were collected from five stages of *Drosophila* development; 12 hr embryo, first instar, third instar, pupae, and adults. Second instar larvae were not collected because of the difficulty in getting a correctly aged and staged population for collection. Stages were collected as described in Section 2.13.8. Primers used in this section were the same used in Section 3.4.1.1(Table 2.4). Levels of *HDACX* throughout development were compared to levels three-day old adult fly levels.

The expression pattern throughout development is very clear (Figure 3.12). The highest levels of *HDACX* mRNA were seen in the adults. There is little expression relative to adults in the 12 hr embryo, with a relative level of 0.06 ± 0.01. The level in first and third instar larvae was also low, with 0.09 ± 0.02, and 0.06 ± 0.03. This indicated low, stable levels of *HDACX*, congruent with FlyAtlas (Chintapalli et al., 2007) data indicating very limited expression in early development.

Expression appears to begin to significantly increase at the pupal stage, with the development of the brain, with relative levels at 0.22 ± 0.04 (Figure 3.12). There is no published data on the expression of *HDACX* at the pupal stage, FlyAtlas (Chintapalli et al., 2007) does not publish pupal mRNA levels. These data agree with an expected increase in expression due to the development of the brain, where *HDACX* is highly expressed in the adults.

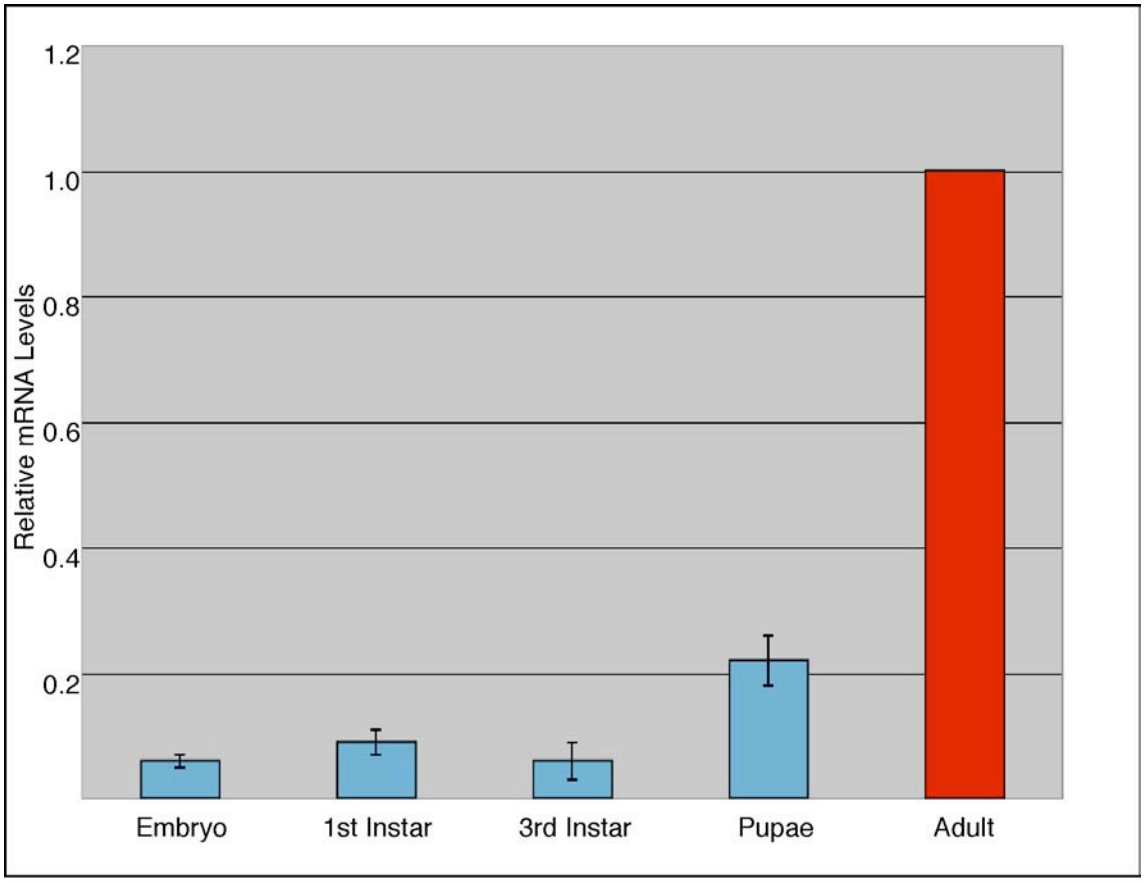

Figure 3.12 Relative mRNA Levels of *HDACX* Through Drosophila Development

Relative mRNA levels of *HDACX* at different points in *Drosophila* Development

3.6 Phenotypic Effect of Inverted Repeat lines

The knockdown of gene expression of a chromatin-modifying enzyme could potentially have dramatic phenotypic consequences due to widespread change in gene expression of downstream genes. In these experiments the GAL4 drivers *GMR*-GAL4 and *arm*-GAL4 were crossed with the inverted repeat lines HDR1, spSR3-3, and M2R3. The offspring of these crosses were examined for atypical eye formation and relative viability.

3.6.1 Phenotypic Effects of Eye Specific Promoter

Flies were anaesthetised, and were imaged using the Olympus SZX12 microscope (Section 2.13.10) (Figure 3.13). There were no observable phenotypic changes caused by these crosses. There was a slight observable alteration of colour of the eyes in all three vectors used, which was most probably due to an effect on the expression of the *miniWhite* gene, independent of any effects of the dsRNA. The knockdown of gene expression of *HDACX*, *pr-Set7*, and *msl*-2 did not effect eye development.

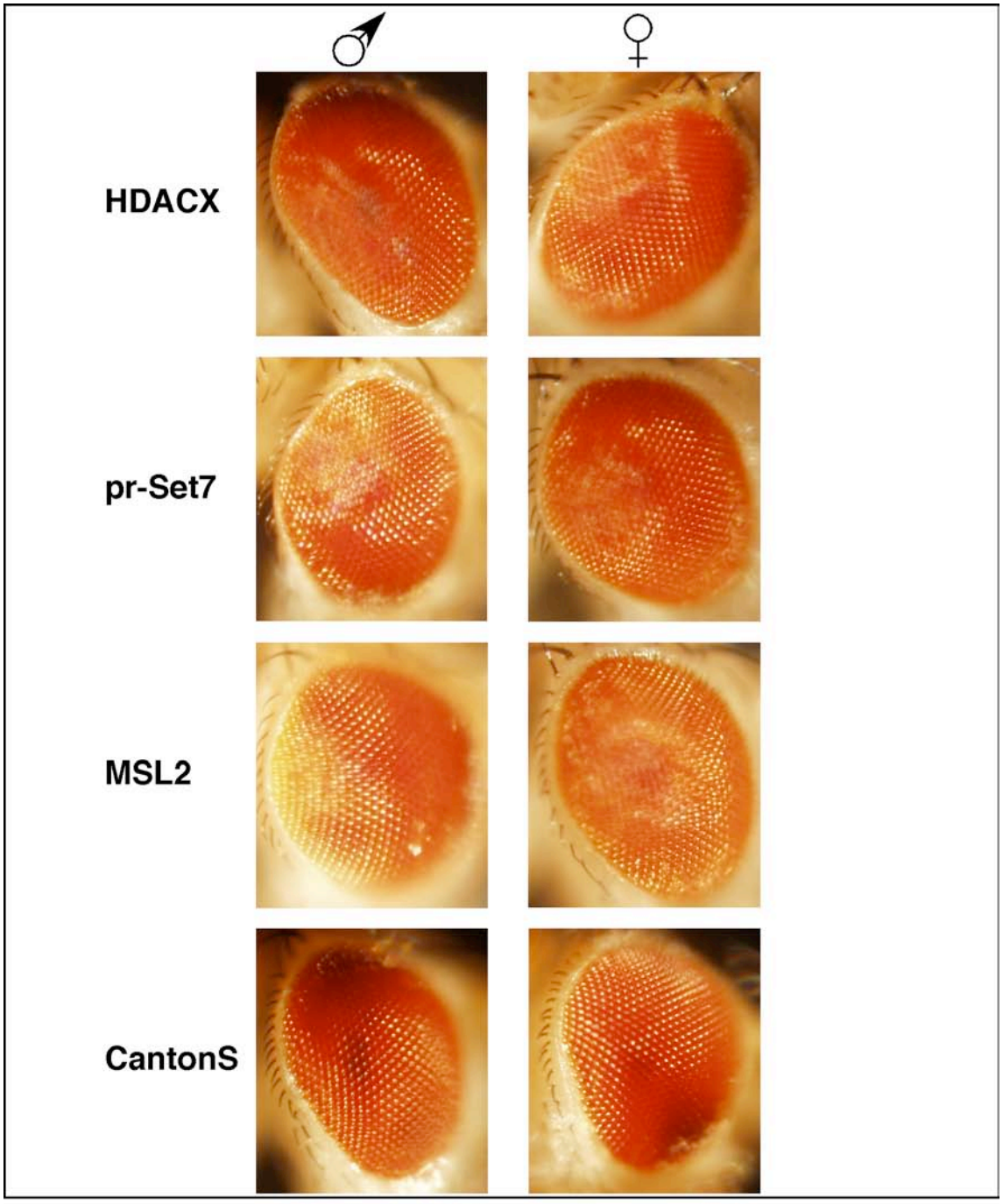

Figure 3.13 Eye specific Promoter of Inverted Repeat Lines

Adult flies that contain the GMR-GAL4 transgene and either, (A) UAS-*HDACX* inverted repeat, (B) UAS-*pr-Set7* inverted repeat, or (C) UAS-*msl-2* inverted repeat. (D) is CantonS wid type.

3.6.2 Effect on Viability of *arm*-Gal4 Induced Transformant Lines

The objective of this section was to observe any effects on viability caused by the constitutive expression of dsRNA. The transformant lines were crossed to a heterozygous *arm*-GAL4 driver over a *CyO* balancer chromosome as described in Section 2.13.13. Wild type CantonS were used as an external control for the *CyO* balancer effect on *Drosophila*. Statistical analysis assumed normal distribution (Appendix 6.8).

The offspring of the CantonS showed no sex bias between the offspring carrying the *arm*-GAL4 transgene, indicating it does not affect male or female viability. There was a small but statistically significant difference between the sex ratios of the CantonS carrying the *CyO* balancer chromosome, with a drop in male viability, at the p=0.05 and p=0.01 level (Figure 3.14). There was also a small but significant difference between the two male genotypes, at the p=0.01 level (Figure 3.14), indicating that the *CyO* balancer chromosome effects male viability.

The HDACX transformant line, crossed to *arm*-GAL4 line, gave no significant difference between the sex ratio of transformant flies carrying the *arm*-GAL4. The HDR1 line carrying the *CyO* balancer chromosome showed a small but significant drop in male viability, at the p=0.05 (Figure 3.14). There was no significant difference between the male genotypes as seen in the CantonS control.

The pr-Set7 transformant line crossed to *arm*-GAL4 line had no significant difference to the p=0.05 level between the males and females. The spSR3-3 line carrying the *CyO* balancer showed a small but significant difference between the sex ratios, with a drop in male viability, at the p=0.05 carrying the *CyO* balancer (Figure 3.14). There was no significant difference between the male genotypes.

The msl-2 transformant line crossed to *arm*-GAL4 line did show a significant difference to the p=0.01 level between the males and females. There was no significant difference between the sex ratio of flies carrying the *CyO* balancer chromosome (Figure 3.14). There was no significant difference between the male genotypes.

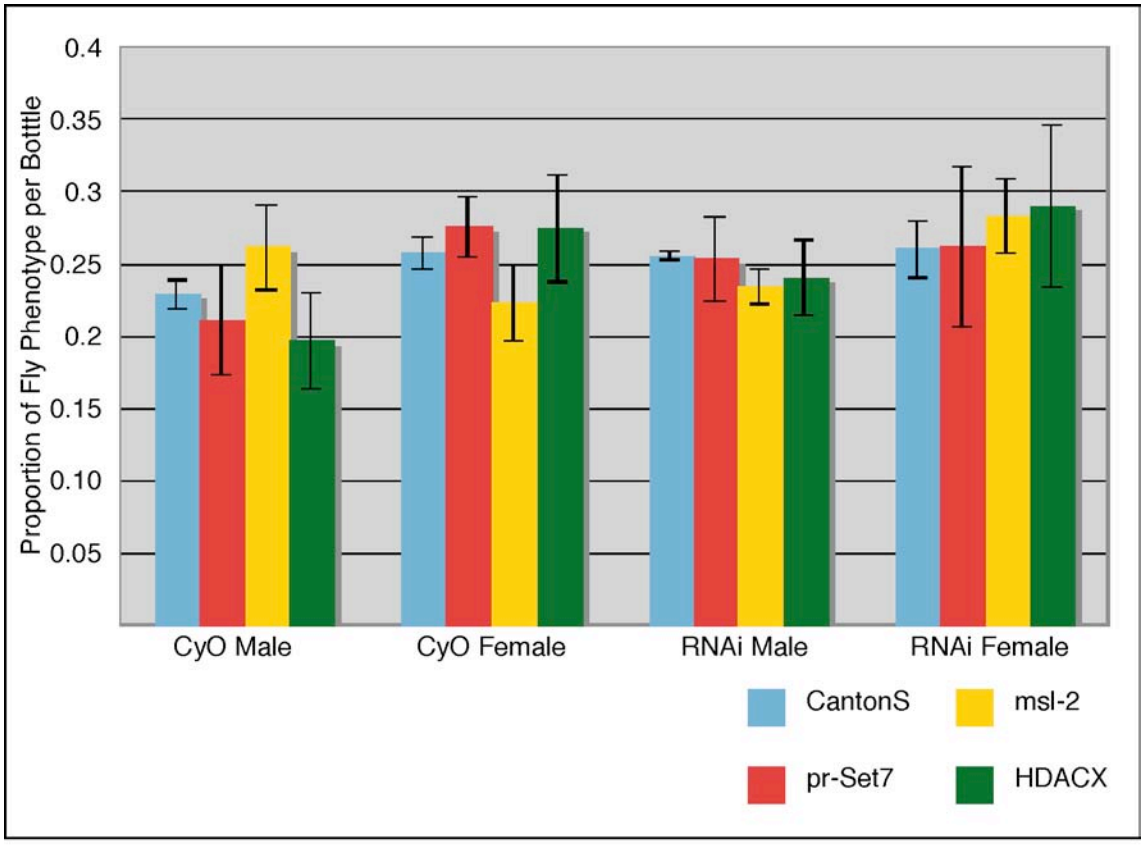

Figure 3.14 Effect of dsRNA on Fly Viability

Transformant lines were crossed to the *arm*-GAL4 driver. The proportion of flies in each bottle are represented above.

3.7 Effect of RNAi-Induced Reduction of Target Gene Expression on Long-Term Memory

The objective of this section was to observe any possible effects the dsRNA knockdown of the target transcripts had on the ability of *Drosophila* to form long-term memory. The *Drosophila* lines HDR1 spSR3-3, CamKII, and CantonS were used in this experiment (Table 2.5 and 2.6). Each transformant line was crossed to MB247 mushroom-body specific GAL4 driver. The long-term memory of the male offspring crosses were assayed using the courtship-conditioning assay (Section 2.14). Each fly line was assayed between 25 and 35 times. Three sets of data are presented for each line assayed. The raw data, showing each individual fly assay, are presented in a scatter plot. The raw data were then analysed as described in Section 2.14, giving the mean and errors to a 95 % confidence. Finally, the data were normalised to the unconditioned data from each fly line (Section 2.14.5). This was done to remove bias between different assay lines that may show a variance in the average courtship index of unconditioned flies. These raw data, along with statistical analysis, are presented in Appendix 6.6.

3.7.1 Behavioural Analysis of CantonS

The CantonS wild type strain were the positive control in this assay, in that they are capable of learning in this paradigm. The raw data (Figure 3.15 A) show two distinct groups in the conditioned line. One group within the conditioned line showed a marked decrease in their courtship index, whereas the second group did not appear to show a decrease (Figure 3.15 A). This is most likely due to the learning paradigm used, as it was not an established protocol within the laboratory. This is the supported by the unconditioned data, as the raw data show a less diverse set of courtship indices (Figure 3.15 A). The statistical analysis of the raw data showed that the conditioned and unconditioned sets had a mean courtship index of 5.9 ± 1.19 and 7.2 ± 0.78, respectively, these data gave a significance at $p=0.06$ (Figure 3.15 B). The data set in Figure 3.15 C shows the normalised data of Figure 3.15 B.

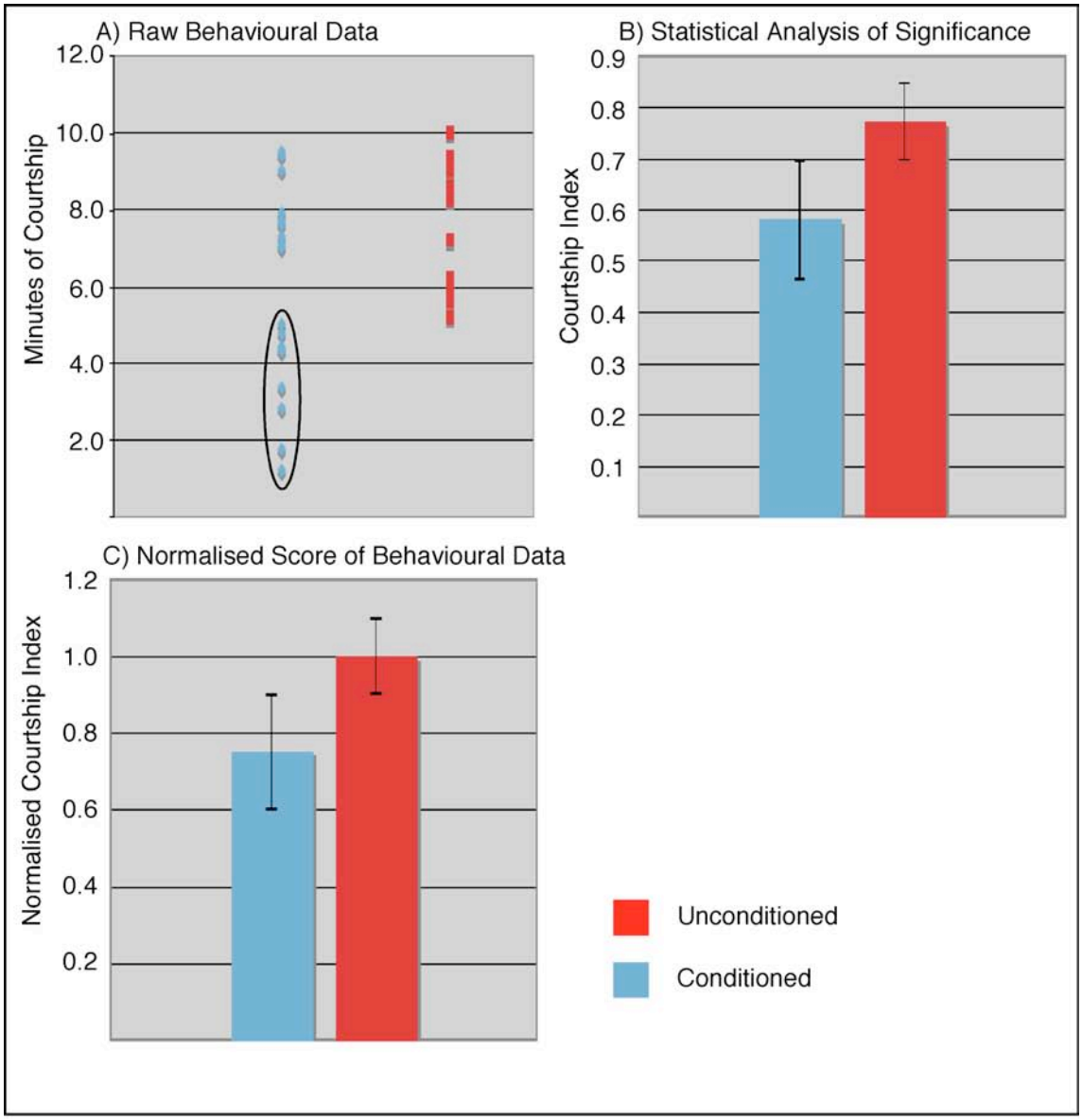

Figure 3.15 Courtship Data of Adult CantonS Flies

Courtship data of adult CantonS . (A) Raw data of individual courtship times. (B) Mean courtship index with 95% confidence shown. (C) Normalised courtship index of data. Circled region in (A) represents a distinctive group within the conditioned group. Unconditioned n value = 19, conditioned n value = 18

3.7.2 Behavioural Analysis of *CamKII* Inverted Repeat

The CamKII inverted repeat line were the negative control in this assay, in that they are unable to form long-term memories (Byrne and Kandel, 1996). The raw data (Figure 3.16 A) shows a wide variance in individual courtship indices in both the conditioned and unconditioned data sets. The statistical analysis of the raw data showed that the conditioned and unconditioned sets had a mean courtship index of 4.5 ± 1.52 and 4.7 ± 1.5, respectively, providing no significant difference to a 95 % confidence (Figure 3.16 B). The large errors produced in the statistical analysis of these data sets reflect the variance of this line within the assay. The data set in Figure 3.16 C shows the normalised data of Figure 3.16 B. This was done to remove the bias of differing unconditioned mean times between this assay line and the CantonS assay line to allow a clearer comparison.

3.7.3 Behavioural Analysis of *HDACX* Inverted Repeat

The HDR1 line was an experimental line in this assay. The raw data (Figure 3.17 A) show very little variance in individual courtship indices in both the conditioned and unconditioned data sets. The courtship indices of both the conditioned and unconditioned groups were high. The statistical analysis of the raw data showed that the conditioned and unconditioned sets had a mean courtship index of 7.9 ± 0.91 and 7.2 ± 0.78, respectively, providing no significant difference to a 95 % confidence (Figure 3.17 B). The data set in Figure 3.17 C shows the normalised data of Figure 3.17 B. This was done to allow analysis with the CantonS control line.

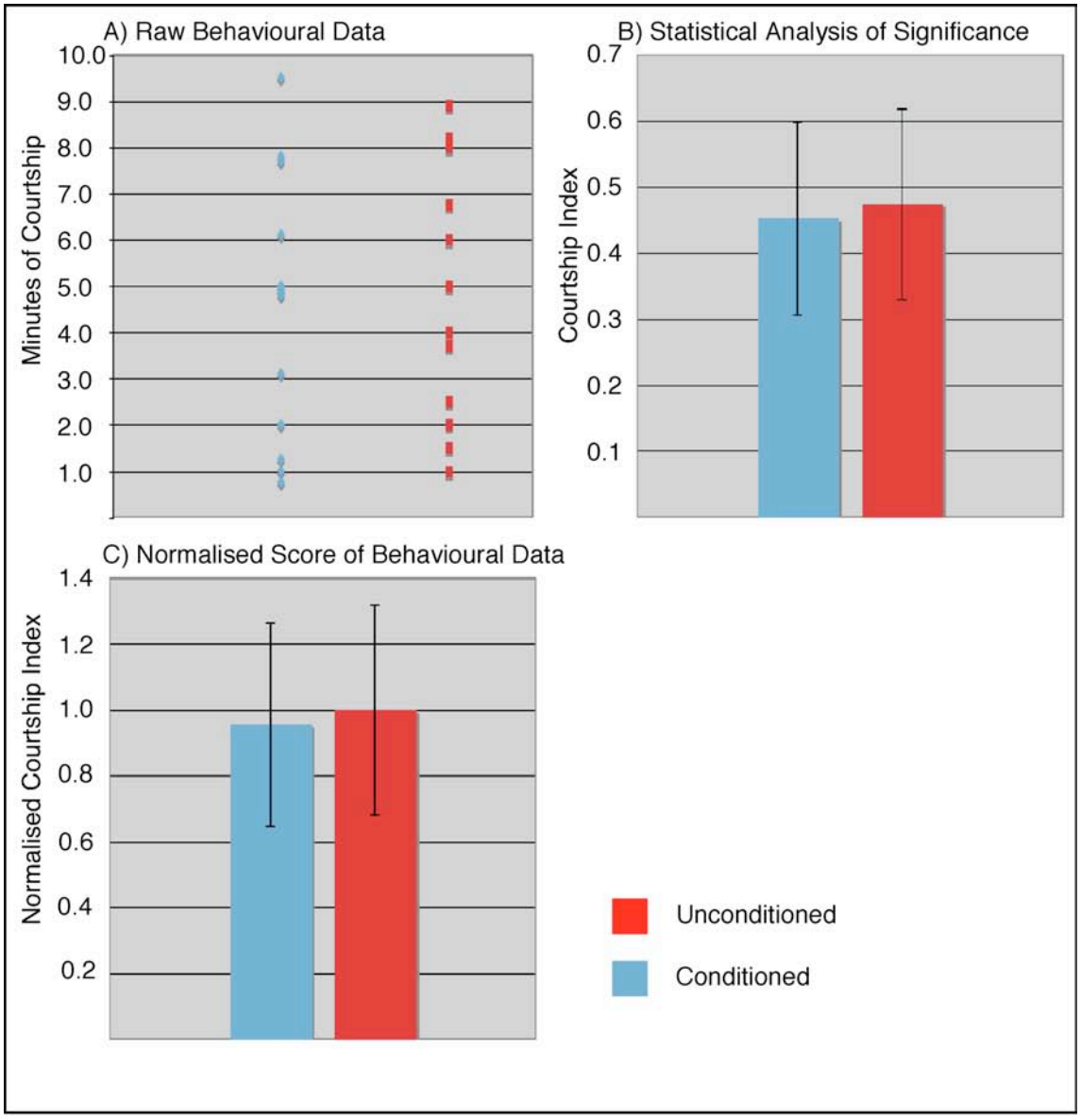

Figure 3.16 Courtship Data of Adult Flies That Express Reduced Levels of CamKII

Courtship data of the off spring of a CamKII inverted repeat transgenic line crossed with MB247 GAL4 driver. (A) Raw data of individual courtship times. (B) Mean courtship index with 95% confidence shown. (C) Normalised courtship index of data. Unconditioned n value = 13, conditioned n value = 13

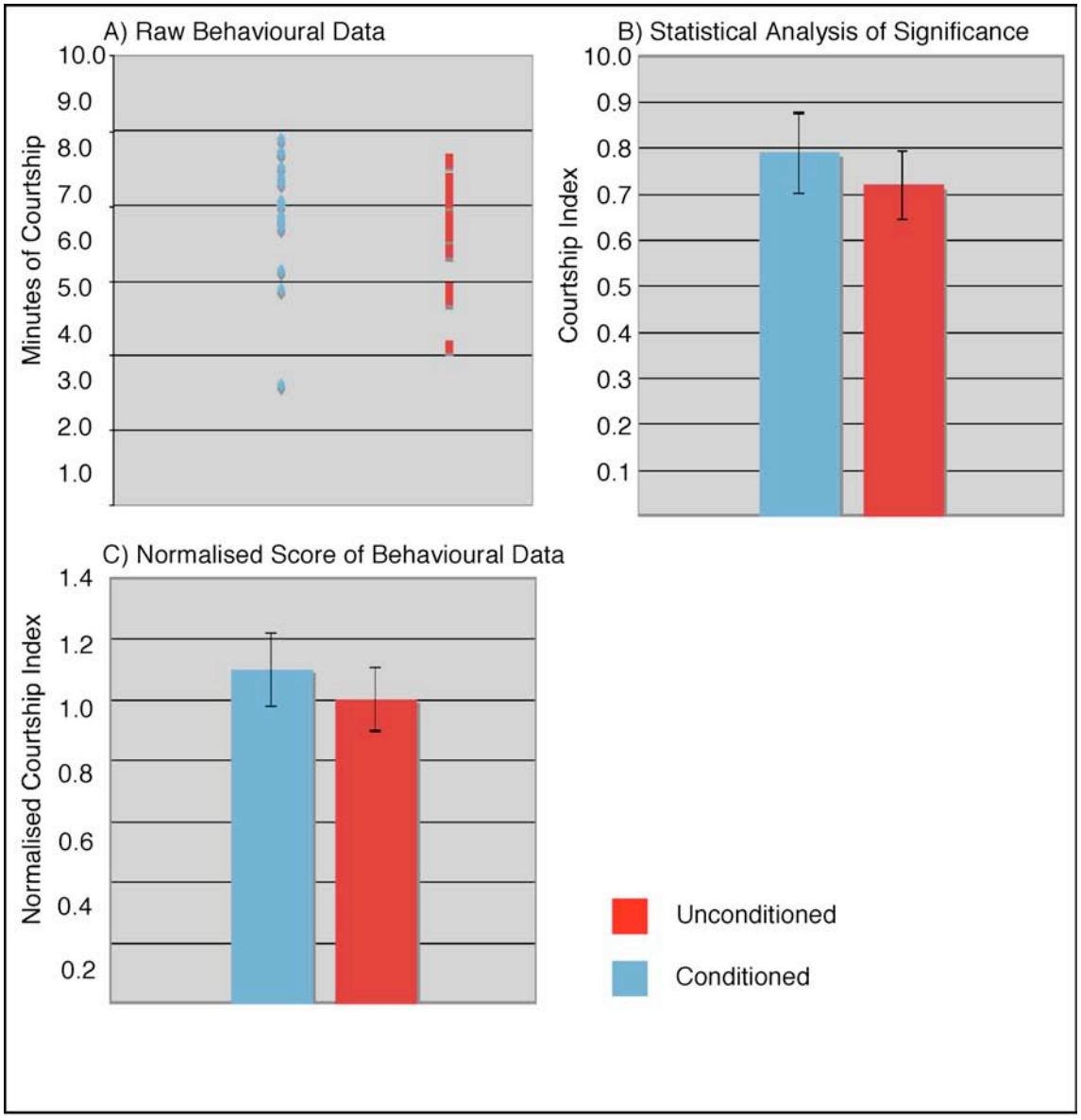

Figure 3.17 Courtship Data of Adult Flies That Express Reduced Levels of *HDACX*

Courtship data of the off spring of a *HDACX* inverted repeat transgenic line crossed with MB247 GAL4 driver. (A) Raw data of individual courtship times. (B) Mean courtship index with 95% confidence shown. (C) Normalised courtship index of data. Unconditioned n value = 14, conditioned n value = 15

3.7.4 Behavioural Analysis of *pr-Set7* Inverted Repeat

The spSR3-3 line was an experimental line in this assay. The raw data (Figure 3.18 A) show a notable amount of variance in individual courtship indices in both the conditioned and unconditioned data sets. The courtship indices of both the conditioned and unconditioned groups were average, compared to the CantonS control line. The statistical analysis of the raw data showed that the conditioned and unconditioned sets had a mean courtship index of 6.8 ± 1.14 and 7.3 ± 1.45 respectively, providing no significant difference to a 95 % confidence (Figure 3.18 B). The data set in Figure 3.18 C shows the normalised data of Figure 3.18 B. This was done to allow analysis with the CantonS control line.

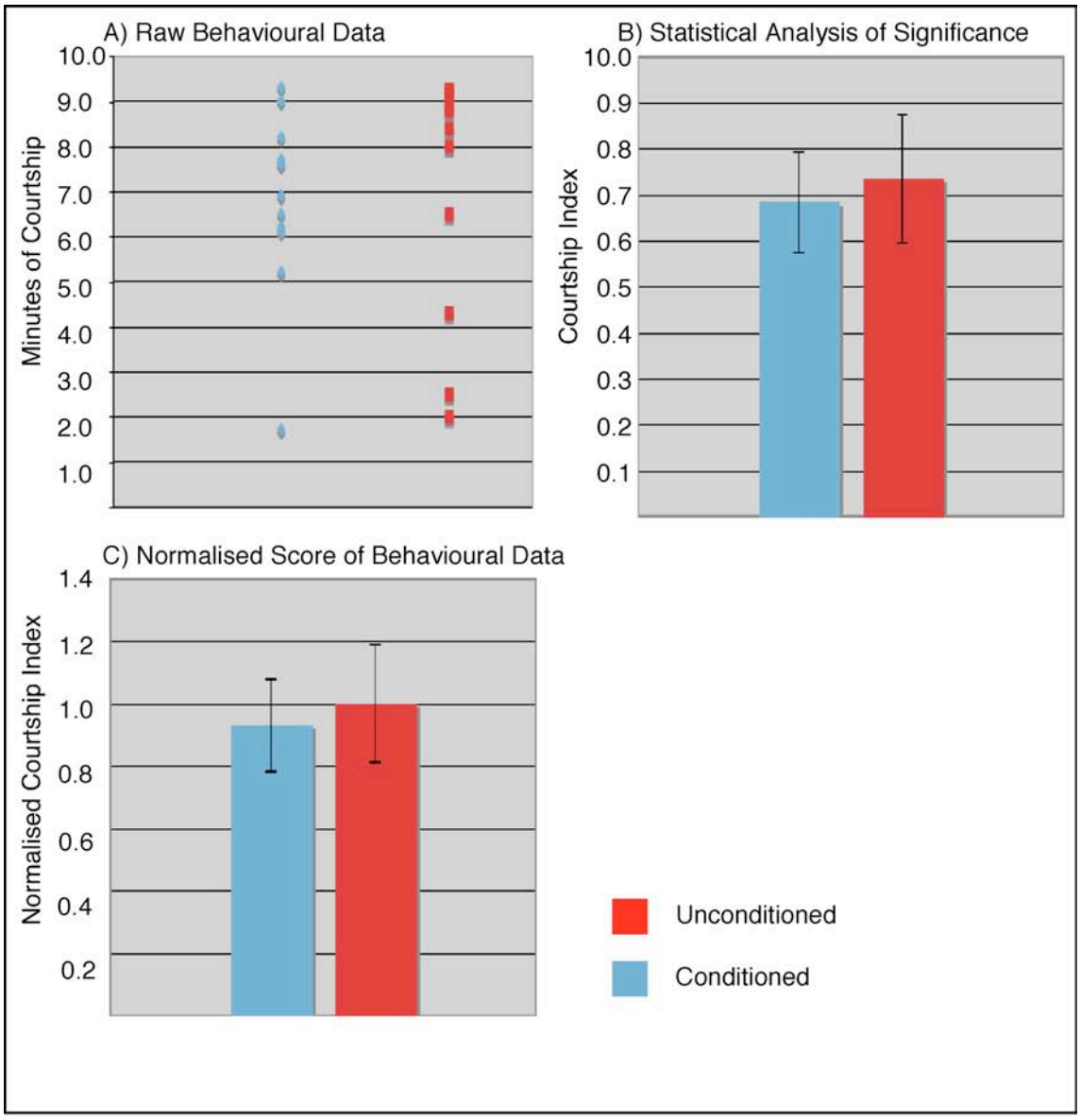

Figure 3.18 Courtship Data of Adult Flies That Express Reduced Levels of *pr-Set7*

Courtship data of the off spring of a *pr-Set7* inverted repeat transgenic line crossed with MB247 GAL4 driver. (A) Raw data of individual courtship times. (B) Mean courtship index with 95% confidence shown. (C) Normalised courtship index of data. Unconditioned n value = 12, conditioned n value = 11

Chapter Four

Discussion

4.1 Creation of UAS-Inverted Repeat Lines

The creation of the vectors carrying the inverted repeats had two issues that needed to be addressed. Firstly, it was anticipated that plasmids containing long inverted repeats would be unstable in *E. coli*. This potential problem was addressed by the use of the recombination deficient Stbl2™cell line. Indeed, analysis of plasmids from individual *E. coli* colonies showed that in general the inverted repeat constructs were not re-arranged due to recombination. The long inverted repeats could potentially have made the transgene unstable in transgenic *Drosophila*. Thus the use of the *CS*2 intron, which provided physical separation of the repeats, also contributed to its stability. Secondly, was the inability to sequence the completed vector, which was most likely due to the inverted repeats causing interference with the genuine sequencing reads. To overcome this, several restriction digests were used to confirm that the second fragment had been sub-cloned, and that it was in the correct orientation. This approach proved to be satisfactory in analysing the second sub-cloning step of this vector, as indicated by subsequent qRT-PCR analysis.

The creation of a vector-target system for targeted integration of a vector within the *Drosophila* genome emerged as a minor objective in this study. Position effects on an insert could alter their expression, and memory assays can be very sensitive to the isogeny of a *Drosophila* population (Sakai et al., 2004). The sub-cloning of an *attB* site into the RNAi vector resulted in the vector being targeted to the chromosome carrying the complementary *attP* site 100 % of the time. Future work would require that inverse PCR be carried out to confirm the insert is targeted to the correct location, and that lines carrying *attP* be backcrossed into the CantonS genetic background for use in memory assays.

4.2 Expression Analysis of GAL4 Drivers

The expression analysis of common GAL4 drivers and mushroom-body specific GAL4 drivers produced both expected and unexpected results. As the DsRed-nls reporter contains a nuclear localisation signal, this produced very bright fluorescence in the cell nucleus rather that being spread across the entire cell body. The fluorescent microscopy analysis of the artificial promoters *Sgs3*-GAL4 and *GMR*-GAL4, which are salivary- and eye-specific respectively, were both very specific for their reported tissues. The *arm*-GAL4 driver did not show the ubiquitous expression that was expected. The *arm*-GAL4 showed punctate expression throughout the body of larvae and adults. The *armadillo* gene is expressed ubiquitously throughout development and in adults (Chintapalli et al., 2007). The *arm*-GAL4 was constructed from a portion of the entire promoter (Vincent et al., 1994); this could result in expression that is not ubiquitous throughout the fly. Alternatively, it is possible that *arm*-GAL4 is expressed in all cells but that the level of expression is much higher in some cells, leading to the punctate expression pattern.

The expression pattern of the BSC 8176 GAL4 driver, which is reported to express in adult muscles and to increase with the age of the adult fly (Bloomington Stock Center) gave extensive expression throughout fly development. The DsRed-nls fluorescence pattern indicates that GAL4 expression begins very early in development and the intensity of fluorescence indicates that it is a strong GAL4 driver. The likely explanation for this expression is that the GAL4 transgene has been integrated into a genomic location that is required to be active for developmental processes but is not exclusive to the adult muscle.

The expression pattern of the mushroom-body drivers MB247, MB739, and MB772, gave expression patterns that did not match their reported expression (Pavlopoulos et al., 2008; Tanaka et al., 2008). The DsRed-nls fluorescence of all three drivers showed expression throughout the development of the larvae and was widespread in the adult fly. This was a surprise, as all three drivers were reported to be mushroom-body specific, and are used in memory assays. The GFP expression, which does not have a nuclear localisation signal, gave some indication as to the possible reasons behind this,

as its fluorescence was much harder to detect and was often obscured by auto-fluorescence in the developing flies. This implies that previously reported expression observed in these mushroom-body drivers may have suffered from the loss of signal due to auto-fluorescence of GFP. I was unable to find any study that had analysed the expression pattern of these drivers using a fluorescence marker with a nuclear localisation signal. Work by Krashes *et al.* (2007) used membrane bound GFP, which appeared to give a clearer pattern of the MB driver expression, however, as it was not nuclear localised and would likely suffer from similar auto-fluorescence as non-localised GFP, possibly leading to a loss of the subtle signals that appear to be present in the DsRed-nls. The expression pattern seen in the DsRed-nls may predict the correct expression of the mushroom-body drivers, as there are very low levels of auto-fluorescence in the developing flies.

The implication for this study is that RNAi may have been active before the adult stage, and the impact on mushroom-body development is therefore unknown, as well as possibly being expressed throughout the brain and body. This is a concern for both the genes analysed, as *HDACX* is highly expressed in the *Drosophila* brain, and therefore may play a crucial role in its development, and *pr-Set7* has an important role in the cell cycle, which could possibly result in a more general defect in the fly brain, body, or behaviour.

Future work to confirm these predictions, and to exclude the possibility that it is some artefact of the experiment, would be to analyse the mRNA levels of an RNAi targeted gene, such as *msl-2*, in male larvae, under the control of the mushroom-body drivers, this would allow for the detection of expression of the MB drivers prior to the development of the brain and MB. Also, analysis of relative levels in the RNAi induced flies between the body and head, when compared to wild type. This would give quantitative data on the practical effects that the apparent widespread GAL4 expression has on UAS_{GAL4} controlled constructs. The *msl-2* gene would make a good target, as it is male specific, the larvae can be sexed, the mRNA is relatively abundant, the transformant lines exist with the same vector constructs used to drive RNAi is this study, and the efficacy of the RNAi has already been established using qRT-PCR.

The fluorescent confocal microscopy of the MB247 driver gave very interesting results, with stark differences between the DsRed-nls and GFP fluorescence. The observable expression of DsRed-nls was much more widespread than the obsevable expression of GFP, and appeared to be present in the majority of cells in the brain. The Kenyon Cell bodies were distinguishable within the mass of fluorescence, appearing as compact groups in the upper mid-brain. The expression of GFP was much clearer than that of DsRed-nls, with the mushroom-bodies being clearly visible. The reason for the difference between the two fluorescent markers is probably due to the nuclear localisation signal of the DsRed-nls, and the absence of this signal for GFP. The DsRed-nls maker had very little auto-fluorescence, and the nuclear localisation signal targeting it to the nucleus, possibly made it more sensitive to detecting the expression at lower levels. The GFP fluorescence, by contrast, gave considerable auto-fluorescence, which could easily obscure low levels of expression. The absence of a nuclear localisation signal on the GFP marker also could have further dispersed the signal from cells that were expressing GAL4, causing further dilution of the GFP signal. The absence of a nuclear localisation signal did provide one clear advantage over the nuclear localised DsRed-nls. The cytoplasmic distribution of the GFP, coupled with the tight axonal bundles of the mushroom-bodies, gave a clear picture of the morphology of the mushroom-bodies (Figure 3.7).

In relation to this study, the expression pattern of MB247 needs to be described at a higher resolution, with continued confocal work. The practical implications of the expression pattern need to be identified, as the ectopic expression of the driver may impact on other regions of the brain. As the ectopic expression may be low, they may not be driving expression at a level that would cause significant impact on expression of a UAS_{GAL4} controlled construct. *In situ* hybridisation analysis, as well as antibody staining, needs to be carried out to analyse whether or not the ectopic expression impacts on mRNA and protein levels in regions other than the mushroom-bodies.

The two properties of the fluorescent markers could be used for a possible future project; the development of an artificial promoter for mushroom-body expression. As has already been discussed, artificial promoters such as *Sgs3*-GAL4 and *GMR*-GAL4 have very tight expression patterns, with no observable ectopic expression. Using the apparent sensitivity of the DsRed-nls for detecting GAL4 expression, a robust assay could be developed to test artificial promoters, using likely promoter candidates from memory-associated genes, to screen for Kenyon Cell specific expression. Coupling this to GFP expression would allow analysis of which groups of Kenyon Cells are associated with which lobes of the mushroom-bodies. The difficultly in this approach is that genes involved in memory are likely to be expressed in other tissues, and fine dissection of the promoter would be necessary to find regions specific for mushroom-body expression. Further to this, it may be necessary to multimerize a small region of the promoter to produce the desired expression pattern, as was done with the eye-specific *GMR* promoter. Coincidentally, identifying promoter regions that produce specific mushroom-body expression may help elucidate important regulator functions involved in memory function.

4.3 Analysis of Relative mRNA Levels and Phenotypic Effects of RNAi

4.3.1 RNAi-mediated Knockdown of Gene Expression

Analysis of the RNAi-induced knockdown by quantitative PCR showed that the level of reduction of gene expression was variable. The *arm*-GAL4 driver induced a significant reduction in mRNA levels of *pr-set7* and *msl-2*. These knockdowns showed a 8- and 15-fold reduction in mRNA levels, respectively, when compared to wild type levels. The change in levels of *HDACX* mRNA was far less dramatic, with less than a 2-fold reduction. This could be due to two reasons, firstly, the dsRNA produced by the inverted repeat could be ineffective at inducing knockdown of the target mRNA, or secondly, the *arm*-GAL4 driver may not express strongly in the cells that express *HDACX* mRNA.

With the MB247 GAL4 driver, both *HDACX* and *pr-Set7* mRNA levels were reduced by less than 2-fold in heads. It is unlikely that the small reduction in *pr-Set7* mRNA

levels could be due to dsRNA efficacy to induce knockdown, as the same inverted repeat line responded very effectively to the *arm*-GAL4 driver. Thus it is more likely that the low reduction suggests that the MB247 driver is only expressed in a small fraction of the cells in the head that actively transcribe the endogenous *pr-Set7* gene. The same argument could explain the low reduction in *HDACX* mRNA levels. This highlights the critical importance of determining exactly which cells in the *Drosophila* brain express HDACX and pr-Set7. This could be accomplished by using *in situ* hybridisation or antibody staining, but the latter would require development of an antibody for HDACX.

4.3.2 Relative *HDACX* mRNA Levels Through Development

The analysis of relative levels of *HDACX* mRNA through development gave an unexpected result. The level of mRNA is very low throughout development, with 12-hour embryos, first instar, and wandering third instar larvae all expressing mRNA levels less the 10 % that of adult flies. The level in pupae is approximately 20 % that of adults. The increase of mRNA levels in the pupae probably reflects the development of the adult brain within the pupae. Genes that are preferentially expressed in adults are relatively rare and are usually involved in eye development (Arbeitman, 2002), although this does not appear to be the case with *HDACX*.

4.3.3 Phenotypic effects of RNA-mediated Knockdown of Gene Expression

The effect on viability and eye phenotype of the RNAi knockdowns showed few meaningful results. There were no profound effects on viability, and no observable eye phenotype. However, both *pr-Set7* and *msl-2* are essential genes, and their levels of mRNA in the knockdown lines were greatly reduced, so some effect on viability was expected in these lines. *HDACX* is expressed in the adult fly, and was not expected to have an effect on viability, however the poor knockdown leaves this open to further analysis. The reason for the RNAi having no real effect on viability could be due to protein levels, as it is possible that the reduction in mRNA does not translate into a reduction in protein. Future work would need to include western blots to analyse relative levels of protein.

4.4 A Possible Role for the HDACX and pr-Set7 Chromatin Modifying Proteins in Long-Term Memory

This study showed that RNAi-induced knockdown of the *HDACX* and *pr-Set7* mRNA in *Drosophila* males disrupted long-term memory in courtship behaviour. Analysis of the positive control, CantonS, indicated long-term memory formation and recollection, with the conditioned line having a reduction in the courtship index. However, the drop in the courtship index was significant at the p=0.06 level, a significance of below p=0.05 would have made the results from these experiments more robust. The negative control, the *CamKII* RNAi induced line, did not have any statistically significant difference between conditioned and unconditioned groups. However, the variance in the courtship index of individual flies within this line was very large. This may indicate that *CamKII* is important for normal courtship behaviour, and further analysis of this line is needed. Flies carrying an uninduced *CamKII* inverted repeat will need to be assayed to test if this line has the ability to be conditioned in the behavioural assay, if this is possible, then it may indicate that *CamKII* could have pleiotropic effects on courtship behaviour. Flies will need to be assayed for normal mobility and other courtship behaviours such as latency of courtship initiation (O'Dell, 2003). This is also necessary to assess whether the apparently widespread expression of MB247 impacts on behaviour and mobility.

The *HDACX* inverted repeat line showed no ability to learn, and their individual courtship indices showed very little variance, indicating that it may play a role in long-term memory function. The qRT-PCR results show very little knockdown of the mRNA, however the relative reduction in the mushroom-bodies may be higher. Future work would need to include *in situ* hybridisation to elucidate the localisation of the *HDACX* mRNA within the *Drosophila* brain, and to monitor any effects on mRNA levels within the mushroom-bodies in RNAi-induced lines.

The *pr-Set7* inverted repeat line also showed no ability to learn, although it did demonstrate slightly more variance in the individual courtship indices. The function that *pr-Set7* has in memory function may not be as straightforward as that of *HDACX*, which is expressed exclusively in adult brains, as *pr-Set7* is expressed throughout development and plays a central role in mitosis. The fluorescent work carried out in this study indicated that MB247 expresses throughout development, and therefore may cause a more systemic disruption to mushroom-body formation. Fluorescent microscopy would need to be carried out to analyse formation of the mushroom-bodies within this line.

If knockdown of pr-Set7 or HDACX is affecting mushroom-body development, the TARGET system could be used to inhibit GAL4 until after development of the adult brain is complete (McGuire et al., 2004). A major future challenge of this project would be to elucidate which genes within the mushroom-bodies are being regulated by HDACX and pr-Set7. A possible approach to this problem is to use the Solexa genome analysis system to analyse expression patterns in both wild type and RNAi lines, before and after conditioning.

4.5 Technical Problems Arising Within this Study

The courtship indices of the flies in this experiment were high, relative to other studies (Sakai et al., 2004), which could be due to the size of the courtship assay chambers. Due to technical constraints, the assay chambers were 13 mm in diameter, compared to 15 mm used in other studies (Sakai et al., 2004). This represents a 25 % reduction in area, and so inherently the flies will come into contact more often. Although the flies were raised at 25 °C in a 12 hour light/dark cycle, the behavioural assay was carried out 21 °C, again due to technical constraints. Solutions to these two problems could greatly improve the efficacy of this behavioural assay. It would require a climate controlled room set at 25 °C to carry out the assays, and a new recording system with a wider field of view to accommodate a larger assay chamber. Further controls to improve the robustness of this experiment would require assaying the uninduced transformant lines to confirm that they are able to form long-term memory when their mRNA levels are not disrupted. Also, the motility of the transformant lines, both induced and uninduced, needs to be assayed to confirm that it is normal. The high courtship index indicates that

their mobility is normal, with the possible exception of the *CamKII* line. Future analysis of memory function in the two experimental lines would require analysis using a different memory assay system, such as an olfactory conditioning assay (McGuire et al., 2006).

The behavioural assay used in this study was initially difficult to establish, as it was a new technique to the laboratory. Methodology and equipment proved difficult to fine-tune, with issues such as assaying at 21 °C instead of 25 °C, and the camera aperture only allowing a 13 mm assay chamber. Removing females from conditioning chambers, as well as transferring flies from conditioning chambers to assay chambers, by aspiration, proved difficult to master, with frequent loss and injury of flies. This study would have benefited greatly from collaboration with a New Zealand laboratory with established memory assays for *Drosophila*, however, this was a unique study within New Zealand and no such collaboration was available.

Chapter Five

References

5. References

Akhtar, A. and Becker, P.B. Activation of transcription through histone H4 acetylation by MOF, an acetyltransferase essential for dosage compensation in Drosophila. *Molecular Cell* **5** (2000), pp. 367-375.

Allfrey, V.G., Faulkner, R. and Mirsky, A.E. Acetylation + Methylation Of Histones + Their Possible Role In Regulation Of Rna Synthesis. *Proceedings Of The National Academy Of Sciences Of The United States Of America* **51** (1964), pp. 786-&.

Altschul, S.F., Gish, W., Miller, W., Myers, E.W. and Lipman, D.J. BASIC LOCAL ALIGNMENT SEARCH TOOL. *Journal of Molecular Biology* **215** (1990), pp. 403-410.

Arbeitman, M.N. Gene expression during the life cycle of Drosophila melanogaster (vol 297, pg 2270, 2002). *Science* **298** (2002), pp. 1172-1172.

Armstrong, J.D., de Belle, J.S., Wang, Z.S. and Kaiser, K. Metamorphosis of the mushroom bodies; Large-scale rearrangements of the neural substrates for associative learning and memory in Drosophila. *Learning & Memory* **5** (1998), pp. 102-114.

Ashburner, M. *Drosophila*: A Laboratory Manual. *New York: Cold Springs Harbor Laboratory Press.* (1989).

Bannister, A.J., Zegerman, P., Partridge, J.F., Miska, E.A., Thomas, J.O., Allshire, R.C. and Kouzarides, T. Selective recognition of methylated lysine 9 on histone H3 by the HP1 chromo domain. *Nature* **410** (2001), pp. 120-124.

Barski, A., Cuddapah, S., Cui, K.R., Roh, T.Y., Schones, D.E., Wang, Z.B., Wei, G., Chepelev, I. and Zhao, K.J. High-resolution profiling of histone methylations in the human genome. *Cell* **129** (2007), pp. 823-837.

Bernstein, E., Caudy, A.A., Hammond, S.M. and Hannon, G.J. Role for a bidentate ribonuclease in the initiation step of RNA interference. *Nature* **409** (2001), pp. 363-366.

Brand, A.H. and Perrimon, N. Targeted Gene-Expression As A Means Of Altering Cell Fates And Generating Dominant Phenotypes. *Development* **118** (1993), pp. 401-415.

Brownell, J.E., Zhou, J.X., Ranalli, T., Kobayashi, R., Edmondson, D.G., Roth, S.Y. and Allis, C.D. Tetrahymena histone acetyltransferase A: A homolog to yeast Gcn5p linking histone acetylation to gene activation. *Cell* **84** (1996), pp. 843-851.

Byrne, J.H. and Kandel, E.R. Presynaptic facilitation revisited: State and time dependence. *Journal of Neuroscience* **16** (1996), pp. 425-435.

Cakouros, D., Daish, T.J., Mills, K. and Kumar, S. An arginine-histone methyltransferase, CARMER, coordinates ecdysone-mediated apoptosis in drosophila cells. *Journal Of Biological Chemistry* **279** (2004), pp. 18467-18471.

Chintapalli, V.R., Wang, J. and Dow, J.A.T. Using FlyAtlas to identify better Drosophila melanogaster models of human disease. *Nature Genetics* **39** (2007), pp. 715-720.

Corona, D.F.V., Clapier, C.R., Becker, P.B. and Tamkun, J.W. Modulation of ISWI function by site-specific histone acetylation. *Embo Reports* **3** (2002), pp. 242-247.

Crittenden, J.R., Skoulakis, E.M.C., Han, K.A., Kalderon, D. and Davis, R.L. Tripartite mushroom body architecture revealed by antigenic markers. *Learning & Memory* **5** (1998), pp. 38-51.

de belle, J.S. and Heisenberg, M. Associative Odor Learning In Drosophila Abolished By Chemical Ablation Of Mushroom Bodies. *Science* **263** (1994), pp. 692-695.

Dietzl, G., Chen, D., Schnorrer, F., Su, K.C., Barinova, Y., Fellner, M., Gasser, B., Kinsey, K., Oppel, S., Scheiblauer, S., Couto, A., Marra, V., Keleman, K. and Dickson, B.J. A genome-wide transgenic RNAi library for conditional gene inactivation in Drosophila. *Nature* **448** (2007), pp. 151-U1.

Dubnau, J., Chiang, A.S., Grady, L., Barditch, J., Gossweiler, S., McNeil, J., Smith, P., Buldoc, F., Scott, R., Certa, U., Broger, C. and Tully, T. The staufen/pumilio pathway is involved in Drosophila long-term memory. *Current Biology* **13** (2003), pp. 286-296.

Feng, Q., Wang, H.B., Ng, H.H., Erdjument-Bromage, H., Tempst, P., Struhl, K. and Zhang, Y. Methylation of H3-lysine 79 is mediated by a new family of HMTases without a SET domain. *Current Biology* **12** (2002), pp. 1052-1058.

Fire, A., Xu, S.Q., Montgomery, M.K., Kostas, S.A., Driver, S.E. and Mello, C.C. Potent and specific genetic interference by double-stranded RNA in Caenorhabditis elegans. *Nature* **391** (1998), pp. 806-811.

Foglietti, C., Filocamo, G., Cundari, E., De Rinaldis, E., Lahm, A., Cortese, R. and Steinkuhler, C. Dissecting the biological functions of Drosophila histone deacetylases by RNA interference and transcriptional profiling. *Journal of Biological Chemistry* **281** (2006), pp. 17968-17976.

Gao, L., Cueto, M.A., Asselbergs, F. and Atadja, P. Cloning and functional characterization of HDAC11, a novel member of the human histone deacetylase family. *Journal Of Biological Chemistry* **277** (2002), pp. 25748-25755.

Gong, Z.F., Xia, S.Z., Liu, L., Feng, C.H. and Guo, A.K. Operant visual learning and memory in Drosophila mutants dunce, amnesiac and radish. *Journal of Insect Physiology* **44** (1998), pp. 1149-1158.

Gregoretti, I.V., Lee, Y.M. and Goodson, H.V. Molecular evolution of the histone deacetylase family: Functional implications of phylogenetic analysis. *Journal of Molecular Biology* **338** (2004), pp. 17-31.

Groth, A.C., Fish, M., Nusse, R. and Calos, M.P. Construction of transgenic Drosophila by using the site-specific integrase from phage phi C31. *Genetics* **166** (2004), pp. 1775-1782.

Guan, Z.H., Giustetto, M., Lomvardas, S., Kim, J.H., Miniaci, M.C., Schwartz, J.H., Thanos, D. and Kandel, E.R. Integration of long-term-memory-related synaptic plasticity involves bidirectional regulation of gene expression and chromatin structure. *Cell* **111** (2002), pp. 483-493.

Gutierrez, E., Wiggins, D., Fielding, B. and Gould, A.P. Specialized hepatocyte-like cells regulate Drosophila lipid metabolism. *Nature* **445** (2007), pp. 275-280.

Hammond, S.M., Bernstein, E., Beach, D. and Hannon, G.J. An RNA-directed nuclease mediates post-transcriptional gene silencing in Drosophila cells. *Nature* **404** (2000), pp. 293-296.

Han, P.L., Levin, L.R., Reed, R.R. and Davis, R.L. PREFERENTIAL EXPRESSION OF THE DROSOPHILA RUTABAGA GENE IN MUSHROOM BODIES, NEURAL CENTERS FOR LEARNING IN INSECTS. *Neuron* **9** (1992), pp. 619-627.

Hannon, G.J. RNA interference. *Nature* **418** (2002), pp. 244-251.

Heisenberg, M. What do the mushroom bodies do for the insect brain? An introduction. *Learning & Memory* **5** (1998), pp. 1-10.

Hubel, D.H., Wiesel, T.N. and Levay, S. PLASTICITY OF OCULAR DOMINANCE COLUMNS IN MONKEY STRIATE CORTEX. *Philosophical Transactions of the Royal Society of London Series B-Biological Sciences* **278** (1977), pp. 377-&.

Inoue, H., Nojima, H. and Okayama, H. HIGH-EFFICIENCY TRANSFORMATION OF ESCHERICHIA-COLI WITH PLASMIDS. *Gene* **96** (1990), pp. 23-28.

Isabel, G., Pascual, A. and Preat, T. Exclusive consolidated memory phases in Drosophila. *Science* **304** (2004), pp. 1024-1027.

Ito, K., Suzuki, K., Estes, P., Ramaswami, M., Yamamoto, D. and Strausfeld, N.J. The organization of extrinsic neurons and their implications in the functional roles of the mushroom bodies in Drosophila melanogaster meigen. *Learning & Memory* **5** (1998), pp. 52-77.

Jenuwein, T. and Allis, C.D. Translating the histone code. *Science* **293** (2001), pp. 1074-1080.

Kandel, E.R. The molecular biology of memory storage: A dialog between genes and synapses. *Bioscience Reports* **21** (2001), pp. 565-611.

Karachentsev, D., Druzhinina, M. and Steward, R. Free and chromatin-associated mono-, di-, and trimethylation of histone H4-lysine 20 during development and cell cycle progression. *Developmental Biology* **304** (2007), pp. 46-52.

Karachentsev, D., Sarma, K., Reinberg, D. and Steward, R. PR-Set7-dependent methylation of histone H4 Lys 20 functions in repression of gene expression and is essential for mitosis. *Genes & Development* **19** (2005), pp. 431-435.

Kato, Y., Kato, M., Tachibana, M., Shinkai, Y. and Yamaguchi, M. Characterization of Drosophila G9a in vivo and identification of genetic interactants. *Genes to Cells* **13** (2008), pp. 703-722.

Kee, N., Teixeira, C.M., Wang, A.H. and Frankland, P.W. Preferential incorporation of adult-generated granule cells into spatial memory networks in the dentate gyrus. *Nature Neuroscience* **10** (2007), pp. 355-362.

Kornberg, R.D. and Lorch, Y.L. Twenty-five years of the nucleosome, fundamental particle of the eukaryote chromosome. *Cell* **98** (1999), pp. 285-294.

Krashes, M.J., Keene, A.C., Leung, B., Armstrong, J.D. and Waddell, S. Sequential use of mushroom body neuron subsets during Drosophila odor memory processing. *Neuron* **53** (2007), pp. 103-115.

Lagarou, A., Mohd-Sarip, A., Moshkin, Y.M., Chalkley, G.E., Bezstarosti, K., Demmers, J.A.A. and Verrijzer, C.P. dKDM2 couples histone H2A ubiquitylation to histone H3 demethylation during Polycomb group silencing. *Genes & Development* **22** (2008), pp. 2799-2810.

Lee, T., Lee, A. and Luo, L.Q. Development of the Drosophila mushroom bodies: sequential generation of three distinct types of neurons from a neuroblast. *Development* **126** (1999), pp. 4065-4076.

Lekven, A.C., Tepass, U., Keshmeshian, M. and Hartenstein, V. faint sausage encodes a novel extracellular protein of the immunoglobulin superfamily required for cell migration and the establishment of normal axonal pathways in the Drosophila nervous system. *Development* **125** (1998), pp. 2747-2758.

Levenson, J.M., O'Riordan, K.J., Brown, K.D., Trinh, M.A., Molfese, D.L. and Sweatt, J.D. Regulation of histone acetylation during memory formation in the hippocampus. *Journal Of Biological Chemistry* **279** (2004), pp. 40545-40559.

Levis, R., Hazelrigg, T. and Rubin, G.M. EFFECTS OF GENOMIC POSITION ON THE EXPRESSION OF TRANSDUCED COPIES OF THE WHITE GENE OF DROSOPHILA. *Science* **229** (1985), pp. 558-561.

Lichtman, J.W. and Colman, H. Synapse elimination and indelible memory. *Neuron* **25** (2000), pp. 269-278.

Ling, X.F., Harkness, T.A.A., Schultz, M.C., FisherAdams, G. and Grunstein, M. Yeast histone H3 and H4 amino termini are important for nucleosome assembly in vivo and in vitro: Redundant and position-independent functions in assembly but not in gene regulation. *Genes & Development* **10** (1996), pp. 686-699.

Liu, H.D., Hu, Q.C., Kaufman, A., D'Ercole, A.J. and Ye, P. Developmental expression of histone deacetylase 11 in the murine brain. *Journal of Neuroscience Research* **86** (2008), pp. 537-543.

Luger, K., Mader, A.W., Richmond, R.K., Sargent, D.F. and Richmond, T.J. Crystal structure of the nucleosome core particle at 2.8A resolution. *Nature* **389** (1997), pp. 251-260.

Ma, Y., Creanga, A., Lum, L. and Beachy, P.A. Prevalence of off-target effects in Drosophila RNA interference screens. *Nature* **443** (2006), pp. 359-363.

McGuire, S.E., Deshazer, M. and Davis, R.L. Thirty years of olfactory learning and memory research in Drosophila melanogaster (vol 76, pg 328, 2005). *Progress in Neurobiology* **79** (2006), pp. 341-342.

McGuire, S.E., Le, P.T. and Davis, R.L. The role of Drosophila mushroom body signaling in olfactory memory. *Science* **293** (2001), pp. 1330-1333.

McGuire, S.E., Mao, Z. and Davis, R.L. Spatiotemporal Gene Expression Targeting with the TARGET and Gene-Switch Systems in *Drosophila*. *Sci. STKE* **pl6** (2004).

Muller, J., Hart, C.M., Francis, N.J., Vargas, M.L., Sengupta, A., Wild, B., Miller, E.L., O'Connor, M.B., Kingston, R.E. and Simon, J.A. Histone methyltransferase activity of a Drosophila polycomb group repressor complex. *Cell* **111** (2002), pp. 197-208.

Nassif, C., Noveen, A. and Hartenstein, V. Embryonic development of the Drosophila brain. I. Pattern of pioneer tracts. *Journal of Comparative Neurology* **402** (1998), pp. 10-31.

Nishioka, K., Rice, J.C., Sarma, K., Erdjument-Bromage, H., Werner, J., Wang, Y.M., Chuikov, S., Valenzuela, P., Tempst, P., Steward, R., Lis, J.T., Allis, C.D. and Reinberg, D. PR-Set7 is a nucleosome-specific methyltransferase that modifies lysine 20 of histone H4 and is associated with silent chromatin. *Molecular Cell* **9** (2002), pp. 1201-1213.

O'Dell, K.M.C. The voyeurs' guide to Drosophila melanogaster courtship. *Behavioural Processes* **64** (2003), pp. 211-223.

Owen, D.J., Ornaghi, P., Yang, J.C., Lowe, N., Evans, P.R., Ballario, P., Neuhaus, D., Filetici, P. and Travers, A.A. The structural basis for the recognition of acetylated histone H4 by the bromodomain of histone acetyltransferase Gcn5p. *Embo Journal* **19** (2000), pp. 6141-6149.

Pascual, A. and Preat, T. Localization of long-term memory within the Drosophila mushroom body. *Science* **294** (2001), pp. 1115-1117.

Pavlopoulos, E., Anezaki, M. and Skoulakis, E.M.C. Neuralized is expressed in the alpha/beta lobes of adult Drosophila mushroom bodies and facilitates olfactory long-term memory formation. *Proceedings of the National Academy of Sciences of the United States of America* **105** (2008), pp. 14674-14679.

Peters, A., Mermoud, J.E., O'Carroll, D., Pagani, M., Schweizer, D., Brockdorff, N. and Jenuwein, T. Histone H3 lysine 9 methylation is an epigenetic imprint of facultative heterochromatin. *Nature Genetics* **30** (2002), pp. 77-80.

Pikaart, M.I., Recillas-Targa, F. and Felsenfeld, G. Loss of transcriptional activity of a transgene is accompanied by DNA methylation and histone deacetylation and is prevented by insulators. *Genes & Development* **12** (1998), pp. 2852-2862.

Rubin, G.M. and Spradling, A.C. GENETIC-TRANSFORMATION OF DROSOPHILA WITH TRANSPOSABLE ELEMENT VECTORS. *Science* **218** (1982), pp. 348-353.

Rudolph, T., Yonezawa, M., Lein, S., Heidrich, K., Kubicek, S., Schafer, C., Phalke, S., Walther, M., Schmidt, A., Jenuwein, T. and Reuter, G. Heterochromatin formation in Drosophila is initiated through active removal of H3K4 methylation by the LSD1 homolog SU(VAR)3-3. *Molecular Cell* **26** (2007), pp. 103-115.

Sakaguchi, A. and Steward, R. Aberrant monomethylation of histone H4 lysine 20 activates the DNA damage checkpoint in Drosophila melanogaster. *Journal of Cell Biology* **176** (2007), pp. 155-162.

Sakai, T., Tamura, T., Kitamoto, T. and Kidokoro, Y. A clock gene, period, plays a key role in long-term memory formation in Drosophila. *Proceedings of the National Academy of Sciences of the United States of America* **101** (2004), pp. 16058-16063.

Sambrook, J., Fitsch, E.F. and Maniatis, T. Molecular Cloning: A Laboratory Manual. *New York: Cold Spring Harbor Laboratory Press.* (1989).

Sewack, G.F., Ellis, T.W. and Hansen, U. Binding of TATA binding protein to a naturally positioned nucleosome is facilitated by histone acetylation. *Molecular And Cellular Biology* **21** (2001), pp. 1404-1415.

Shirahata, T., Tsunoda, M., Santa, T., Kirino, Y. and Watanabe, S. Depletion of serotonin selectively impairs short-term memory without affecting long-term memory in odor learning in the terrestrial slug Limax valentianus. *Learning & Memory* **13** (2006), pp. 267-270.

Spradling, A.C. and Rubin, G.M. TRANSPOSITION OF CLONED P ELEMENTS INTO DROSOPHILA GERM LINE CHROMOSOMES. *Science* **218** (1982), pp. 341-347.

Strahl, B.D. and Allis, C.D. The language of covalent histone modifications. *Nature* **403** (2000), pp. 41-45.

Tanaka, N.K., Tanimoto, H. and Ito, K. Neuronal assemblies of the Drosophila mushroom body. *Journal of Comparative Neurology* **508** (2008), pp. 711-755.

Thorpe, H.M. and Smith, M.C.M. In vitro site-specific integration of bacteriophage DNA catalyzed by a recombinase of the resolvase/invertase family. *Proceedings of the National Academy of Sciences of the United States of America* **95** (1998), pp. 5505-5510.

Trievel, R.C. Structure and function of histone methyltransferases. *Critical Reviews In Eukaryotic Gene Expression* **14** (2004), pp. 147-169.

Tschiersch, B., Hofmann, A., Krauss, V., Dorn, R., Korge, G. and Reuter, G. THE PROTEIN ENCODED BY THE DROSOPHILA POSITION-EFFECT VARIEGATION SUPPRESSOR GENE SU(VAR)3-9 COMBINES DOMAINS OF ANTAGONISTIC REGULATORS OF HOMEOTIC GENE COMPLEXES. *Embo Journal* **13** (1994), pp. 3822-3831.

Tse, C., Sera, T., Wolffe, A.P. and Hansen, J.C. Disruption of higher-order folding by core histone acetylation dramatically enhances transcription of nucleosomal

arrays by RNA polymerase III. *Molecular And Cellular Biology* **18** (1998), pp. 4629-4638.

Tully, T., Preat, T., Boynton, S.C. and Delvecchio, M. Genetic Dissection Of Consolidated Memory In Drosophila. *Cell* **79** (1994), pp. 35-47.

Turner, B.M. Histone acetylation as an epigenetic determinant of long-term transcriptional competence. *Cellular And Molecular Life Sciences* **54** (1998), pp. 21-31.

Verdin, E., Dequiedt, F. and Kasler, H.G. Class II histone deacetylases: versatile regulators. *Trends in Genetics* **19** (2003), pp. 286-293.

Vincent, J.P., Girdham, C.H. and Ofarrell, P.H. A CELL-AUTONOMOUS, UBIQUITOUS MARKER FOR THE ANALYSIS OF DROSOPHILA GENETIC MOSAICS. *Developmental Biology* **164** (1994), pp. 328-331.

Wade, P.A. Transcriptional control at regulatory checkpoints by histone deacetylases: molecular connections between cancer and chromatin. *Human Molecular Genetics* **10** (2001), pp. 693-698.

Wang, Y.M., Zhang, W.G., Jin, Y., Johansen, J. and Johansen, K.M. The JIL-1 tandem kinase mediates histone H3 phosphorylation and is required for maintenance of chromatin structure in Drosophila. *Cell* **105** (2001), pp. 433-443.

Xiao, B., Jing, C., Kelly, G., Walker, P.A., Muskett, F.W., Frenkiel, T.A., Martin, S.R., Sarma, K., Reinberg, D., Gamblin, S.J. and Wilson, J.R. Specificity and mechanism of the histone methyltransferase Pr-Set7. *Genes & Development* **19** (2005), pp. 1444-1454.

Zamore, P.D., Tuschl, T., Sharp, P.A. and Bartel, D.P. RNAi: Double-stranded RNA directs the ATP-dependent cleavage of mRNA at 21 to 23 nucleotide intervals. *Cell* **101** (2000), pp. 25-33.

Zars, T., Fischer, M., Schulz, R. and Heisenberg, M. Localization of a short-term memory in Drosophila. *Science* **288** (2000), pp. 672-675.

Zhu, X.J. and Stein, D. RNAi-mediated inhibition of gene function in the follicle cell layer of the Drosophila ovary. *Genesis* **40** (2004), pp. 101-108.

Chapter Six

Appendices

Appendix 6.1 Vector Map of pUAS-HDACX$_{IR}$.CS2$_{intron}$ and Predicted Restriction Fragments

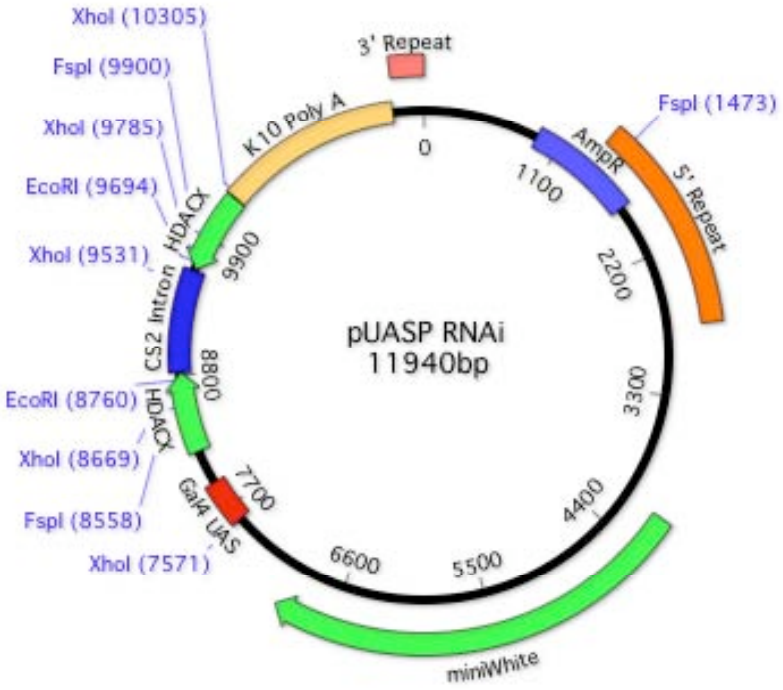

Digest with *Xho* I:

Fragment Size	From:To	Overhang
9206	10306:7571	4
1098	7572:8669	4
862	8670:9531	4
520	9786:10305	4
254	9532:9785	4

Digest with *Eco* RI:

Fragment Size	From:To	Overhang
11006	9695:8760	4
934	8761:9694	4

Digest with *Fsp* I:

Fragment Size	From:To	Overhang
7085	1474:8558	0
3513	9901:1473	0
1342	8559:9900	0

Appendix 6.2 Vector Map of pUAS-prSet7$_{IR}$.CS2$_{intron}$ and Predicted Restriction Fragments

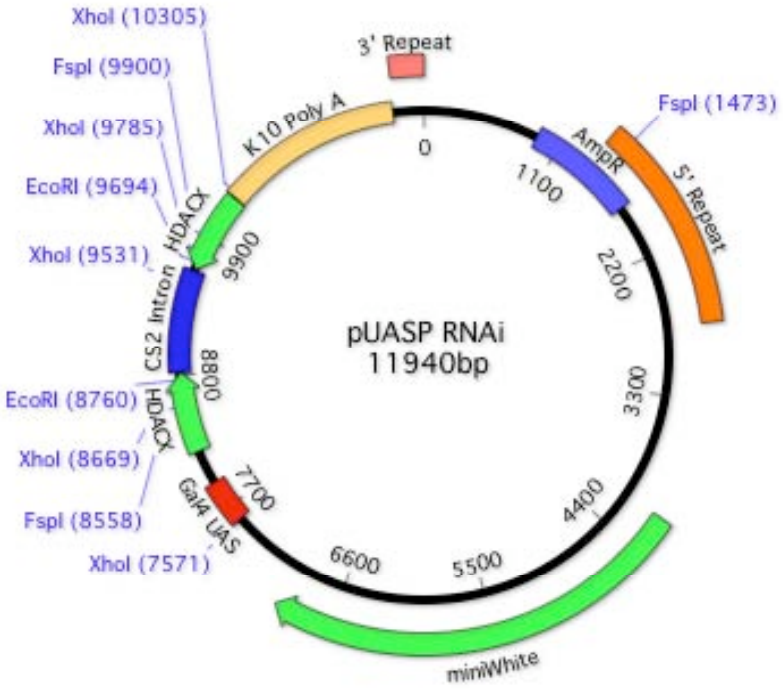

Digest with *Afl* II:

Fragment Size	From:To	Overhang
7929	10361:6899	4
3461	6900:10360	4

Digest with *Bst* BI:

Fragment Size	From:To	Overhang
4259	3975:8233	2
3747	228:3974	2
1719	9899:227	2
1440	8234:9673	2
225	9674:9898	2

Digest with *Xho* I:

Fragment Size	From:To	Overhang
9206	9756:7571	4
1685	7572:9256	4
499	9257:9755	4

Appendix 6.3 Vector Map of pUAS-MSL2$_{IR}$.CS2$_{intron}$ and Predicted Restriction Fragments

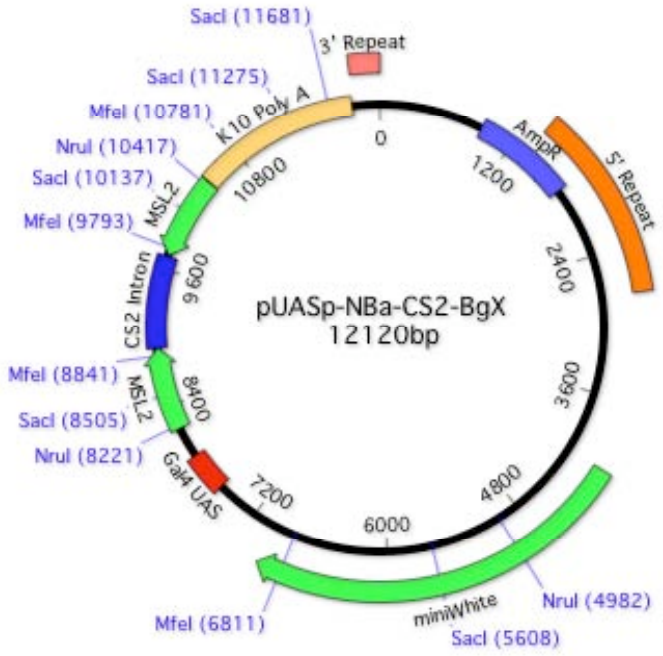

Digest with MfeI:

Fragment Size	From:To	Overhang
8150	10782:6811	4
2030	6812:8841	4
988	9794:10781	4
952	8842:9793	4

Digest with NruI:

Fragment Size	From:To	Overhang
6685	10418:4982	0
3239	4983:8221	0
2196	8222:10417	0

Digest with SacI:

Fragment Size	From:To	Overhang
6047	11682:5608	4
2897	5609:8505	4
1632	8506:10137	4
1138	10138:11275	4
406	11276:11681	4

Appendix 6.4 Vector Map of pUASp-NBa-CS2-BgX

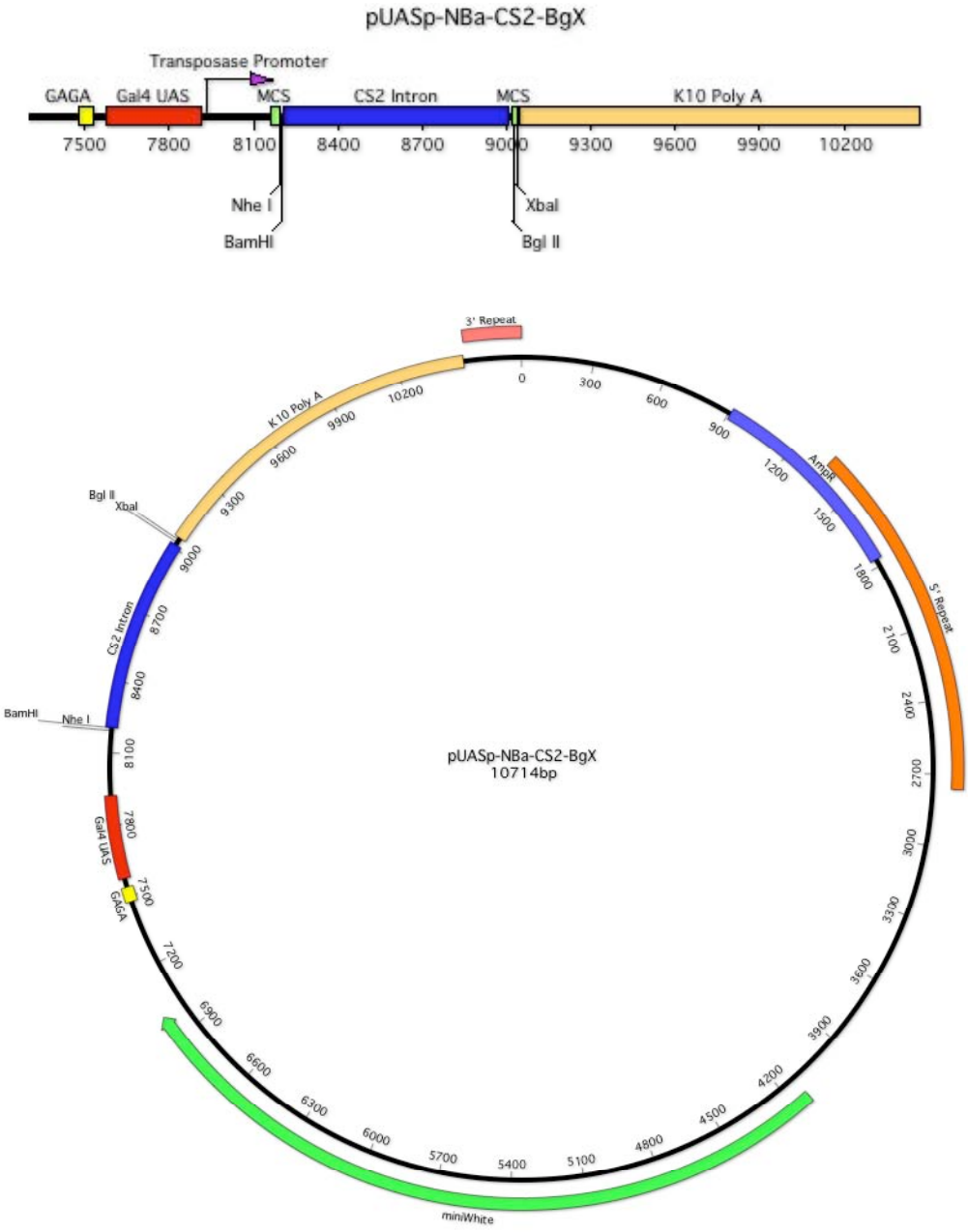
pUASp-NBa-CS2-BgX
Transposase Promoter
GAGA
Gal4 UAS
MCS
CS2 Intron
MCS
K10 Poly A
7500
7800
8100
8400
8700
9000
9300
9600
9900
10200
Nhe I
BamHI
XbaI
Bgl II
3' Repeat
Amp R
5' Repeat
pUASp-NBa-CS2-BgX
10714bp
miniWhite

Appendix 6.5 Vector Maps of pUASp-RNAi-attB

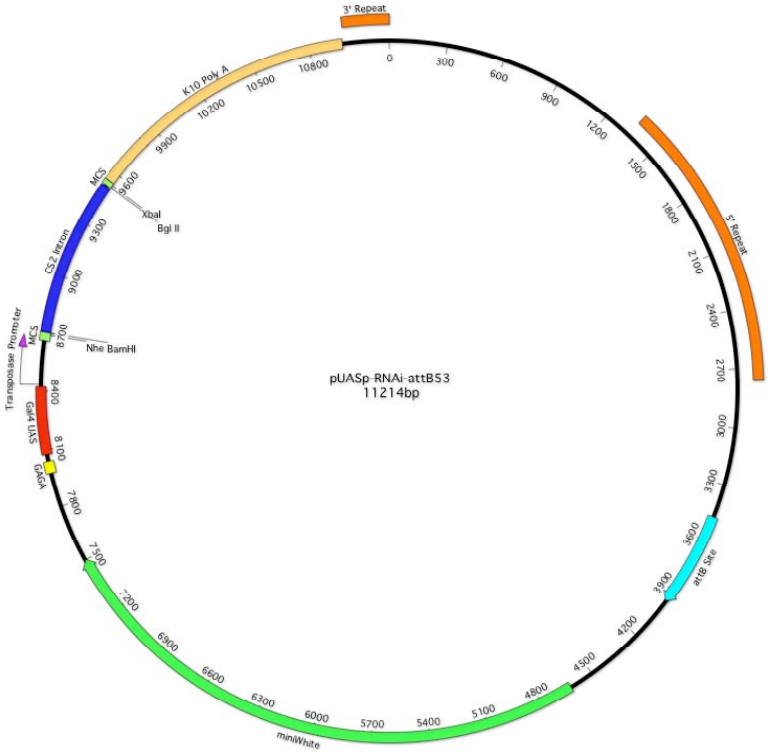

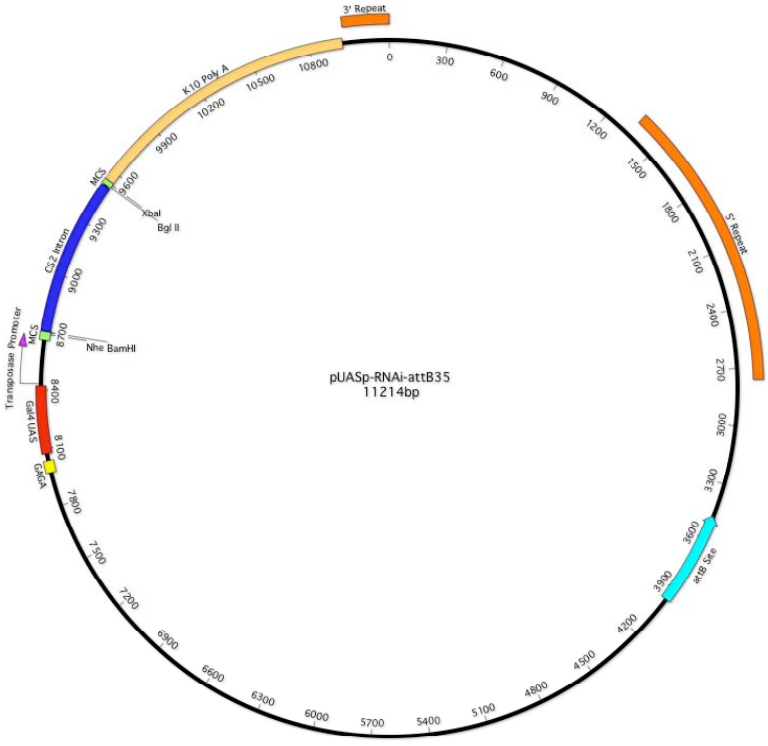

Appendix 6.6 Courtship Conditioning Assay Data

	CantonS		pr-Set7	
	Conditioned	Unconditioned	Conditioned	Unconditioned
	1.2	5.2	7.6	9.25
	1.75	5.6	9.3	8.8
	2.8	5.75	6.5	8.4
	3.35	6	6.2	4.3
	4.3	6.1	8.2	9.25
	4.33	6.1	6.9	6.5
	4.4	6.2	7.7	8.9
	4.75	6.25	5.2	2
	5	7.2	6.1	2.5
	7	8.25	7.6	8
	7.1	8.6	1.7	9.1
	7.27	8.6	9	9.25
	7.6	9		9.2
	7.7	9.2		
	7.9	9.3		
	9	9.4		
	9.4	10		
	9.5	10		
		10		
Average	5.797222222	7.723684211	6.833333333	7.342307692
STD	2.590924899	1.736005026	2.014643363	2.669491693
95% Confidence	1.148575934	0.749057778	1.093827139	1.392509086

	CamKII		HDACX	
	Conditioned	Unconditioned	Conditioned	Unconditioned
	0.75	1	3.2	4.25
	1	1.5	5.75	5.5
	1.25	2	6.25	5.6
	2	2.5	7.4	5.75
	3.1	3.7	7.6	6.8
	4.8	4	7.7	7.2
	4.9	4	8	7.5
	4.9	5	8.1	7.5
	5	6	8.6	7.7
	6.1	6.75	8.75	8.1
	7.7	8	9	8.3
	7.8	8.2	9.4	8.5
	9.5	8.9	9.4	8.7
			9.4	9.2
			9.75	
Average	4.523076923	4.734615385	7.886666667	7.185714286
STD	2.805174934	2.658115295	1.74145533	1.435863258
95% Confidence	1.463286661	1.443192727	0.875365571	0.749001257

6.7 Data from qRT-PCR Experiments

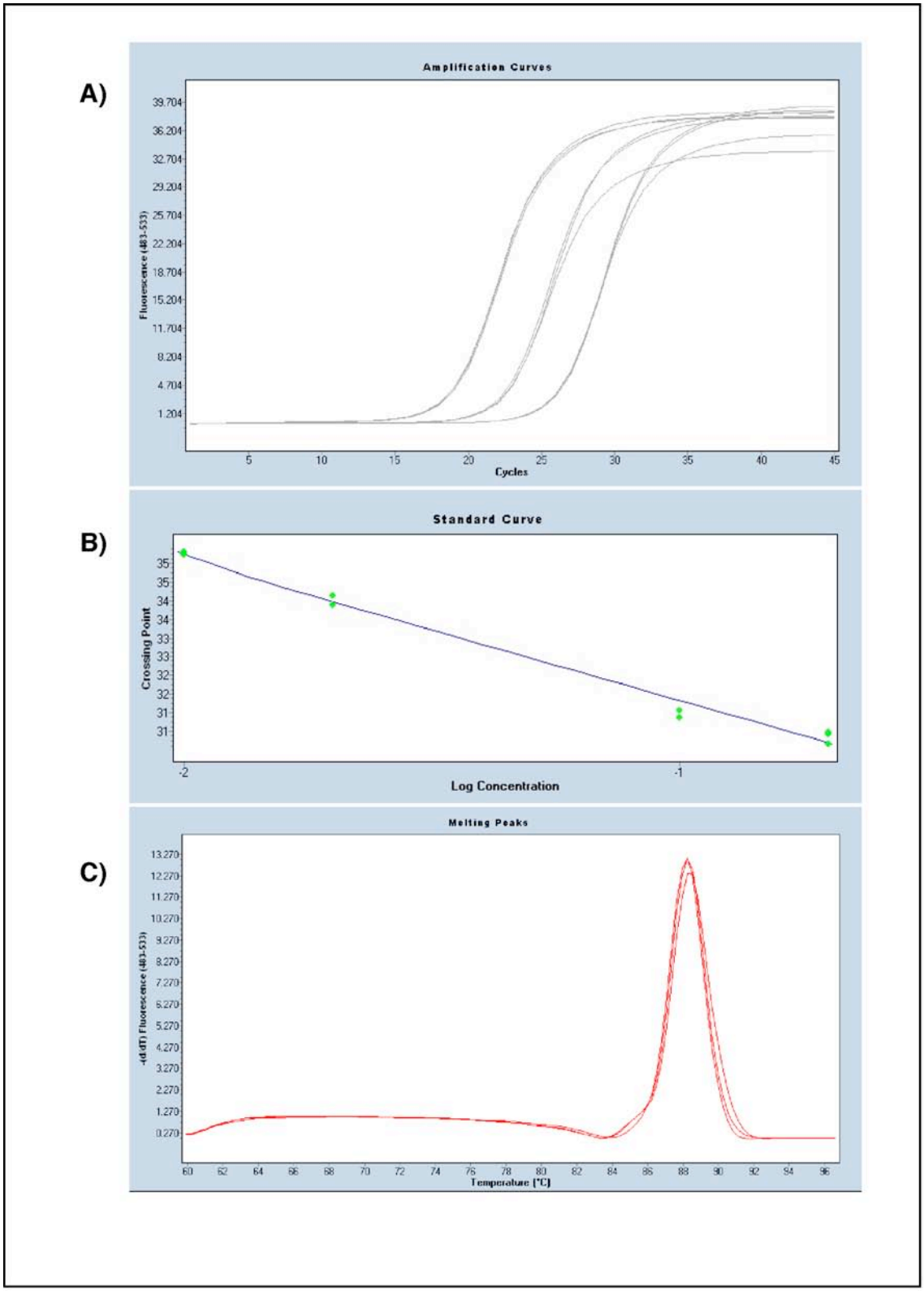

qRT-PCR Data of primer pair HDACX showing (A) reproducibility, (B) Standard curve, and (C)Melting point

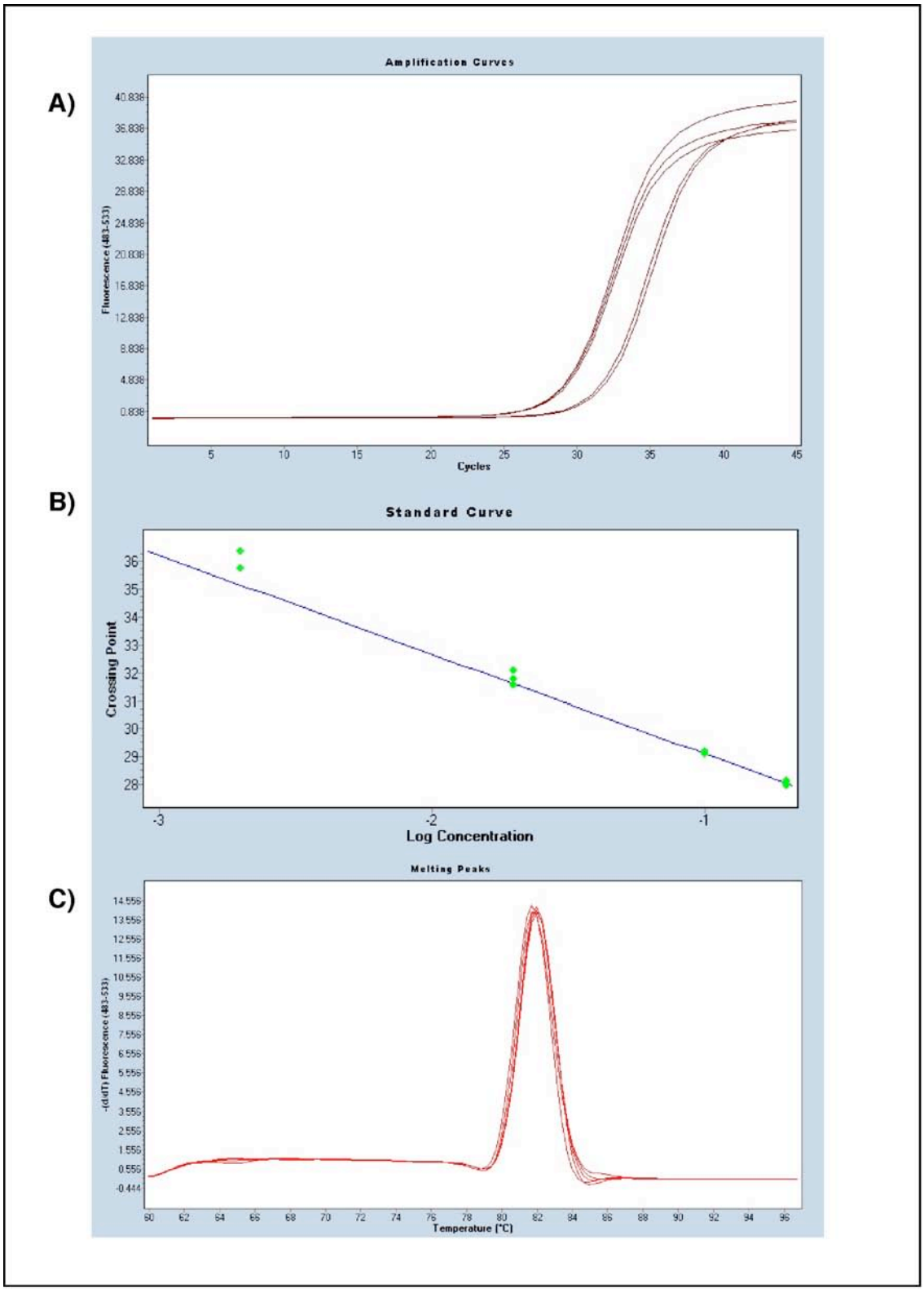

qRT-PCR Data of primer pair pr-Set7 showing (A) reproducibility, (B) Standard curve, and (C)Melting point

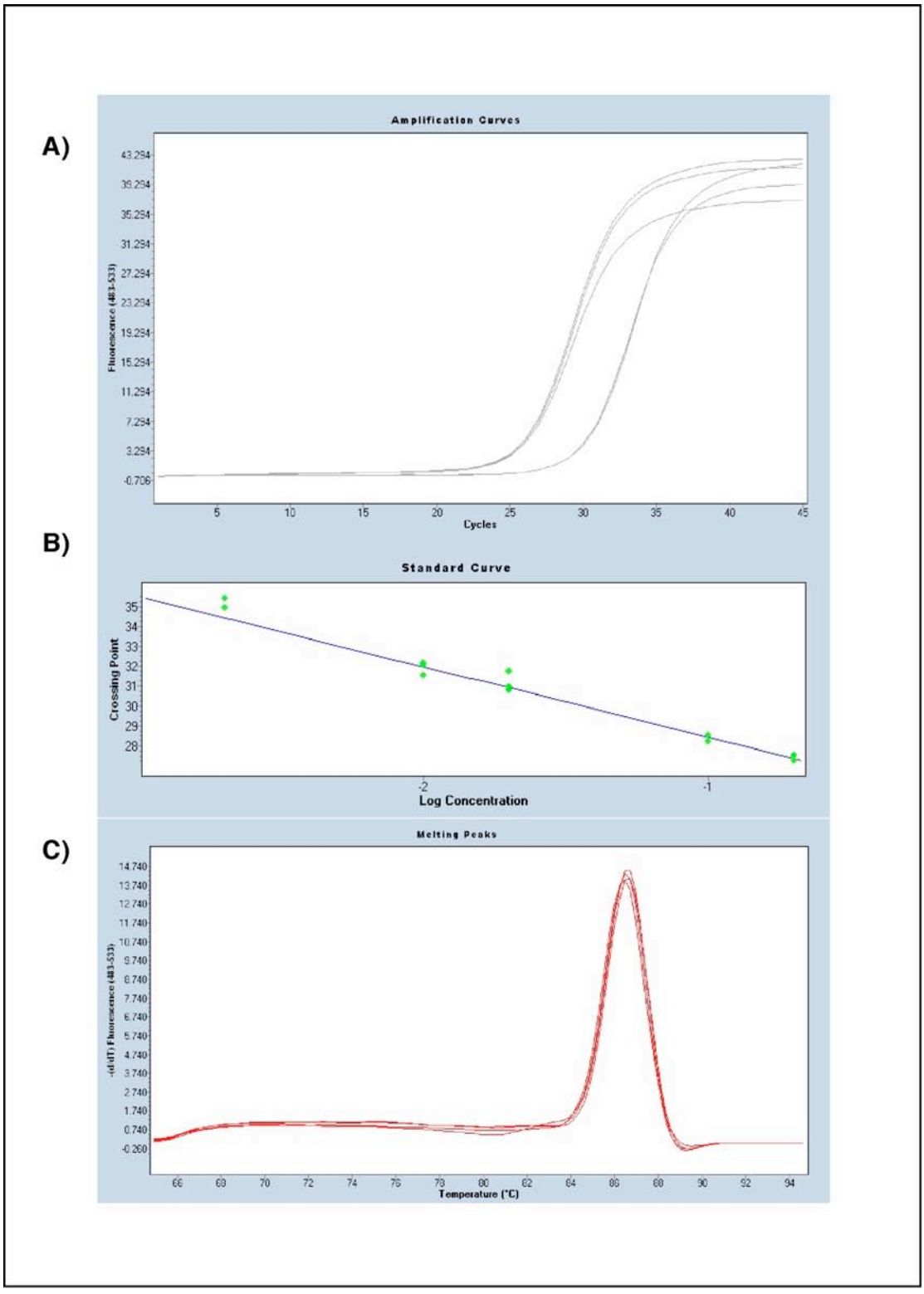

qRT-PCR Data of primer pair msl-2 showing (A) reproducibility, (B) Standard curve, and (C)Melting point

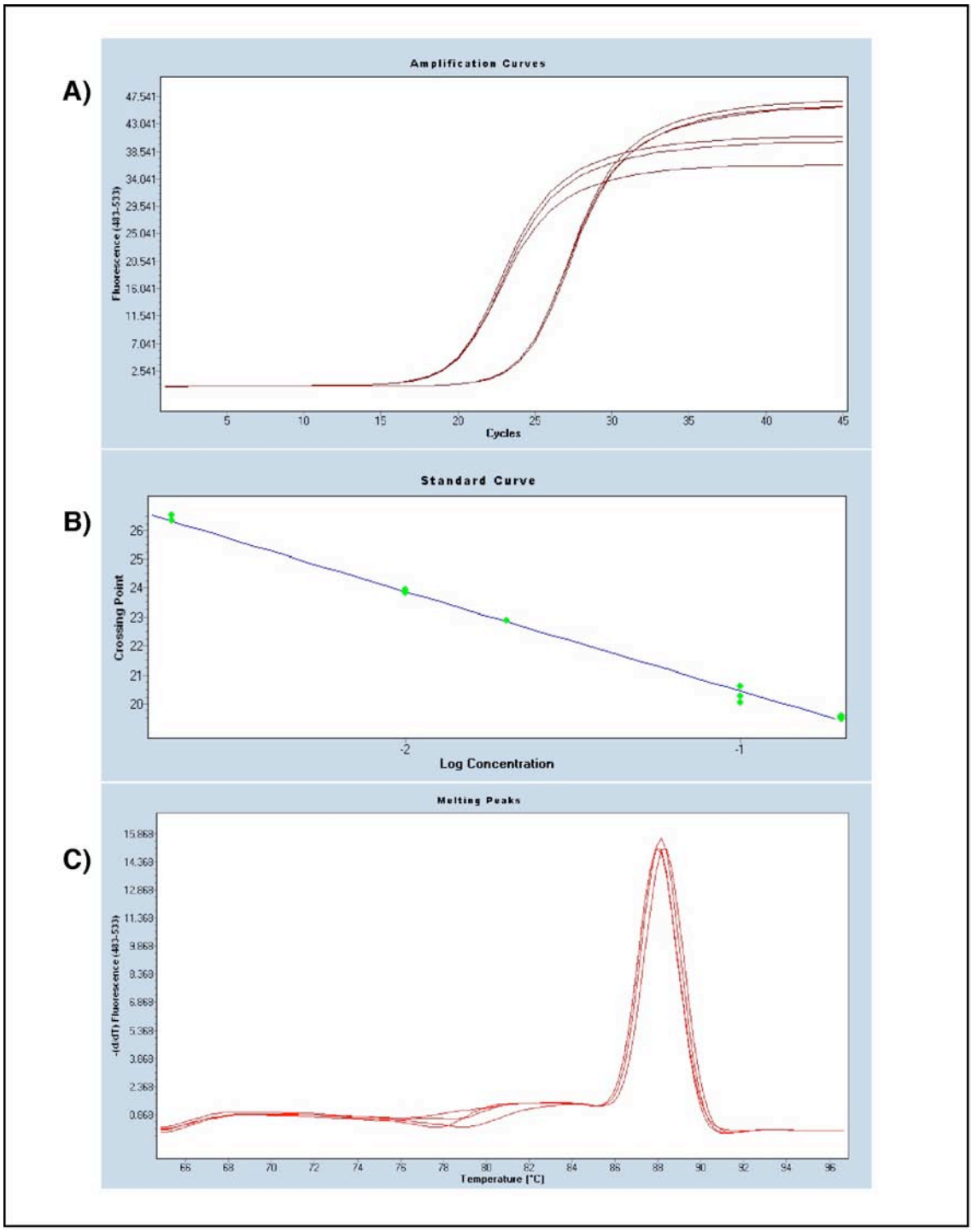

qRT-PCR Data of primer pair Rp49 showing (A) reproducibility, (B) Standard curve, and (C)Melting point

Appendix 6.8 Viability Assay Data

HDACX	CyO Male	CyO Female	RNAi Male	RNAi Female	Total
	170	211	170	191	742
	195	261	231	209	896
	92	130	158	216	596
	134	221	152	224	731
Total	591	823	711	840	2965
Percentage	0.229110512	0.284366577	0.229110512	0.257412399	1
	0.217633929	0.291294643	0.2578125	0.233258929	1
	0.154362416	0.218120805	0.265100671	0.362416107	1
	0.183310534	0.302325581	0.207934337	0.306429549	1
Average	0.196104348	0.274026902	0.239989505	0.289879246	1
STD	0.033955855	0.037997327	0.026420422	0.057141536	
95% Confidence	0.033276126	0.037236697	0.025891538	0.055997676	

pr-Set7	CyO Male	CyO Female	Arm Male	Arm Female	Total
	121	154	157	129	561
	169	206	160	166	701
	132	194	189	240	755
Total	422	554	506	535	2017
Percentage	0.215686275	0.274509804	0.279857398	0.229946524	1
	0.241084165	0.293865906	0.228245364	0.236804565	1
	0.174834437	0.256953642	0.250331126	0.317880795	1
Average	0.210534959	0.275109784	0.252811296	0.261543961	1
STD	0.033423924	0.018463444	0.025895249	0.048909481	
95% Confidence	0.037822035	0.02089297	0.029302695	0.05534527	

msl-2	CyO Male	CyO Female	Arm Male	Arm Female	Total
	243	177	187	230	837
	187	153	172	228	740
	200	207	204	221	832
Total	630	537	563	679	2409
Percentage	0.290322581	0.211469534	0.223416965	0.27479092	1
	0.252702703	0.206756757	0.232432432	0.308108108	1
	0.240384615	0.248798077	0.245192308	0.265625	1
Average	0.261136633	0.222341456	0.233680568	0.282841343	1
STD	0.026015351	0.023032958	0.010941196	0.022356444	
95% Confidence	0.0294386	0.026063767	0.012380901	0.025298233	

CantonS	CyO Male	CyO Female	Arm Male	Arm Female	Total
	166	189	193	199	747
	197	221	209	198	825
	160	178	181	194	713

Total	523	588	583	591	2285
Percentage	0.222222222	0.253012048	0.258366801	0.266398929	1
	0.238787879	0.267878788	0.253333333	0.24	1
	0.224403927	0.249649369	0.253856942	0.272089762	1
Average	0.228471343	0.256846735	0.255185692	0.25949623	1
STD	0.00900073	0.009700853	0.002767333	0.017122314	
95% Confidence	0.010185098	0.010977347	0.003131474	0.019375366	

Appendix 6.9 *Chitin Synthase 2* Intron Alignment

>gb|AE014296.4| *Drosophila melanogaster* chromosome 3L, complete sequence

```
Query  2         AGGTAAGTGGGAGTCGCTTCCTGCAGAATTGAGTGCTTCAAATCAGGTGCGAGGAAAGTT  61
                 ||||  ||||||||||||||||||||||||||||||||||||||||||||||||||||||
Sbjct  21958350  AGGTGAGTGGGAGTCGCTTCCTGCAGAATTGAGTGCTTCAAATCAGGTGCGAGGAAAGTT  21958409

Query  62        GAGGGCATGTTAATGAATTATTGAAATCAGGCGCCTGCTTAGCATCAATCATCTCGCTAA  121
                 ||||||||||||||||||||||||||||||||||||||||||||||||||||||||||||
Sbjct  21958410  GAGGGCATGTTAATGAATTATTGAAATCAGGCGCCTGCTTAGCATCAATCATCTCGCTAA  21958469

Query  122       GTTCGCAGCTTCCTGCAGCTCTTGTGCCAATCCGTGCACCCACATCCATTTTTGACTATT  181
                 ||||||||||||||||||||||||||||||||||||||||||||||||||||||||||||
Sbjct  21958470  GTTCGCAGCTTCCTGCAGCTCTTGTGCCAATCCGTGCACCCACATCCATTTTTGACTATT  21958529

Query  182       CCGGCGGAGGGGGCCCGGACTGCCGGCACTACTGATGAGCGCTTCAAATGTCAGGCAATG  241
                 ||||||||||||||||||||||||||||||||||||||||||||||||||||||||||||
Sbjct  21958530  CCGGCGGAGGGGGCCCGGACTGCCGGCACTACTGATGAGCGCTTCAAATGTCAGGCAATG  21958589

Query  242       TAATTAAGTTAAATGACGGGGAAACTGCAAAGTTCAGGAAATGTTTGTGTTTCGTCCTTT  301
                 ||||||||||||||||||||||||||||||||||||||||||||||||||||||||||||
Sbjct  21958590  TAATTAAGTTAAATGACGGGGAAACTGCAAAGTTCAGGAAATGTTTGTGTTTCGTCCTTT  21958649

Query  302       TCGGGGAGGGGCACGGCTAGGATGCCAGTACTGGGATGGGTTTTCGGTGGGTGTAAACTT  361
                 ||||||||||||||||||||||||||||||||||||||||||||||||||||||||||||
Sbjct  21958650  TCGGGGAGGGGCACGGCTAGGATGCCAGTACTGGGATGGGTTTTCGGTGGGTGTAAACTT  21958709

Query  362       AATTAAAAGTGCTTCAGCTCCACTCGCATGTTTTCGGGGCCTACCCAGTATAAAGACATT  421
                 ||||||||||||||||||||||||||||||||||||||||||||||||||||||||||||
Sbjct  21958710  AATTAAAAGTGCTTCAGCTCCACTCGCATGTTTTCGGGGCCTACCCAGTATAAAGACATT  21958769

Query  422       AAAGTAATTAAAATCAGGGCATACGAGTTGATTTTAAGGGCATAATTTAGGGGCCATGCG  481
                 ||||||||||||||||||||||||||||||||||||||||||||||||||||||||||||
Sbjct  21958770  AAAGTAATTAAAATCAGGGCATACGAGTTGATTTTAAGGGCATAATTTAGGGGCCATGCG  21958829

Query  482       AATTATGTGCATTCGTAATAGCCTTGCTACATTAGGCAGGCGGAACCGACCTTTAAGTCC  541
                 ||||||||||||||||||||||||||||||||||||||||||||||||||||||||||||
Sbjct  21958830  AATTATGTGCATTCGTAATAGCCTTGCTACATTAGGCAGGCGGAACCGACCTTTAAGTCC  21958889

Query  542       TTAAAATCCGTGACATATTAATAAAAACTTTCATTCTAGTTAGGATTAATCTGCTGTATT  601
                 ||||||||||||||||||||||||||||||||||||||||||||||||||||||||||||
Sbjct  21958890  TTAAAATCCGTGACATATTAATAAAAACTTTCATTCTAGTTAGGATTAATCTGCTGTATT  21958949

Query  602       GCATACCAAACACATTGCTTAACATGAAATGAATTTTGAGGTTTATCTTGTGTGCAGTTG  661
                 ||||||||||||||||||||||||||||||||||||||||||||||||||||||||||||
Sbjct  21958950  GCATACCAAACACATTGCTTAACATGAAATGAATTTTGAGGTTTATCTTGTGTGCAGTTG  21959009

Query  662       TGTTCTGTTGCCAAATTAATGCCGGAGCCCTTGCCAAGAATTTTCGTGCTCTCGAGGCTC  721
                 ||||||||||||||||||||||||||||||||||||||||||||||||||||||||||||
Sbjct  21959010  TGTTCTGTTGCCAAATTAATGCCGGAGCCCTTGCCAAGAATTTTCGTGCTCTCGAGGCTC  21959069

Query  722       CGCAAATACCGCATTGGATTTCTGAAATACCCACTTGGTATGCACTGCAATCATTCGGAG  781
                 ||||||||||||||||||||||||||||||||||||||||||||||||||||||||||||
Sbjct  21959070  CGCAAATACCGCATTGGATTTCTGAAATACCCACTTGGTATGCACTGCAATCATTCGGAG  21959129

Query  782       CTTAAACTAAACCCACCTGCATCTGTTT  809
                 |||||||||||||||||||||||||||
Sbjct  21959130  CTTAAACTAAACCCACCTGCATCTGTTT  21959157
```

Appendix 6.10 *HDACX* Sequence Alignment

>gb|AE014297.2| *Drosophila melanogaster* chromosome 3R, complete sequence

```
Query  5         ATTCAGCGTTCCTATTTGCGACCCATGCGCTTTCAAGCAGCCGGTTCCATTTTGGCCGGT  64
                 ||||||||||||||||||||||||||||||||||||||||||||||||||||||||||||
Sbjct  20681493  ATTCAGCGTTCCTATTTGCGACCCATGCGCTTTCAAGCAGCCGGTTCCATTTTGGCCGGT  20681434

Query  65        AAGCTGGCATTGGATTATGGTTGGGCCATCAACCTGGGCGGTGGGTTCCATCACTGTTGC  124
                 ||||||||||||||||||||||||||||||||||||||||||||||||||||||||||||
Sbjct  20681433  AAGCTGGCATTGGATTATGGTTGGGCCATCAACCTGGGCGGTGGGTTCCATCACTGTTGC  20681374

Query  125       TCGTACAGAGGCGGTGGTTTCTGTCCATATGCTGACATCTCGCTGCTCATCGTCAGGCTG  184
                 ||||||||||||||||||||||||||||||||||||||||||||||||||||||||||||
Sbjct  20681373  TCGTACAGAGGCGGTGGTTTCTGTCCATATGCTGACATCTCGCTGCTCATCGTCAGGCTG  20681314

Query  185       TTCGAGCAGGAACCATTCCGGGTGCGCCGCATAATGATTGTGGACCTGGATGCCCATCAG  244
                 ||||||||||||||||||||||||||||||||||||||||||||||||||||||||||||
Sbjct  20681313  TTCGAGCAGGAACCATTCCGGGTGCGCCGCATAATGATTGTGGACCTGGATGCCCATCAG  20681254

Query  245       GGCAATGGGCACGAGCGGGACTTCAATAACGTGGCAGCCGTCTACATTTTCGACATGTAC  304
                 ||||||||||||||||||||||||||||||||||||||||||||||||||||||||||||
Sbjct  20681253  GGCAATGGGCACGAGCGGGACTTCAATAACGTGGCAGCCGTCTACATTTTCGACATGTAC  20681194

Query  305       AATGCCTTTGTCTATCCGCGGGATCATGTGGCCAAGGAGAGCATTCGGTGTGCGGTGGAG  364
                 ||||||||||||||||||||||||||||||||||||||||||||||||||||||||||||
Sbjct  20681193  AATGCCTTTGTCTATCCGCGGGATCATGTGGCCAAGGAGAGCATTCGGTGTGCGGTGGAG  20681134

Query  365       CTGCGCAACTACACGGAGGATGGATTCTACCTGCGGCAACTAAAACGCTGCCTGATGCAG  424
                 ||||||||||||||||||||||||||||||||||||||||||||||||||||||||||||
Sbjct  20681133  CTGCGCAACTACACGGAGGATGGATTCTACCTGCGGCAACTAAAACGCTGCCTGATGCAG  20681074

Query  425       TCCCTGGCCGAGTTCCGTCCAGATATGGTCGTCTATAATGCGGGAACCGATGTGCTCGAG  484
                 ||||||||||||||||||||||||||||||||||||||||||||||||||||||||||||
Sbjct  20681073  TCCCTGGCCGAGTTCCGTCCAGATATGGTCGTCTATAATGCGGGAACCGATGTGCTCGAG  20681014

Query  485       GGCGATCCATTGGGCAACCTGGCTATTTCCGCGGAGGGCGTTATTGAGCGGGATCGGTTG  544
                 ||||||||||||||||||||||||||||||||||||||||||||||||||||||||||||
Sbjct  20681013  GGCGATCCATTGGGCAACCTGGCTATTTCCGCGGAGGGCGTTATTGAGCGGGATCGGTTG  20680954

Query  545       GTATTTAGTACATTTCGGGCATTAGGAATTCCGGTGGTGATGCTGCTGAGTGGTGGCTAC  604
                 ||||||||||||||||||||||||||||||||||||||||||||||||||||||||||||
Sbjct  20680953  GTATTTAGTACATTTCGGGCATTAGGAATTCCGGTGGTGATGCTGCTGAGTGGTGGCTAC  20680894

Query  605       TTGAAGGCATCCGCAGGGGT  624
                 ||||||||||||||||||||
Sbjct  20680893  TTGAAGGCATCCGCAGGGGT  20680874
```

Appendix 6.11 *pr-Set7* Sequence Alignment

>gb|AE014297.2| Drosophila melanogaster chromosome 3R, complete sequence.
Features in this part of subject sequence: CG3307-PA, CG3307-PB

```
Query  6         CCCACCAAAGCCTCCAGCATAAAGATCAATCGGAGCTTCGAACTGGCCGGAGCCGTATTC  65
                 ||||||||||||||||||||||||||||||||||||||||||||||||||||||||||||
Sbjct  10143212  CCCACCAAAGCCTCCAGCATAAAGATCAATCGGAGCTTCGAACTGGCCGGAGCCGTATTC  10143271

Query  66        TCATCACCTCCGTCGGTGCTAAACGCCTGTCTCAATGGACGCTTCAATCAAATAGTAAGC  125
                 ||||||||||||||||||||||||||||||||||||||||||||||||||||||||||||
Sbjct  10143272  TCATCACCTCCGTCGGTGCTAAACGCCTGTCTCAATGGACGCTTCAATCAAATAGTAAGC  10143331

Query  126       CTGAATGGACAAAAGGAGGCGCTGGACTTGCCGCACTTCGATTTGGATCAACATGACAGT  185
                 ||||||||||||||||||||||||||||||||||||||||||||||||||||||||||||
Sbjct  10143332  CTGAATGGACAAAAGGAGGCGCTGGACTTGCCGCACTTCGATTTGGATCAACATGACAGT  10143391

Query  186       AGTTCTTGCGACAGCGGAGTAGCCTGTGGTCTCACTGCCAATACAGAATCGCCAGCGGGG  245
                 ||||||||||||||||||||||||||||||||||||||||||||||||||||||||||||
Sbjct  10143392  AGTTCTTGCGACAGCGGAGTAGCCTGTGGTCTCACTGCCAATACAGAATCGCCAGCGGGG  10143451

Query  246       CAACCCCGACGCAGAAAACCAGCCACACCGCATCGCATCCTCTGCCCCTCGCCAATCAAA  305
                 ||||||||||||||||||||||||||||||||||||||||||||||||||||||||||||
Sbjct  10143452  CAACCCCGACGCAGAAAACCAGCCACACCGCATCGCATCCTCTGCCCCTCGCCAATCAAA  10143511

Query  306       ACGGCTTTGAAGGTAACTGGAGGGATTTGCAAGGTCGGATCTGCGGATC  354
                 |||||||||||||||||||||||||||||||||||||||||||||||||
Sbjct  10143512  ACGGCTTTGAAGGTAACTGGAGGGATTTGCAAGGTCGGATCTGCGGATC  10143560
```

Appendix 6.12 *msl-2* Sequence Alignment

>gb|EU167118.1| *Drosophila melanogaster* isolate male-specific lethal 2 (*msl*-2) gene.

```
Query  6    CCCAAAACCACACAGGAGTTCATTCGCGAGGGCTCAAACATCTCCGACACTTTTGACATC  65
            ||||||||||||||||||||||||||||||||||||||||||||||||||||||||||||
Sbjct  225  CCCAAAACCACACAGGAGTTCATTCGCGAGGGCTCAAACATCTCCGACACTTTTGACATC  284

Query  66   TTTCTGCCCCAGCCGGATTTGCCGTTCCTCAAGGACATGCCCACATCGCTGCCTGCGGAG  125
            |||||||||||||||||||||||||||||||||||||||||||||||||||| ||||||
Sbjct  285  TTTCTGCCCCAGCCGGATTTGCCGTTCCTCAAGGACATGCCCACATCGCTGCCCGCGGAG  344

Query  126  ACGCCGCCTACGTCGGCGGTCACGACTCCGGAACTGCCCTATGATCACCACCTCAACATC  185
            ||||||||||||||||||||||||||||||||||||||||||||||||||||||||||||
Sbjct  345  ACGCCGCCTACGTCGGCGGTCACGACTCCGGAACTGCCCTATGATCACCACCTCAACATC  404

Query  186  AGCGACATTGAGGCGGAGGCGGCGGCCACAGCGGAGCAGGGTCACTTCTCGCCGCTTCCC  245
            ||||||||||||||||||||||||||||||||||||||||||||||||||||||||||||
Sbjct  405  AGCGACATTGAGGCGGAGGCGGCGGCCACAGCGGAGCAGGGTCACTTCTCGCCGCTTCCC  464

Query  246  CTGCTGCCCACAGGATCTCGCATGGGCATGCTCTCCCACGCCGGGCAAATAGTCATTGCC  305
            |||||||||||||||||||||||||||||| ||||||||||||||||||||||||||||
Sbjct  465  CTGCTGCCCACAGGATCTCGCATGGGCATGCTTTCCCACGCCGGGCAAATAGTCATTGCC  524

Query  306  ACCGAGAGCTCGGAGTCGGGCTTCATGGACCAAGCGTGGACGGATCAGGTAGACCTGTCT  365
            ||||||||||||||||||||||||||||||||||||||||||||||||||||||||||||
Sbjct  525  ACCGAGAGCTCGGAGTCGGGCTTCATGGACCAAGCGTGGACGGATCAGGTAGACCTGTCT  584

Query  366  GGCACGGTTTCGGTGTCCAAATACACAAATAGCGGCAACAACTTTGCTGTCTCCTACGTG  425
            ||||||||||||||||||||||||||||||||||||||||||||||||||||||||||||
Sbjct  585  GGCACGGTTTCGGTGTCCAAATACACAAATAGCGGCAACAACTTTGCTGTCTCCTACGTG  644

Query  426  ATGCCCACCTCTGCGACCACGAAGTTCGATCCACAGGAACTGCAAATCGGCCAGGTGGTG  485
            ||||||| ||||||||||||||||||||||||||||||||||||||||||||||||||||
Sbjct  645  ATGCCCAACTCTGCGACCACGAAGTTCGATCCACAGGAACTGCAAATCGGCCAGGTGGTG  704

Query  486  CAAATGGCGGACTCCACACAGTTGGCTGTGCTGGCTGCCGTTGAGGAGACCGTTGAGACG  545
            ||||||||||||||||||||||||||||||||||||||||||||||||||||||||||||
Sbjct  705  CAAATGGCGGACTCCACACAGTTGGCTGTGCTGGCTGCCGTTGAGGAGACCGTTGAGACG  764

Query  546  TCCACACAGTTGACTGTGCTCTCCACCACCGTTGAGGAGACCGTTGAAACATCCACGCAG  605
            ||||||||||||||||||||||||||||||||||||||||||||||||||||||||||||
Sbjct  765  TCCACACAGTTGACTGTGCTCTCCACCACCGTTGAGGAGACCGTTGAAACATCCACGCAG  824

Query  606  CTAGACGTGCTTACCTCCGCTGAGGAACCCAACGAAATCTCTGATCAATTGGCTAATTTG  665
            ||||||||||||||||||||||||||||||||||||||||||||||||||||||||||||
Sbjct  825  CTAGACGTGCTTACCTCCGCTGAGGAACCCAACGAAATCTCTGATCAATTGGCTAATTTG  884

Query  666  CAAGTTGAGGAATCTGATGAGGCTCTGGTTGAAGAGACCGTTGAAGAGGC  715
            |||||||||||||||||||||||||||||||||| ||||||||||||||
Sbjct  885  CAAGTTGAGGAATCTGATGAGGCTCTGGTTGAAGAGGCCGTTGAAGAGGC  934
```

Appendix 6.13 Map of pCaSpeR Vector

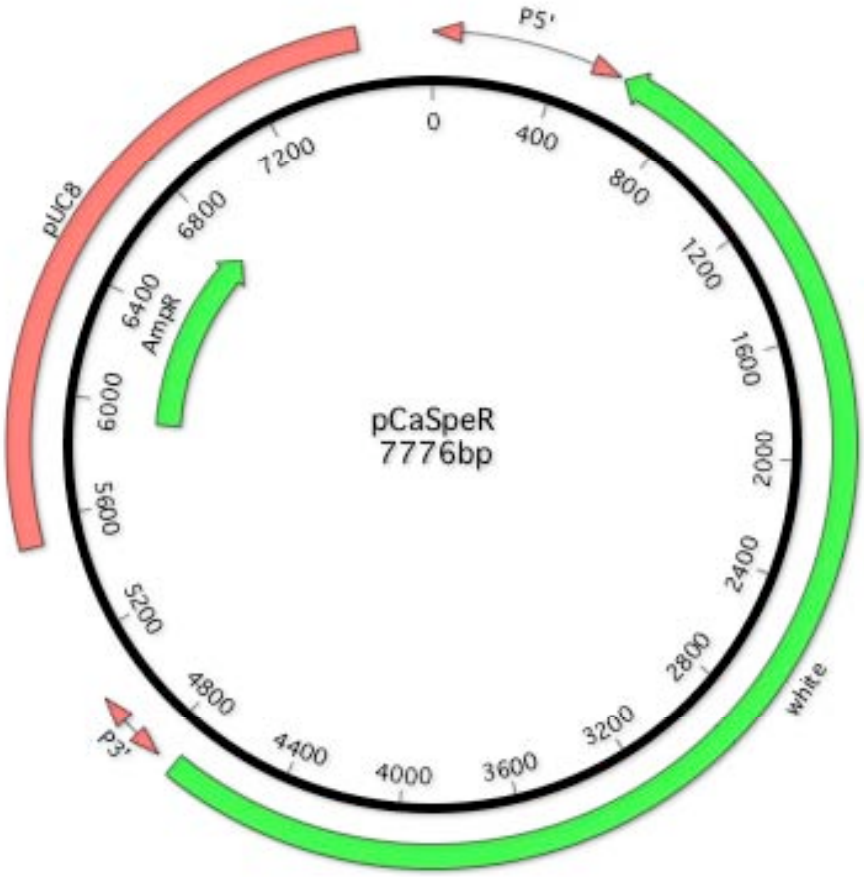

Appendix 6.14 Injection Data

Construct	No. Eclosed	No. of Fertile Crosses	No. of Transgenic
HDACX	12	6	1
pr-Set7	25	18	4
msl-2	20	13	3

Appendix 6.15 Inverse PCR Sequence Alignment

HDACX iPCR Sequence Alignment

>gb|AE013599.4| *Drosophila melanogaster* chromosome 2R, complete sequence
Features in this part of subject sequence:
CG33183-PD, isoform D
CG33183-PC, isoform C

```
Query  85       ACGAAGAAAGCCACGGGGTGTAAAAAGAGAGAGAGCAGAGATAACAGCTGATTATGACTC  144
                ||||||||||||||||||||||||||||||||||||||||||||||||||||||||||||
Sbjct  6115800  ACGAAGAAAGCCACGGGGTGTAAAAAGAGAGAGAGCAGAGATAACAGCTGATTATGACTC  6115741

Query  145      TTTTCTTCGCCGAGCGGTTGCCATAGCGAATGAACGGCACAAAGCGGACGAGGCAAAAGT  204
                ||||||||||||||||||||||||||||||||||||||||||||||||||||||||||||
Sbjct  6115740  TTTTCTTCGCCGAGCGGTTGCCATAGCGAATGAACGGCACAAAGCGGACGAGGCAAAAGT  6115681

Query  205      GGGTGTGATGGTGGCAGCGGGGCGGGGGCTTGGGGCAGCGAACTGAAGAAGTCATCGGCA  263
                ||||||||||||||||||||||||||||||||||||||||||||||||||||||||||||
Sbjct  6115680  GGGTGTGATGGTGGCAGCGGGGCGGGGGCTTGGGGCAGCGAACTGAAGAAGTCATCGGCA  6115621

Query  264      CAGAGACACATATACCCACTTCTCTCTCTTGCGC  297
                |||||||||||||||||||||||||||||||||
Sbjct  6115620  CAGAGACACATATACCCACTTCTCTCTCTTGCGC  6115587
```

pr-Set7 iPCR iPCR Sequence Alignment

>gb|AE013599.4| Drosophila melanogaster chromosome 2R, complete sequence
Features flanking this part of subject sequence:
13814 bp at 5' side: CG12464-PA
31388 bp at 3' side: CG17716-PA

```
Query  1        TGGCCCACAGCATCGGGCTGTTATACGCGAGTGTTATACGACTTGCCGCCTTCCAGCGAG  60
                ||||||||||||||||||||||||||||||||||||||||||||||||||||||||||||
Sbjct  9510514  TGGCCCACAGCATCGGGCTGTTATACGCGAGTGTTATACGACTTGCCGCCTTCCAGCGAG  9510455

Query  61       AGCGAGAGCGC  71
                ||||||||||||
Sbjct  9510454  AGCGAGAGCGC  9510444
```

msl-2 iPCR iPCR Sequence Alignment

>gb|AE014297.2| Drosophila melanogaster chromosome 3R, complete sequence
Features flanking this part of subject sequence:
892 bp at 5' side: CG31092-PD, isoform D
1289 bp at 3' side: CG31094-PC, isoform C

```
Query  82        GGAACCGTCTTAGAAACTTCGGCAGTGCTCGTCTTTCGTTCGGCAACGAACCGACGATCG  141
                 ||||||||||||||||||||||||||||||||||||||||||||||||||||||||||||
Sbjct  21566224  GGAACCGTCTTAGAAACTTCGGCAGTGCTCGTCTTTCGTTCGGCAACGAACCGACGATCG  21566283

Query  142       CCACGCGTACCATATCACACCTGCGAAGAGAAAAGAGAGTGTCGACGTCATCATCGGGGG  201
                 ||||||||||||||||||||||||||||||||||||||||||||||||||||||||||||
Sbjct  21566284  CCACGCGTACCATATCACACCTGCGAAGAGAAAAGAGAGTGTCGACGTCATCATCGGGGG  21566343

Query  202       GAGCCCCAAAGCGTTGAAAATCAAAAGCCTCGATCTCCAACACAAAGAGAAGACAAAGCT  261
                 ||||||||||||||||||||||||||||||||||||||||||||||||||||||||||||
Sbjct  21566344  GAGCCCCAAAGCGTTGAAAATCAAAAGCCTCGATCTCCAACACAAAGAGAAGACAAAGCT  21566403

Query  262       ACCAGTGCGC  271
                 ||||||||||
Sbjct  21566404  ACCAGTGCGC  21566413
```

Appendix 6.16 Sequence of pUASp-NBa-CS2-BgX Region of Interest

AAAGAGATAGCGGACGCAGCGGCGAAAGAGACGGCGATATTTCTGTGGACAGAGAAGGAGGCAAACAGCG
CTGACTTTGAGTGGAATGTCATTTTGAGTGAGAGGTAATCGAAAGAACCTGGTACATCAAATACCCTTGG
ATCGAAGTAAATTTAAAACTGATCAGATAAGTTCAATGATATCCAGTGCAGTAAAAAAAAAAAATGTTTTT
TTTATCTACTTTCCGCAAAAATGGGTTTTATTAACTTACATACATACTAGAATTGGCCGCTCTAGCCCCC
CCTCGAATGTTCTCTCTCTTCTCTTCTCTCTCTCTTTCTCGAATGTTCTCTCTCTTCTCTTCTCTCTCTC
TTTCTCGAGGTCATCAAGCTTAGGCCTCCAAGGCGGAGTACTGTCCTCCGGGCTGGCGGAGTACTGTCCT
CCGGCAAGGCGGAGTACTGTCCTCCGGGCTGGCGGAGTACTGTCCTCCGGCAAGGCGGAGTACTGTCCTC
CGGGCTGGCGGAGTACTGTCCTCCGGCAAGGCGGAGTACTGTCCTCCGGGCTGGCGGAGTACTGTCCTCC
GGCAAGGCGGAGTACTGTCCTCCGGGCTGGCGGAGTACTGTCCTCCGGCAAGGCGGAGTACTGTCCTCCG
GGCTGGCGGAGTACTGTCCTCCGGCAAGGCGGAGTACTGTCCTCCGGGCTGGCGGAGTACTGTCCTCCGG
CAAGGGTCGAGTCGATAGCCGAAGCTTACCGAAGTATACACTTAAATTCAGTGCACGTTTGCTTGTTGAG
AGGAAAGGTTGTGTGCGGACGAATTTTTTTTTGAAAACCGGTGATAGAGCCTGAACCAGAAAAGATAAAA
GAAGGCTATACCAGTGGGAGTACACAAACAGAGTAAGTTTGAATAGTAAAAAAAATCATTTATGTAAACA
ATAACGTGACTGTGCGTTAGGTCCTGTTCATTGGTACCCGCCCGGGGATCAGATCCGCGGCCGCTAGCGA
ATTCGGATCCAGGTAAGTGGGAGTCGCTTCCTGCAGAATTGAGTGCTTCAAATCAGGTGCGAGGAAAGTT
GAGGGCATGTTAATGAATTATTGAAATCAGGCGCCTGCTTAGCATCAATCATCTCGCTAAGTTCGCAGCT
TCCTGCAGCTCTTGTGCCAATCCGTGCACCCACATCCATTTTTGACTATTCCGGCGGAGGGGGCCCGGAC
TGCCGGCACTACTGATGAGCGCTTCAAATGTCAGGCAATGTAATTAAGTTAAATGACGGGGAAACTGCAA
AGTTCAGGAAATGTTTGTGTTTCGTCCTTTTCGGGGAGGGGCACGGCTAGGATGCCAGTACTGGGATGGG
TTTTCGGTGGGTGTAAACTTAATTAAAAGTGCTTCAGCTCCACTCGCATGTTTTCGGGGCCTACCCAGTA
TAAAGACATTAAAGTAATTAAAATCAGGGCATACGAGTTGATTTTAAGGGCATAATTTAGGGGCCATGCG
AATTATGTGCATTCGTAATAGCCTTGCTACATTAGGCAGGCGGAACCGACCTTTAAGTCCTTAAAATCCG
TGACATATTAATAAAAACTTTCATTCTAGTTAGGATTAATCTGCTGTATTGCATACCAAACACATTGCTT
AACATGAAATGAATTTTGAGGTTTATCTTGTGTGCAGTTGTGTTCTGTTGCCAAATTAATGCCGGAGCCC
TTGCCAAGAATTTTCGTGCTCTCGAGGCTCCGCAAATACCGCATTGGATTTCTGAAATACCCACTTGGTA
TGCACTGCAATCATTCGGAGCTTAAACTAAACCCACCTGCATCTGTTTTTTTTTTAGGAGATCTTACGTA
TCTAGAGTCGACCTCGAACGTTAACGTTAACGTAACGTTAACTCGAGGAGCTTGATAACATTATACCTAA
ACCCATGGTCAAGAGTAAACATTTCTGCCTTTGAAGTTGAGAACACAATTAAGCATCCCCTGGTTAAACC
TGACATTCATACTTGTTAATAGCGCCATAAACATAGCACCAATTTCGAAGAAATCAGTTAAAAGCAATTA
GCAATTAGCAATTAGCAATAACTCTGCTGACTTCAAAACGAGAAGAGTTGCAAGTATTTGTAAGGCACAG
TTTATAGACCACCGACGGCTCATTAGGGCTCGTCATGTAACTAAGCGCGGTGAAACCCAATTGAACATAT
AGTGGAATTATTATTATCAATGGGGAAGATTTAACCCTCAGGTAGCAAAGTAATTTAATTGCAAATAGAG
AGTCCTAAGACTAAATAATATATTTAAAAATCTGGCCCTTTGACCTTGCTTGTCAGGTGCATTTGGGTTC
AATCGTAAGTTGCTTCTATATAAACACTTTCCCCATCCCCGCAATAATGAAGAATACCGCAGAATAAAGA
GAGATTTGCAACAAAAAATAAAGGCATTGCGAAAACTTTTTATGGGGGATCATTACACTCGGGCCTACGG
TTACAATTCCCAGCCACTTAAGCGACAAGTTTGGCCAACAATCCATCTAATAGCTAATAGCGCAATCACT
GGTAATCGCAAGAGTATATAGGCAATAGAACCCATGGATTTGACCAAAGGTAACCGAGACAATGGAGAAG
CAAGAGGATTTCAAACTGAACACCCACAGTGCTGTGTACTACCACTGGCGCGTTTGGGAGCTCACTGGCC
TGATGCGTCCTCCGGGCGTTTCAAGCCTGCTTTACGTGGTATACTCCATTACGGTAACTTGGTGGTCACC
GTGCTGTTTCCCTTGAGCTTGCTGGCCAGGCTGCTGTTCACCACCAACATGGCCGGATTGTGCGAGAACC
TGACCATAACTATTACCGATATTGTGGCCAATTTGAAGTTTGCGAATGTGTACATGGTGAGGAAGCAGCT
CCATGAGATTCGCTCTCTCCTAAGGCTCATGGACGCTAGAGCCCGGCTGGTGGGCGATCCCGAGGAGATT
TCTGCCTTGAGGAAGGAAGTGAATATGCACAGGGCACTTTCCGCACCTTTGCCAGTATTTTCGTATTTGG
CACTACTTTGAGTTGCGTCCGCGTGGTCGTTCGCCCGGATCGAGAGCTCCTGTATCCGGCCTGGTTCGGC
GTTGACTGGATGCACTCCACCAGAAACTATGTGCTCATCAATATCTACCAGCTCTTCGGCTTGATAGTGC
AGGCTATACAGAACTGCGCTAGTGACTCCTATCCGCCTGCGTTTCTCTGCCTGCTCACGGGTCATATGCG
TGCTTTGGAGCTGAGGGTGCGGCGGATTGGCTGCAGCCAAGCTTTGCGTACTCGCAAATTATTAAAAATA
AAACTTTAAAAATAATTTCGTCTAATTAATATTATGAGTTAATTCAAACCCCACGGACATGCTAAGGGTT
AATCAACAATCATATCGCTGTCTCACTCAGACTCAATACGACACTCAGAATACTATTCCTTTCACTCGCA
CTTATTGCAAGCATACGTTAAGTGGATGTCTCTTG

6.17 Sequence of PCR to confirm *attB* insert

pUASp-RNAi-attB35

ATGCGTCGTTTAGAGCAGCAGCCGAATTAATTCTAGTTCCAGTGAAATCCAAGCATTTTCTAAATTAAAT
GTATTCTTATTATTATAGTTGTTATTTTTGATATATATAAACAACACTATTATGCCCACCATTTTTTTGA
GAGACATGCCCGCCGTGACCGTCGAGAACCCGCTGACGCTGCCCCGCGTATCCGCACCCGCCGACGCCGT
CGCACGTCCCGTGCTCACCGTGACCACCGCGCCCAGCGGTTTCGAGGGCGAGGGCTTCCCGGTGCGCCGC
GCGTTCGCCGGGATCAACTACCGCCACCTCGACCCGTTCATCATGATGGACCAGATGGGTGAGGTGGAGT
ACGCGCCCGGGGAGCCCAAGGGCACGCCCTGGCACCCGCACCGCGGCTTCGAGACCGTGACCTACATCGT
CTCTACACAAGGAACAAACACTGGATGTCACTTTCAGTTCAAATTGTAACGCTAATCACTCCGAACAGGT
CACAA

pUASp-RNAi-attB53

AATGCGTCGTTTAGAGCAGCAGCCGAATTAATTCTAGTTCCAGTGAAATCCAAGCATTTTCTAAATTAAA
TGTATTCTTATTATTATAGTTGTTATTTTTGATATATATAAACAACACTATTATGCCCACCATTTTTTTG
AGAGACATGCCCGCCGTGACCGTCGAGAACCCGCTGACGCTGCCCCGCGTATCCGCACCCGCCGACGCCG
TCGCACGTCCCGTGCTCACCGTGACCACCGCGCCCAGCGGTTTCGAGGGCGAGGGCTTCCCGGTGCGCCG
CGCGTTCGCCGGGATCAACTACCGCCACCTCGACCCGTTCATCATGATGGACCAGATGGGTGAGGTGGAG
TACGCGCCCGGGGAGCCCAAGGGCACGCCCTGGCACCCGCACCGCGGCTTCGAGACCGTGACCTACATCG
TCTCTACACAAGGAACAAACACTGGATGTCACTTTCAGTTCAAATTGTAACGCTAATCACTCCGAACAGG
TCACAA